Ann Med Res

Annals of Medical Research

The Official Journal of Inonu University Faculty of Medicine

Ann Med Res | Volume: 32 | Issue: 11 | November 2025

Original Articles

Case Reports

Ann Med Res

Annals of Medical Research

The Official Journal of Inonu University Faculty of Medicine

Editorial Board | Volume: 32 | Issue: 11 | November 2025

Ann Med Res

Annals of Medical Research

The Official Journal of Inonu University Faculty of Medicine

Editorial Advisory Board | Volume: 32 | Issue: 11 | November 2025

Ann Med Res

Annals of Medical Research

The Official Journal of Inonu University Faculty of Medicine

Table of Contents | Volume: 32 | Issue: 11 | November 2025

Original Articles

Case Reports

Ann Med Res

Current issue list available at Ann Med Res

Annals of Medical Research

journal page: annalsmedres.org

Effect of methylphenidate treatment on macula and optic disc microvascularity in children with attention-deficit/hyperactivity disorder: A retrospective study

Serhat Ermis [a,*], Duygu Kinay Ermis [b], Yusuf Cem Yilmaz [a], Serife Ciloglu Hayat [a], Petek Aksoz [a]

[a]*University of Health Sciences, Basaksehir Cam and Sakura City Hospital, Department of Ophthalmology, Istanbul, Türkiye*
[b]*University of Health Sciences, Basaksehir Cam and Sakura City Hospital, Department of Child and Adolescent Psychiatry, Istanbul, Türkiye*
**Corresponding author: serhatermis87@gmail.com (Serhat Ermis)*

MAIN POINTS

- This study is among the first to investigate the effects of methylphenidate (MPH) treatment on retinal and optic nerve head microvasculature in children with attention-deficit/hyperactivity disorder (ADHD).
- Significant increases in superficial and deep capillary plexus vessel densities were observed after MPH treatment.
- Radial peripapillary capillary plexus vessel density showed no significant change between pre- and post-treatment measurements.
- These findings suggest that MPH may exert regional and limited effects on retinal microcirculation, and that OCTA could serve as a sensitive tool for monitoring retinal vascular changes in children with ADHD.

Cite this article as: Ermis S, Kinay Ermis D, Yilmaz YC, Ciloglu Hayat S, Aksoz P. Effect of methylphenidate treatment on macula and optic disc microvascularity in children with attention-deficit/hyperactivity disorder: A retrospective study. *Ann Med Res*. 2025;32(11):474–480. doi: 10.5455/annalsmedres.2025.05.114.

ABSTRACT

Aim: This study aimed to investigate macular and optic nerve head (ONH) microvascularization in children diagnosed with attention deficit hyperactivity disorder (ADHD) before and 6 months after the initiation of methylphenidate (MPH) treatment, and to compare these findings with a healthy control group.

Materials and Methods: This retrospective study included 66 eyes of 66 patients with ADHD and 74 eyes of 74 healthy controls, all aged 6–17 years. Participants were grouped as follows: newly diagnosed treatment-naive ADHD patients, the same patients after 6 months of MPH treatment, and healthy controls. Specular microscopy findings, pupil size (PS), anterior chamber depth (ACD), and lens thickness (LT) values of participants were recorded. Additionally, retinal nerve fiber layer (RNFL) thickness, central macular thickness (CMT), and optic nerve head (ONH) radial peripapillary capillary plexus (RPCP), superficial capillary plexus (SCP), and deep capillary plexus (DCP) vessel density (VD) parameters were measured.

Results: Statistically significant increases in whole-image VD values for SCP and DCP were observed following MPH treatment (both $p<0.001$). Additionally, SCP VD values were significantly lower in treatment-naive children with ADHD compared to healthy controls, while RPCP VD values were higher ($p = 0.006$ and $p = 0.010$, respectively). No statistically significant differences in CMT, RNFL thickness, or anterior segment parameters (PS, ACD, LT) were observed either after MPH treatment within the ADHD group or between the control group and treatment-naive ADHD patients.

Conclusion: In children diagnosed with ADHD, significant increases in SCP and DCP values were observed following MPH treatment. These findings indicate the need for further studies to evaluate the effects and clinical significance of MPH treatment on retinal microvasculature.

Keywords: Attention deficit hyperactivity disorder, Methylphenidate, Optical coherence tomography angiography

Received: May 12, 2025 **Accepted:** Jul 25, 2025 **Available Online:** Nov 25, 2025

INTRODUCTION

Attention deficit hyperactivity disorder (ADHD) is a neurodevelopmental disorder characterized by inattention, hyperactivity, and impulsivity, resulting from the interaction of genetic and environmental factors [1,2]. Neuroimaging studies have elucidated the neural basis of the disorder by revealing structural differences in the brain [3-7]. Neurotransmitter imbalance in the prefrontal cortex forms the basis of methylphenidate (MPH) treatment [8,9].

Studies indicate that ocular parameters have been investigated to identify biomarkers associated with ADHD. In this context, the macula and optic nerve head (ONH) have become

focal points, with ocular findings being evaluated in detail using imaging techniques such as optical coherence tomography (OCT) and optical coherence tomography angiography (OCTA). Based on the vascular theory of neurodevelopmental disorders, it has been suggested that individuals with ADHD may exhibit significant alterations in the vascular structures of the macula and ONH [4-10].

Methylphenidate, commonly used in the treatment of ADHD, is known to alter sympathetic activation in the central nervous system through its effects on neurotransmitter systems. It is thought that this effect could influence the circulation and density of microvascular structures within the retina and ONH. Additionally, considering the potential effects of MPH treatment on anterior segment structures, particularly the corneal endothelium, our study evaluated anterior segment parameters including corneal endothelial cell density (ECD) measured by specular microscopy, anterior chamber depth (ACD), and lens thickness (LT).

This study aimed to evaluate superficial capillary plexus (SCP), deep capillary plexus (DCP), and radial peripapillary capillary plexus (RPCP) vessel density (VD) values in treatment-naive children with ADHD, to determine the changes in these values after six months of MPH treatment, and to investigate the potential effects of MPH on retinal and ONH microvascular structures by comparing these results with healthy controls.

MATERIALS AND METHODS

This retrospective case-control study was conducted retrospectively following approval by the ethics committee and in accordance with the principles of the Declaration of Helsinki. (Ethics approval code: KAEK/2022.05.153).

Given the retrospective nature of the study, existing patient data were anonymized to ensure confidentiality in accordance with ethical principles.

The study was conducted on patients diagnosed with ADHD between January 2020 and September 2022 at the Child and Adolescent Psychiatry Clinic of our hospital, who were subsequently referred to the Ophthalmology Clinic for routine ocular examinations. Two groups of participants were included in the study. Group 1 included randomly selected 66 eyes from 66 ADHD patients who were treatment-naive before MPH initiation, along with the evaluations performed on the same patients after 6 months of oral MPH treatment. Group 2 included 74 randomly selected eyes from 74 healthy children matched to the ADHD group in terms of age and gender.

All participants were evaluated by child and adolescent psychiatrists using the Schedule for Affective Disorders and Schizophrenia for School-Age Children - Present and Lifetime Version Turkish Form (K-SADS-PL-T) [11,12].

The inclusion criteria were: Best-corrected visual acuity (BCVA) $\geq$20/20, spherical equivalent (SE) (KR-8900, Topcon Corporation, Japan) refractive error within ±3 diopters as assessed by cycloplegic refraction, and intraocular pressure (IOP) $\leq$21 mmHg.

Exclusion criteria included: History of intraocular surgery, presence of any systemic or ocular disease, individuals with inadequate image quality due to media opacity, and participants unable to sufficiently cooperate during ocular examination or imaging procedures. Additionally, individuals with a history of psychiatric disorders, learning or behavioral changes, or medication use were excluded from the study.

During ophthalmological examinations, participants underwent Snellen best-corrected visual acuity (BCVA) measurement, intraocular pressure (IOP) measurement using applanation tonometry, axial length measurement via optical biometry (Tomey Optical Biometry OA-2000 Opt-Meas V.4E) and imaging using swept-source OCT (SS-OCT) and OCT angiography (OCTA). Additionally, to assess the potential effects of MPH treatment on anterior segment structures, corneal ECD was measured using specular microscopy (Tomey EM-4000, Japan), and parameters such as ACD, pupil size (PS) and LT were recorded. The presence of lens opacities was evaluated subjectively via slit-lamp biomicroscopic examination. All measurements were performed by an experienced retina specialist (SE).

Swept-Source OCT imaging protocol

OCT imaging was performed using the Topcon DRI OCT Triton (Topcon Corporation, Tokyo, Japan), which utilizes a laser source with a wavelength of 1050 nm and an A-scan rate of 100,000 scans per second. For macular evaluation, a raster scanning pattern within a 6×6 mm area centered on the macula was employed. Central macular thickness (CMT) was measured using the Early Treatment Diabetic Retinopathy Study grid, specifically within the central 1-mm subfield. Retinal nerve fiber layer (RNFL) assessment was conducted using a 6×6 mm scanning area centered on the optic disc. The device's internal eye-tracking system and artifact removal algorithm were actively utilized to enhance image quality and consistency. A minimum OCT image quality score of 90 was required for acceptance.

Swept-Source OCT angiography imaging protocol

Macular OCTA imaging was performed over a 3×3 mm scanning area centered on the macula. Optic disc OCTA imaging for RPCP was conducted over a 4.5×4.5 mm scanning area centered on the optic disc. Each OCTA scan cube comprised 320 B-scan clusters, with automated segmentation of all vascular plexuses performed using IMAGEnet6 software. Manual segmentation corrections were applied when necessary. RPCP was defined as the vascular structures between the internal limiting membrane and the lower boundary of the RNFL. A minimum image quality score of 70 was required for OCTA images to be included in the analysis.

To ensure measurement reliability and optimal image quality in young patients with ADHD, all examinations were con-

https://doi.org/10.5455/annalsmedres.2025.05.114

ducted by the same investigator under conditions designed to optimize patient attention levels. Furthermore, to minimize diurnal variation, all assessments were performed between 09:00 AM and 11:00 AM [13].

Statistical analysis

In this study, continuous variables were expressed as mean ± standard deviation, while categorical variables were presented as numbers and percentages. The normality distribution of continuous variables was assessed using the Kolmogorov-Smirnov test. To compare individuals with ADHD and the control group, an independent samples t-test was utilized for variables with normal distribution, whereas the Mann-Whitney U test was used for those not normally distributed. For variables analyzed using non-parametric tests, descriptive statistics were presented as median (interquartile range) or median (minimum–maximum), in accordance with best statistical practices. Pre- and post-treatment values of patients with ADHD were compared using the paired samples t-test for normally distributed variables and the Wilcoxon signed-rank test for non-normally distributed variables. Associations between categorical variables were evaluated using the Chi-square test. The 95% confidence intervals (CI) for differences between groups were calculated and reported as footnotes beneath the respective tables. Statistical analyses were conducted using IBM SPSS Statistics, Version 28.0 (Armonk, NY: IBM Corp.), with a significance level set at $p<0.05$. The minimum required sample size was calculated using G*Power software (version 3.1.9.7, Heinrich Heine University, Düsseldorf, Germany). A priori power analysis was performed for a two-tailed paired-samples t-test with an alpha level of 0.05, statistical power ($1-\beta$) of 0.80, and a medium effect size of 0.50, as defined by Cohen. The analysis revealed that a minimum of 34 participants would be necessary to detect a significant within-subject difference. Given that our study included 66 treatment-naive ADHD patients, the statistical power was deemed sufficient.

RESULTS

A total of 140 eyes from 140 participants were included in this study. No significant differences were observed between groups regarding demographic and clinical characteristics, including age, sex distribution, cycloplegic SE values, IOP, ECD, axial length, ACD, PS, LT, CMT, RNFL thickness, and rim volume. These findings indicate that the study groups were comparable, sharing similar baseline ocular characteristics. Additionally, among the ADHD patients, no statistically significant changes were observed in the previously mentioned parameters at the 6-month evaluation after MPH treatment compared to baseline ($p>0.05$ for all parameters). At the 6-month follow-up, no participants developed lens opacity.

IOP; intraocular pressure, ECD; endothelial cell density, ACD; anterior chamber depth, PS: pupil size, LT; lens thickness, CMT; central Macular thickness, RNFL; retinal nerve fiber layer

Values are expressed as mean ± standard deviation. The 95% confidence intervals (CI) for differences between groups are as follows: age (-1.60; 0.20), IOP (-0.90; 0.50), ECD (-27.50; 160.50), axial length (-0.85; 0.05), ACD (-0.25; 0.05), PS (-0.01; 0.81), LT (-0.06; 0.04), CMT (-4.20; 14.40), RNFL (-7.30; 10.30), and rim volume (-0.07; 0.07).

In the treatment-naive ADHD group (Group 1a), the mean whole-image SCP VD was significantly lower compared to healthy controls (Group 2) ($p = .006$). Post-treatment (Group 1b), a significant increase was observed in the whole-image SCP ($p < .001$). Although SCP values in the superior quadrant were numerically higher in treatment-naive ADHD patients compared to healthy controls, this difference was not statistically significant ($p = .177$). Following MPH treatment, there was a significant increase in the superior quadrant ($p < .001$); however, no statistically significant changes were observed in temporal, inferior, and nasal quadrants compared to pre-treatment values. These findings suggest that MPH treatment may exert region-specific effects on SCP.

Regarding DCP VD, pre-treatment values in the ADHD group (Group 1a) showed no statistically significant differences compared to healthy controls. Following MPH treatment, DCP values significantly increased in the whole image, temporal, and nasal quadrants ($p < .001$, $p < 0.001$, and $p = .025$, respectively), while a statistically significant but small decrease was observed in the superior and inferior quadrants ($p = .037$ and $p = .049$). These findings suggest that MPH treatment may exert region-specific effects on deep retinal microvascular density. Detailed results are presented in Table 2.

In the treatment-naive ADHD group (Group 1a), the RPCP VD of the ONH was significantly higher in the whole-image and superior quadrant averages compared to healthy controls (Group 2). Following MPH treatment, no significant differences in RPCP vessel density were observed when comparing pre-treatment (Group 1a) and post-treatment (Group 1b) measurements of the same patients. A comparison between the post-treatment patient group (Group 1b) and healthy controls (Group 2) was not performed. These findings suggest that MPH treatment does not have a pronounced effect on RPCP vessel density. Detailed results of the RPCP vessel density analysis are summarized in Table 3.

DISCUSSION

Attention deficit hyperactivity disorder is a complex and multifactorial neurodevelopmental disorder investigated through various ocular structures and parameters [1,4,10]. As extensions of the central nervous system, the retina and ONH can provide important insights into the pathophysiology of ADHD. Recent advances in OCT technology have enabled the identification of alterations in ONH and macular parameters, highlighting retinal manifestations of neuropsychiatric disorders [4,14-19]. Grönlund et al. reported significant morphological changes in the SCP, DCP, and ONH in children

https://doi.org/10.5455/annalsmedres.2025.05.114

Table 1. Demographic and clinic characteristics of the study participants.

	Group 1 (a) (treatment naive)	Group 1 (b) (post-treatment)	Group 2 (control)	p 1(a) &1(b)	p 1(a) & 2
Age (years)	9 (8-10.5)	-	10.5 (9-13)	-	0.122[a]
Sex (female/male)	30/36	-	36/38	-	0.874[b]
Spherical equivalent (D)	0.00±0.60	0.05±0.40	--0.08±0.45	0.574[c]	0.388[c]
IOP (mmHg)	14.2±1.7	14.3±1.5	14.4±3.0	0.721[c]	0.924[c]
ECD (cells/mm^2)	3022.3±222.5	3020.1±212.6	2955.8±323.7	0.954[c]	0.164[c]
Axial length (mm)	23.0±0.5	23.1±0.5	23.4±1.3	0.936[c]	0.089[c]
ACD (mm)	3.78 (3.67--3.93)	3.78 (3.67--3.93)	3.71 (3.19--4.41)	1.0[a]	0.075[a]
PS (mm)	7.3 (6.73--8.08)	6.99 (6.36--7.84)	6.86 (6.05--7.95)	0.103[a]	0.054[a]
LT (mm)	3.49 (3.43--3.57)	3.49 (3.43--3.57)	3.48 (3.37--3.63)	1.0[a]	0.200[a]
CMT (μm)	278.1 (259.70--302.90)	277.71 (270.29--287.71)	274.13 (262.23--290.17)	0.589[a]	0.105[a]
RNFL (μm)	79.69 (61.23--104.57)	80.34 (63.32--103.28)	80.05 (72.29--90.51)	0.941[a]	0.634[a]
Rim volume(mm^3)	0.38 (0.29--0.49)	0.37 (0.28--0.50)	0.37 (0.26--0.52)	1.0[a]	0.630[a]

[a] Mann–Whitney U test, [b] Chi-square test, [c] Independent-samples t-test, [d] Paired-samples t-test. Values are expressed as median (interquartile range) for variables analyzed using non-parametric tests (Mann–Whitney U test), and as mean ± standard deviation for variables analyzed using parametric tests (independent- or paired-samples t-test). Categorical variables are presented as counts and percentages. *p < 0.05. Bold values represent the variables which show statistical significance.

Table 2. Vessel density values of the superficial and deep capillary plexus in the study participants.

		Group 1 (a) (treatment naive)	Group 1 (b) (post-treatment)	Group 2 (control)	p 1(a) &1(b)	p 1(a) & 2
SCP VD (%)	Whole Image	43.07 (39.45--47.95)	44.34 (41.70--47.90)	45.18 (42.19--49.21)	**<0.001*,b**	**0.006*,a**
	Superior	46.42 (44.81--48.59)	47.26 (45.88--49.12)	44.89 (42.53--48.07)	**<0.001*,b**	0.177[a]
	Temporal	44.65 (43.21--46.59)	44.57 (43.25--46.35)	44.30 (42.00--47.40)	0.368[b]	0.086[a]
	Inferior	46.32 (44.71--48.49)	45.88 (44.62--47.59)	44.41 (41.59--48.21)	0.060[b]	0.397[a]
	Nasale	44.88 (43.04--47.36)	44.91 (43.24--47.16)	44.92 (42.73--47.86)	0.276[b]	0.071[a]
DCP VD (%)	Whole Image	45.53 (41.68--50.72)	48.01 (44.62--52.58)	46.09 (41.43--52.37)	**<0.001*,b**	0.142[a]
	Superior	48.36 (46.41--51.00)	47.83 (46.28--49.92)	46.66 (44.70--49.30)	**0.037*,b**	0.101[a]
	Temporal	48.61 (46.37--51.63)	49.63 (48.08--51.72)	48.64 (46.57--51.43)	**<0.001*,b**	0.351[a]
	Inferior	48.04 (46.54--50.05)	47.87 (46.55--49.65)	45.69 (43.33--48.87)	**0.049*,b**	0.231[a]
	Nasale	49.15 (46.56--52.64)	50.25 (48.81--52.19)	48.41 (46.17--51.43)	**0.025*,b**	0.391[a]

[a] Mann–Whitney U test, [b] Wilcoxon signed-rank test. Values are expressed as median (interquartile range) for all parameters, as they were analyzed using non-parametric tests. *p < 0.05. Bold values represent the variables which show statistical significance.SCP: Superficial Capillary Plexus, DCP: Deep Capillary Plexus VD: Vessel Density.Values are expressed as mean ± standard deviation. The 95% CI for differences between groups are as follows: For comparison between Group 1(a) and Group 1(b): SCP whole image (-1.72; -0.48), superior quadrant (-1.26; -0.34), temporal quadrant (-0.43; 0.63), inferior quadrant (-0.02; 1.02), nasal quadrant (-0.56; 0.56); DCP whole image (-3.48; -1.32), superior quadrant (0.04; 1.16), temporal quadrant (-1.42; -0.38), inferior quadrant (0.00; 0.40), nasal quadrant (-1.68; -0.12).For comparison between Group 1(a) and Group 2: SCP whole image (-3.41; -0.59), superior quadrant (-0.48; 3.28), temporal quadrant (-0.11; 0.51), inferior quadrant (-1.10; 2.40), nasal quadrant (-0.09; 0.29); DCP whole image (-1.63; 0.23), superior quadrant (-0.33; 1.73), temporal quadrant (-0.44; 0.44), inferior quadrant (-0.18; 2.58), nasal quadrant (-0.81; 2.41).

Table 3. Optic nerve head radial peripapillary capillary plexus vessel density of the study participants.

		Group 1 (a) (treatment naive)	Group 1 (b) (post-treatment)	Group 2 (control)	p 1(a) &1(b)	p 1(a) & 2
RPCP VD (%)	Whole Image	55.39 (53.61--57.79)	55.47 (53.57--58.03)	53.80 (51.50--56.90)	0.313[b]	**0.010*,a**
	Superior	57.76 (56.38--59.62)	57.62 (56.01--59.79)	55.94 (53.87--58.73)	0.594[b]	**0.035*,a**
	Temporal	54.20 ± 2.20	54.30 ± 2.00	54.20 ± 3.40	0.185[c]	0.066[a]
	Inferior	57.67 (56.35--59.45)	57.75 (56.31--59.69)	56.55 (54.54--59.26)	0.313[b]	0.100[a]
	Nasale	57.10 ± 2.70	57.20 ± 2.80	56.30 ± 3.70	0.219[d]	0.730[a]

[a] Mann–Whitney U test, [b] Wilcoxon signed-rank test, [c] Paired-samples t-test, [d] Independent-samples t-test. Values are presented as median (interquartile range) for variables analyzed using non-parametric tests (Wilcoxon signed-rank test), and as mean ± standard deviation for those analyzed using parametric tests (paired-samples t-test), specifically in the temporal and nasal quadrants. *p < 0.05. Bold values indicate statistically significant differences. RPCP: Radial peripapillary capillary plexus, VD: Vessel Density. Values are expressed as mean ± standard deviation. The 95% confidence intervals (CI) for differences between groups were as follows:For comparison between Group 1(a) and Group 1(b): RPCP whole image (-0.40; 0.80), superior quadrant (-0.29; 0.49), temporal quadrant (-0.74; 0.14), inferior quadrant (-0.29; 0.49), nasal quadrant (-0.51; 0.31). For comparison between Group 1(a) and Group 2: RPCP whole image (0.61; 4.39), superior quadrant (0.12; 3.68), temporal quadrant (-0.62; 0.02), inferior quadrant (-0.22; 2.42), nasal quadrant (-1.12; 3.32).

with ADHD, suggesting that these findings may reflect early developmental impairments in neural and vascular tissues of the brain [14]. In the present study, we investigated alterations in macular and ONH microvasculature, as well as the potential effects of MPH treatment on these structures.

In our study, no differences were detected among the groups regarding global RNFL thickness, which is consistent with previous studies [1,4,20]. This finding supports the idea

https://doi.org/10.5455/annalsmedres.2025.05.114

that ADHD is a neurodevelopmental disorder rather than a neurodegenerative one. Additionally, no significant differences were observed in quadrant analyses of RNFL thickness. Similarly, CMT did not differ significantly among the three groups, aligning well with existing literature [4,21,22]. Nevertheless, conflicting findings have also been reported in other studies [23,24]. These discrepancies may arise from technical differences among OCT devices (e.g., variations in resolution and segmentation algorithms). Although such technical differences would affect all participants similarly within a given study, inconsistencies between different studies may result from the utilization of various OCT devices. Furthermore, demographic characteristics (e.g., age, gender distribution, ethnicity) and clinical conditions (e.g., refractive errors, concurrent systemic diseases, medication usage) of study populations could represent confounding factors affecting OCT measurements. Thus, it is crucial to consider these potential confounders when interpreting results across different studies.

Literature regarding microvascular parameters of the macular region is limited. To date, only one previous study has compared OCTA values of the macula in individuals diagnosed with ADHD who were treated with MPH versus those who were not. Tarakcioglu et al. conducted a cross-sectional analysis of 80 treatment-naive children with ADHD and 106 children with ADHD treated with MPH, finding differences in choriocapillaris flow between the groups [10]. However, no significant differences were observed between the groups in SCP and DCP analyses. Researchers suggested that MPH may have only a limited effect on retinal blood flow. In contrast, our study compared OCTA values within the same individuals before and after MPH treatment. By using this within-subject comparative method, heterogeneity caused by inter-individual variability was minimized, leading to potentially more reliable and consistent results. Using this approach, we observed significant increases in SCP measurements in the whole image and superior quadrants. Regarding DCP, MPH treatment led to significant increases in the whole image, temporal, and nasal quadrants, but small yet statistically significant decreases in the superior and inferior quadrants, suggesting region-specific vascular responses. These findings suggest that MPH treatment may cause regional variations in retinal microvasculature. MPH inhibits the reuptake of dopamine and norepinephrine, thereby increasing levels of these neurotransmitters in the synaptic cleft. It has been hypothesized that this increase may lead to vasodilation of cerebral and retinal microvascular structures, enhancing blood flow [25]. This mechanism could explain the observed regional increases in retinal microvascular parameters following MPH treatment in our study. Additionally, these results support the idea that MPH might have quadrant-specific effects on retinal microvascular structures, further highlighting OCTA as a sensitive tool for assessing retinal blood flow in ADHD patients. Our study is the first to compare macular OCTA parameters before and after treatment within the same subjects, which reduces potential confounding effects arising from inter-individual variability.

Recent studies have demonstrated that OCTA is effective for assessing ONH microvascularization [26-29]. Wang et al. [27] reported decreased ONH VD in neurodegenerative diseases such as multiple sclerosis, while Asanad et al. found reduced temporal peripapillary VD in patients with schizophrenia [28]. In our study, treatment-naive ADHD patients exhibited significantly higher RPCP VD values, especially in the superior quadrant and whole-image areas, compared to healthy controls. While neuronal cell loss in neurodegenerative diseases typically leads to reduced retinal and optic nerve head vessel densities, neurodevelopmental disorders may exhibit increased microvascular density due to heightened sympathetic activation and differences in autoregulatory mechanisms [27,28]. This variation could be associated with increased vascular reactivity observed in cerebral and retinal vascular structures in ADHD.

RPCP VD did not show a significant change after MPH treatment compared to pretreatment values. This suggests that MPH may have a limited effect on potential increases in vascular reactivity. However, the absence of a post-treatment comparison with healthy controls limits definitive conclusions. Therefore, further prospective comparative studies involving healthy controls are needed, particularly to evaluate post-treatment changes.

MPH, commonly used in the treatment of ADHD, is an α1-sympathomimetic amine with adrenergic and anticholinergic properties, potentially causing ocular side effects such as mydriasis, accommodation disturbances, and transient visual disturbances [10,14,30-33]. In our study, a minimal but statistically insignificant increase in pupil diameter was observed after MPH treatment. Although previous reports indicate that MPH may transiently elevate IOP our findings suggest that MPH treatment is not associated with clinically significant changes in IOP [30,31,33]. Despite earlier reports proposing that MPH could significantly decrease ACD after cycloplegia and thereby increase glaucoma risk, no significant differences were found regarding this parameter in our study [31]. Additionally, despite the suggestion that long-term MPH use may induce lens opacities, we did not detect any lens opacity during the 6-month follow-up period [27]. These findings suggest that ocular side effects related to MPH may vary based on duration and dosage. A previous study reported that MPH does not exhibit significant toxic effects on ECD [34]. Our study also supports this, demonstrating no significant change in corneal endothelial cell density associated with MPH treatment. However, due to the retrospective design of our study, our results indicate associations rather than causality and should therefore be interpreted with caution. Prospective longitudinal studies are needed to clarify these causal relationships.

One of the significant strengths of our study is the compar-

https://doi.org/10.5455/annalsmedres.2025.05.114

ison of pre- and post-treatment data within the same individuals, enhancing methodological consistency and homogeneity of data. However, our study has several limitations. Firstly, the retrospective design of the study itself constitutes a primary limitation. Additionally, our sample size was relatively small. MPH doses were standardized, and thus, the dose-response relationship was not investigated. The relatively short duration of the study limits the evaluation of long-term effects. Furthermore, the absence of 6-month follow-up data for the healthy control group restricts our ability to differentiate whether microvascular changes observed in the ADHD group were directly related to MPH treatment or resulted from natural developmental processes. Future prospective studies with larger sample sizes, inclusion of healthy controls, and extended follow-up periods are necessary to better understand the long-term effects of MPH on retinal microvascular structures. Furthermore, although the study was initially labeled as cross-sectional, its retrospective nature—characterized by reliance on previously recorded data and the inclusion of both within-subject (pre- and post-treatment) and between-group (ADHD vs. control) comparisons—more accurately reflects a retrospective study design. This clarification has been implemented throughout the manuscript to enhance methodological accuracy.

CONCLUSION

In conclusion, this study demonstrates that MPH treatment in children with ADHD significantly increases SCP and DCP vessel density in certain regions of the macula but does not lead to a significant change in RPCP vessel density. These findings suggest that MPH may exert specific and regional effects on retinal microvascular circulation, whereas its impact on optic disc perfusion appears to be limited. We propose that OCTA may serve as a clinical monitoring tool for assessing retinal vascular effects associated with MPH treatment in individuals diagnosed with ADHD. Further comprehensive studies are needed to better elucidate potential microvascular changes related to MPH therapy.

Ethics Committee Approval: Ethical approval for this study was received from Başakşehir Çam ve Sakura City Hospital Clinical Research Ethics Committee (Date: 20.09.2022, Decision no: KAEK/2022.05.153).

Informed Consent: Informed consent was obtained from the patients.

Peer-review: Externally peer-reviewed.

Conflict of Interest: None of the authors have any potential conflicts of interest to disclose.

Author Contributions: Concept: SE, DKE, YCY, ŞÇH, PA; Design: SE, DKE, YCY, ŞÇH, PA; Supervision: SE, DKE, YCY, ŞÇH, PA; Materials: SE, DKE, YCY, ŞÇH, PA; Data Collection and/or Processing: SE, DKE, YCY, ŞÇH, PA; Analysis and Interpretation: SE, DKE, YCY, ŞÇH, PA; Literature Review: SE, DKE, YCY, ŞÇH, PA; Writing Manuscript: SE, DKE, YCY, ŞÇH, PA; Critical Review: SE, DKE, YCY, ŞÇH, PA.

Financial Disclosure: This research did not receive any specific grant from funding agencies in the public, commercial, or not-for-profit sectors.

REFERENCES

1. Işik U, Kaygisiz M. Assessment of intraocular pressure, macular thickness, retinal nerve fiber layer, and ganglion cell layer thicknesses: ocular parameters and optical coherence tomography findings in attention-deficit/hyperactivity disorder. *Braz J Psychiatry.* 2020;42(3):309-313. doi: 10.1590/1516-4446-2019-0606.
2. Thapar A, Cooper M, Eyre O, Langley K. What have we learnt about the causes of ADHD. *J Child Psychol Psychiatry.* 2013;54(1):3–16. doi: 10.1111/j.1469-7610.2012.02611.x.
3. Işık Ü, Bilgiç A, Toker A, Kilincç İ. Serum levels of cortisol, dehydroepiandrosterone, and oxytocin in children with attention-deficit/hyperactivity disorder combined presentation with and without comorbid conduct disorder. *Psychiatry Res.* 2018;261:212-219. doi: 10.1016/j.psychres.2017.12.076.
4. Hergüner A, Alpfidan I, Yar A, et al. Retinal nerve fiber layer thickness in children with ADHD. *J Atten Disord.* 2018;22(7):619-26. doi: 10.1177/1087054716664412.
5. Bilgiç A, Toker A, Işık Ü, Kilinç İ. Serum brain-derived neurotrophic factor, glial-derived neurotrophic factor, nerve growth factor, and neurotrophin-3 levels in children with attention-deficit/hyperactivity disorder. *Eur Child Adolesc Psychiatry.* 2017;26(3):355-63. doi: 10.1007/s00787-016-0898-2.
6. Valera EM, Faraone SV, Murray KE, Seidman LJ. Meta-analysis of structural imaging findings in attention-deficit/hyperactivity disorder. *Biol Psychiatry.* 2007;61(12):1361-9. doi: 10.1016/j.biopsych.2006.06.011.
7. Friedman LA, Rapoport JL. Brain development in ADHD. *Curr Opin Neurobiol.* 2015;30:106-11. doi: 10.1016/j.conb.2014.11.007.
8. Pliszka SR. Pharmacologic treatment of attention-deficit/hyperactivity disorder: efficacy, safety and mechanisms of action. *Neuropsychol Rev.* 2007;17(1):61-72. doi: 10.1007/s11065-006-9017-3.
9. Sharma A, Couture J. A review of the pathophysiology, etiology, and treatment of attention-deficit hyperactivity disorder (ADHD). *Ann Pharmacother.* 2014;48(2):209-225. doi: 10.1177/1060028013510699.
10. Tarakcioglu HN, Yilmaz S, Kara T, Yildiz AM, Yiğit U, Ozkaya A. Foveal avascular zone and vessel density in children with attention deficit hyperactivity disorder. Int Ophthalmol. 2020;40(5):1155-1162. doi: 10.1007/s10792-019-01281-8.
11. Gökler B. Reliability and validity of Schedule for affective disorders and schizophrenia for school age children-present and lifetime version Turkish version (K-SADS-PL-T). *Turkish J Child Adolesc Ment Health.* 2004;11:109–116.
12. Kaufman J, Birmaher B, Brent D, et al. Schedule for affective disorders and schizophrenia for school age children-present and lifetime version (K-SADS-PL): initial reliability andvalidity data. *J Am Acad Child Adolesc Psychiatry.* 1997;36(7):980–8. doi: 10.1097/00004583-199707000-00021.
13. Hagag AM, Gao SS, Jia Y, Huang D. Optical coherence tomography angiography: technical principles and clinical applications in ophthalmology. *Taiwan J Ophthalmol.* 2017;7(3):115–129. doi: 10.4103/tjo.tjo_31_17.
14. Grönlund MA, Aring E, Landgren M, Hellstrom A. Visual function and ocular features in children and adolescents with attention deficit hyperactivity disorder, with and without treatment with stimulants. *Eye (Lond).* 2015;21(4):494–502. doi: 10.1038/sj.eye.6702240.

https://doi.org/10.5455/annalsmedres.2025.05.114

15. Hu S-J, You Y-A, Zhang Y. A study of retinal parameters measured by optical coherence tomography in patients with multiple sclerosis. *Int J Ophthalmol.* 2015;8(6):1211-4. doi: 10.3980/j.issn.2222-3959.2015.06.24.
16. van Koolwijk LM, Despriet DD, Van Duijn CM, et al. Association of cognitive functioning with retinal nerve fiber layer thickness. *Invest Ophthalmol Vis Sci.* 2009;50(10):4576-80. doi: 10.1167/iovs.08-3181.
17. Yılmaz U, Küçük E, Ülgen A, et al. Retinal nerve fiber layer and macular thickness measurement in patients with schizophrenia. *Eur J Ophthalmol.* 2016;26(4):375–8. doi: 10.5301/ejo.5000723.
18. Mehraban A, Samimi SM, Entezari M, Seifi MH, Nazari M, Yaseri M. Peripapillary retinal nerve fiber layer thickness in bipolar disorder. *Graefes Arch Clin Exp Ophthalmol.* 2016;254(2):365–71. doi: 10.1007/s00417-015-2981-7.
19. Al-Haddad C, Barikian A, Jaroudi M, Massoud V, Tamim H, Noureddin B. Spectral domain optical coherence tomography in children: normative data and biometric correlations. *BMC Ophthalmol.* 2014;14:53. doi: 10.1186/1471-2415-14-53.
20. Bodur S, Kara H, Acikel B, Yaşar E. Evaluation of the ganglion cell layer thickness in children with attention deficit hyperactivity disorder and comorbid oppositional defiant disorder. *Turkish J Clin Psy.* 2018;21(3):222-230. doi: 10.5505/kpd.2018.37450.
21. Bae S, Kim JT, Han JM, Han DH. Pilot study: an ocular biomarker for diagnosis of attention deficit hyperactivity disorder. *Psychiatry Investig.* 2019;16(5):370-8. doi: 10.30773/pi.2019.02.26.1.
22. Pérez-García D, Ibanez-Alperte J, Remón L, Cristobal JA, Sanchez -Cano A, Pinilla I. Study of spectral-domain optical coherence tomography in children: normal values and influence of age, sex, and refractive status. *Eur J Ophthalmol.* 2016;26(2):135–41. doi: 10.5301/ejo.5000665.
23. Hanumunthadu D, Keane PA, Balaskas K, et al. Agreement Between Spectral-Domain and Swept-Source Optical Coherence Tomography Retinal Thickness Measurements in Macular and Retinal Disease. *Ophthalmol Ther.* 2021;10(4):913-922. doi: 10.1007/s40123-021-00377-8.
24. García-Franco R, Méndez-Marín D, García-Roa M, Ramirez-Neria P, Valera-Cornejo D, Lansingh VC. Central Macular Thickness in a Healthy Mexican Population Using Huvitz Optical Coherence Tomography. *Clin Ophthalmol.* 2020;14:3931-3940. doi: 10.2147/OPTH.S272431.
25. Faraone SV. The pharmacology of amphetamine and methylphenidate: Relevance to the neurobiology of attention-deficit/hyperactivity disorder and other psychiatric comorbidities. *Neurosci Biobehav Rev.* 2018;87:255-270. doi: 10.1016/j.neubiorev.2018.02.001.
26. Jia Y, Morrison JC, Tokayer J, et al. Quantitative OCT angiography of optic nerve head blood flow. *Biomed Opt Express.* 2012;3(12):3127–37. doi: 10.1364/BOE.3.003127.
27. Wang X, Jia Y, Spain R, et al. Optical coherence tomography angiography of optic nerve head and parafovea in multiple sclerosis. *Br J Ophthalmol.* 2014;98(10):1368–73. doi: 10.1136/bjophthalmol-2013-304547.
28. Asanad S, Addis H, Chen S, et al. Retinal thickness and vascular pathology as ocular biomarkers for schizophrenia: morphometric analysis of the peripapillary and macular regions using OCT and OCTA in vivo. *Invest Ophthalmol Vis Sci.* 2020;61(7):5105.
29. Jia Y, Wei E, Wang X, et al. Optical coherence tomography angiography of optic disc perfusion in glaucoma. *Ophthalmology.* 2014;121(7):1322–32. doi: 10.1016/j.ophtha.2014.01.021.
30. Duman NS, Duman R, Sarı Gökten E, Duman R. Lens opacities in children using methylphenidate hydrochloride. *Cutan Ocul Toxicol.* 2017;36(4):362–365. doi: 10.1080/15569527.2017.1300161.
31. Larranaga-Fragoso P, Noval S, Rivero JC, Boto-de-los-Buesis A. The effects of methylphenidate on refraction and anterior segment parameters in children with attention deficit hyperactivity disorder. *J AAPOS.* 2015;19(4):322–326. doi: 10.1016/j.jaapos.2015.04.005.
32. Lachkar Y, Bouassida W. Drug-induced acute angle closure glaucoma. *Curr Opin Ophthalmol.* 2007;18(2):129-33. doi: 10.1097/ICU.0b013e32808738d5.
33. Güvenmez O, Cubuk M, Gunes S. The effects of medication on intraocular pressure in children with attention deficit hyperactivity disorder: A prospective study. *J Popul Ther Clin Pharmacol.* 2020;27(2):e45-50. doi: 10.15586/jptcp.v27i2.665.
34. Koc H, Önal BS, Hoşoğlu E. Evaluation of corneal endothelial cell morphology off and on treatment by specular microscopy in children and adolescents with attention deficit hyperactivity disorder. *Cutan Ocul Toxicol.* 2024;43(2):120-123. doi: 10.1080/15569527.2024.2303442.

https://doi.org/10.5455/annalsmedres.2025.05.114

Ann Med Res

Current issue list available at Ann Med Res

Annals of Medical Research

journal page: annalsmedres.org

Functional and radiological comparison of lateral pinning versus cross pinning in displaced pediatric supracondylar humerus fractures

Baris Acar [a,*], Saltuk Bugra Tekin [a], Ahmet Sinan Kalyenci [a], Ahmet Senel [a]

[a] *Istanbul Training and Research Hospital, Clinic of Orthopaedic and Traumatology, Istanbul, Türkiye*
**Corresponding author: brs.acar90@gmail.com (Baris Acar)*

MAIN POINTS

- Supracondylar humerus fractures are the most common pediatric elbow fractures.
- Lateral pinning and cross pinning provide comparable radiological and functional outcomes.
- Medial pinning may carry a risk of ulnar nerve injury, especially when performed without a mini incision.
- We recommend using a mini medial incision over the medial epicondyle to reduce ulnar nerve injury risk.

Cite this article as: Acar B, Tekin SB, Kalyenci AS, Senel A. Functional and radiological comparison of lateral pinning versus cross pinning in displaced pediatric supracondylar humerus fractures. *Ann Med Res*. 2025;32(11):481--485. doi: 10.5455/annalsmedres.2025.06.143.

ABSTRACT

Aim: The aim of this study is to compare the commonly used cross pinning and lateral pinning techniques in the surgical treatment of pediatric supracondylar humerus fractures by evaluating clinical and radiological outcomes.

Materials and Methods: Between 2018 and 2024, patients who had surgical treatment for Gartland type 3 supracondylar humerus fractures were included in the study. Patients were divided into two groups based on the surgical technique: lateral pinning (Group 1) and cross pinning (Group 2). Patients with a minimum folloe-up of 6 months were included in the study. Demographic data inlcuidng age, sex, side, mechanism of trauma were recorded. Clinical evaluation was performed using Flynn's criteria. Radiological evaluation included assessment of fracture union, Baumann's angle and its change from 0 to 6 months, carrying angle, lateral humerocapitellar angle (LHCA), and its 0 to 6-month change. Complications and additional procedures were also recorded.

Results: Group 1 consisted of 32 patients, while Group 2 included 28 patients. The demographic data showed no statistically significant differences between the two groups. Based on Flynn's criteria, outcomes in Group 1 were classified as excellent in 24 (75%) patients, good in 5 (15.6%), fair in 3 (9.4%), and none were considered poor. In Group 2, 20 (71.4%) patients achieved excellent results, 7 (25%) were rated as good, 1 as fair (3.6%), and no poor outcomes were observed. Functional outcomes were similar in both groups (p: 0.488). The groups showed comparable results in terms of both the Baumann's angle and its change, carrying angle, LHCA and its change. Ulnar nerve injury developed in 2 patients in Group 2 and resolved with conservative follow-up.

Conclusion: In the management of pediatric supracondylar humerus fractures, lateral and cross pinning techniques yield comparable clinical and radiological results. To prevent ulnar nerve palsy in the cross-pinning technique, a mini medial incision can be used to protect the ulnar nerve.

Keywords: Gartland, Pediatric, Pinning, Supracondylar

Received: Jun 05, 2025 **Accepted:** Aug 04, 2025 **Available Online:** Nov 25, 2025

INTRODUCTION

Supracondylar humerus fractures represent the most frequent type of elbow fracture in children, comprising about 3–5% of all pediatric fractures and 50–60% of those involving the elbow [1,2]. These fractures predominantly occur in children aged about 6 years and are caused by low-energy trauma [3]. Closed reduction with percutaneous pinning remains the widely accepted method of treatment; however, the optimal pinning configuration that provides stability and best clinical outcomes is still debated [4].

Lateral pinning and medial-lateral crossed pinning are the two commonly used techniques for supracondylar humerus fracture fixation. Lateral pinning is favored for reducing iatrogenic ulnar nerve injury, while medial-lateral crossed pinning is considered biomechanically superior in terms of rotational stability [5]. Despite the biomechanical advantages of medial-lateral crossed pinning, the risk of ulnar nerve injury remains a major concern. Studies have reported an incidence of iatrogenic ulnar nerve injury ranging from 2% to 15% with crossed pinning techniques [5]. This has led many surgeons to prefer lateral pinning, particularly in cases where adequate stability can be achieved without a medial pin. However, clinical

https://doi.org/10.5455/annalsmedres.2025.06.143

studies have reported comparable functional and radiological outcomes between the two techniques [6].

The choice between lateral and crossed pinning is often influenced by fracture pattern, experience of the surgeon, and patient-specific anatomical characteristics. In this study, we aim to evaluate and compare the clinical outcomes of lateral pinning and medial-lateral cross pinning in displaced pediatric supracondylar humerus fractures.

MATERIALS AND METHODS

This retrospective study was initiated with the approval of our hospiral Ethics Committee (91 decision numbered and 18.04.2025 dated). Patients under 12 years of age who underwent surgery for displaced supracondylar humerus fractures between 2018 and 2024 were included. Open fractures, Gartland type I and II fractures, fractures with concomitant injuries, and cases requiring open reduction were excluded. Group 1 included patients who underwent lateral pinning, while Group 2 consisted of those treated with cross pinning.

Surgical procedure

Closed reduction was attempted in all patients, and if successful, percutaneous pinning was performed. In the lateral pinning group, two or three parallel or divergent K-wires were inserted through the lateral condyle, ensuring stability. In the crossed pinning group to all patients, after inserting two lateral K-wires, the elbow was extended to less than 45° to palpate the medial epicondyle and minimize the risk of ulnar nerve injury before placing the medial K-wire. Additionally, the ulnar nerve was palpated and pushed posteriorly to protect it. If the medial epicondyle could not be palpated due to edema, a stab incision was made to expose the medial epicondyle for K-wire placement. A mini medial incision was performed in 10 patients due to local edema obscuring anatomical landmarks (Figure 1).

Postoperative care and rehabilitation

All patients were immobilized with a long-arm brace postoperatively. Pin site dressings were performed every 2–3 days. At the 4th week, the brace was removed, and passive range of motion exercises were initiated. K-wires were removed once callus formation was observed, typically around the 6th week, and patients were referred to the physical therapy department for rehabilitation.

Functional and radiological evaluation

Demographic data, including age, sex, dominant hand, mechanism of injury, and follow-up duration, were recorded. At the final follow-up, range of motion and carrying angle were measured. Functional outcomes were assessed using Flynn's criteria, which include two factors: cosmetic and functional. Based on these criteria, patients were categorized as poor, fair, good, or excellent. Radiological evaluation included measurements of Baumann's angle and the lateral humerocapitellar angle (LHCA) on postoperative radiographs. Changes in these angles were assessed on follow-up radiographs at 6 months. Additionally, carrying angles were measured during the latest clinical follow-up. The carrying angle describes the angle between the axes of the arm and forearm in the coronal plane. The Baumann angle is the angle between the longitudinal axis of the humeral shaft and the physeal line of the lateral condyle on an anteroposterior (AP) radiograph of the elbow. The Lateral Capitellohumeral Angle (LCHA) is the angle between the longitudinal axis of the humeral shaft and the axis of the capitellum on a lateral elbow radiograph (Figure 2).

Statistical analysis

Statistical analysis was performed using IBM SPSS Statistics version 23.0 (Armonk, NY: IBM Corp.). We used the independent samples t-test to analyze continuous variables, including age, operative time, and radiographic angles (Baumann's angle, Lateral Humerocapitellar Angle (LHCA), and carrying angle). Normality was assessed using the Shapiro–Wilk test, and homogeneity of variances was evaluated with Levene's test. For categorical variables such as sex, dominant side, and mechanism of injury, we used the chi-square test, applying Yates' continuity correction for all 2×2 tables. Fisher's exact test was used for comparisons involving complications due to small expected frequencies. We also compared Flynn's functional scores between the groups using a Pearson's chi-square test on a 4×2 contingency table. Additionally, a post-hoc power analysis was conducted based on the difference in the LHCA between the groups. The observed mean difference was 3.7○ with a pooled standard deviation of 4.78○, which corresponds to a Cohen's d effect size of 0.776. This analysis indicated an achieved power of 83.9% at a significance level of $p<0.05$, confirming that we had sufficient power to detect meaningful differences. A p-value of less than 0.05 was considered statistically significant.

RESULTS

The study included 32 patients in Group 1 and 28 patients in Group 2. The mean age of the patients was 6.99±0.87 years, with a mean follow-up duration of 64.25±22.9 months. The most common mechanism of injury for the majority of patients in both groups was a fall from the same level. In Group 1, 28.1% of patients had a fracture on their dominant side, compared to 21.4% (6 patients) in Group 2. A comparison of demographic data revealed no significant differences between the groups (Table 1).

Functional and radiological outcomes

According to the Flynn's criteria, 24 patients in Group 1 and 20 patients in Group 2 achieved an excellent outcome, and no patient in either group was classified as having a poor outcome. There was no statistically significant difference in car-

https://doi.org/10.5455/annalsmedres.2025.06.143

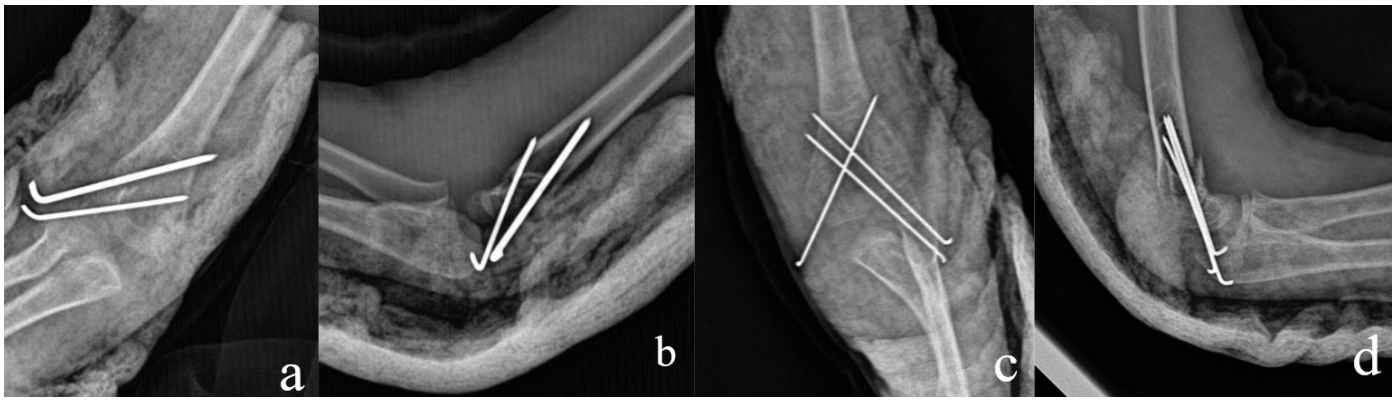

Figure 1. a) Lateral pinning at anteroposterior elbow graphy, b) Lateral pinning at lateral elbow graphy, c) Cross pinning at anteroposterior elbow graphy, d) Cross pinning at lateral graphy.

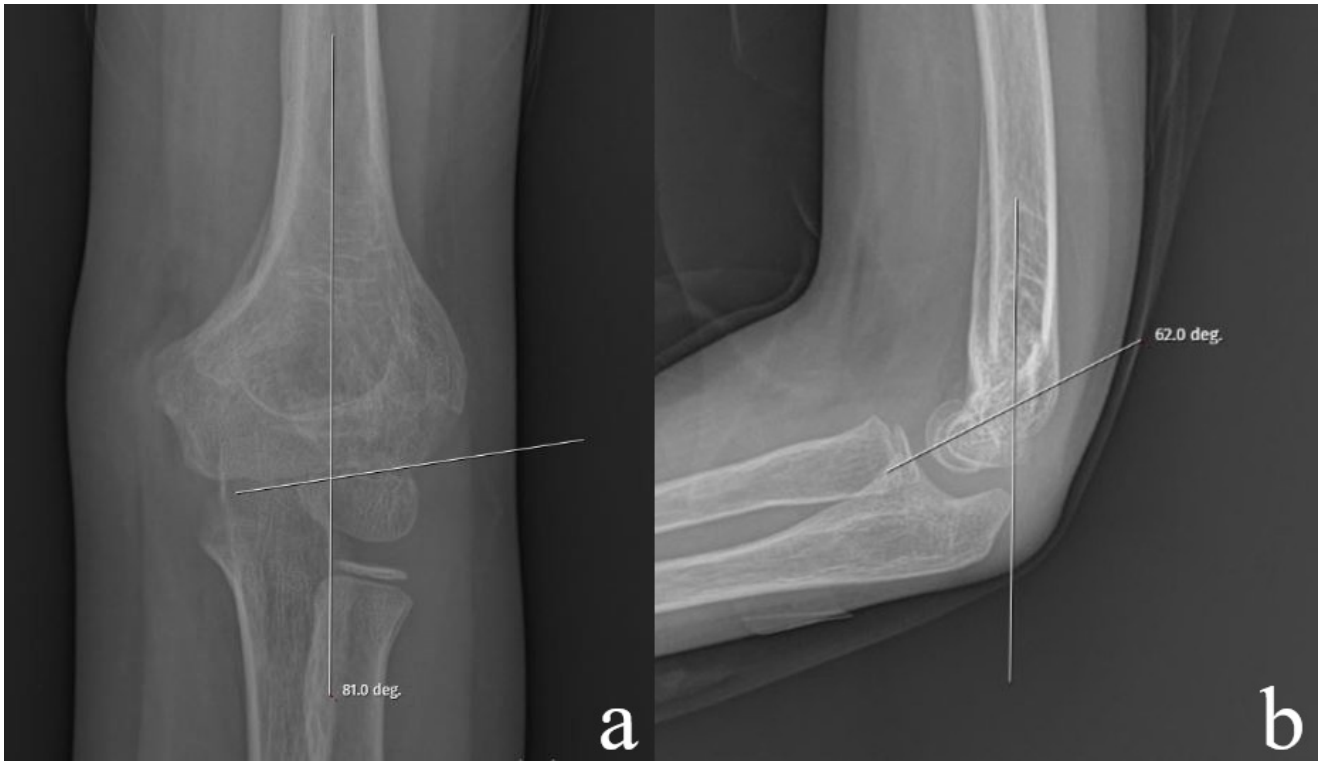

Figure 2. a) Baumann angle b) Lateral Capitellohumeral angle.

Table 1. Demographic data of the patients included in the study.

	Group 1 (n:32) (lateral pinning)	Group 2 (n:28) (cross pinning)	P value
Age	6.8 ± 0.9	7.2 ± 0.8	0.075
Follow-up (months)	35.25 ± 15.2	29 ± 17.1	0.134
Female/Male	12/20	9/19	0.871*
Dominant Side	9 (28.1%)	6 (21.4%)	0.765*
Falling from height	12 (37.5%)	9 (32.1%)	0.871*
Fall from the same level	20 (62.5%)	19 (67.9%)	0.871*

* Yates corrected chi-square.

rying angles between the two groups (p=0.246). Radiological comparisons showed that the mean Baumann's angle was 78±3.2○ in Group 1 and 78.6±3.1○ in Group 2. The mean Lateral Humerocapitellar Angle (LHCA) was 41.1±5.7○ in Group 1 and 44.8±3.6○in Group 2, a difference that was not statistically significant (p=0.179). At the 6-month follow-up, changes in both the Baumann's angle and LHCA were similar between the groups (p=0.607 and p=0.146, respectively) (Table 2).

Complications

No patient in either group experienced a nonunion. Pin-site infections occurred in three patients in the lateral pinning group and two patients in the cross-pinning group; all were successfully treated with local pin-site care. Ulnar nerve injury developed in two patients in Group 2 (the cross-pinning group), with complete recovery observed during follow-up. Both patients with ulnar nerve palsy had undergone closed medial pinning without a mini-incision (Table 1).

https://doi.org/10.5455/annalsmedres.2025.06.143

Table 2. Clinical and radiological comparison.

	Group 1 (n:32) (lateral)	Group 2 (n:28) (cross)	P value
Carrying angle	9.9 ± 2.4	9.2 ± 2.2	0.246
Baumann's angle	78 ± 3.2	78.6 ± 3.1	0.465
Change in Baumann's angle	2.0 ± 0.7	2.1 ± 0.8	0.607
LHCA	41.1 ± 5.7	44.8 ± 3.6	0.179
Change in LHCA	3.2 ± 0.9	3.6 ± 1.2	0.146
Union	32 (100%)	28 (100%)	1
Flynn's score			0.488
Excellent	24 (75%)	20 (71.4%)	
Good	5 (15.6%)	7 (25%)	
Fair	3 (9.4%)	1 (3.6%)	
Poor	0 (0.0%)	0 (0.0%)	
Complications			
-Ulnar nerve injury	0 (0.0%)	2 (7.1%)	0.214*
-Compartman syndrome	0 (0.0%)	0 (0.0%)	1*
-Infection	3 (9.4%)	2 (7.1%)	1*

*Fisher's exact test.

DISCUSSION

In our cohort, the majority of patients shared similar demographic characteristics and trauma mechanisms, which were primarily low-energy falls from the same level. This finding is consistent with previous reports highlighting the frequent occurrence of supracondylar humerus fractures in young children due to low-energy falls [7-9]. Most patients in both groups sustained fractures on their non-dominant side, and there was no significant difference in laterality between the groups. This finding aligns with prior studies that show no significant dominance-related difference in the distribution of these pediatric fractures.Functional outcome evaluations, using Flynn's criteria, revealed no significant difference between the two groups. The majority of patients in both groups achieved excellent results, reflecting the overall success of both surgical techniques. This is consistent with other studies reporting comparable functional outcomes with both methods despite their biomechanical differences [10, 11]. The absence of any patients with poor outcomes further supports the effectiveness of both techniques when applied appropriately.

The decision to use two or three lateral pins was based on an intraoperative assessment of fracture stability. In most cases, two divergent lateral pins provided sufficient fixation, especially when the medial cortex remained intact after reduction. However, a third lateral pin was inserted to enhance mechanical stability in fractures exhibiting medial comminution, rotational instability, or inadequate purchase with only two pins. This approach is supported by studies indicating that two properly placed lateral pins can offer comparable biomechanical strength to cross-pinning in certain fracture types [12,13]. Nevertheless, in unstable or high-grade Gartland type III fractures, additional fixation may be necessary to prevent loss of reduction. Therefore, the pin configuration should be customized based on the specific fracture pattern and intraoperative findings.

From a radiological standpoint, we found no significant differences in the Baumann angle or the Lateral Humerocapitellar Angle (LHCA) between the groups. The Baumann angle, a key measure for assessing distal humerus alignment, was similar in both groups and fell within the expected range for optimal alignment. Similarly, the LHCA, which evaluates the relationship between the humeral shaft and the capitellum, showed no significant difference at initial presentation or at the 6-month follow-up. Our results are consistent with a meta-analysis by Zhao et al., which found no difference in the Baumann angle between the two techniques [14]. Yawar et al. similarly reported that both the Baumann angle and LHCA were within normal limits and comparable between groups [15]. A meta-analysis by Na et al. also concluded that both techniques provided comparable radiological healing [16].

Our study's complication rates were low, with no instances of nonunion in either group. Pin-site infections were relatively uncommon and were successfully managed with local care, which is consistent with findings in the literature [17]. Ulnar nerve injury, a well-known concern with the medial pinning technique, was reported in two patients in the cross-pinning group. In both cases of transient ulnar nerve palsy, serial neurological assessments were performed at one, three, and six weeks postoperatively. Both patients achieved a full recovery by three months without the need for surgical intervention. Although patient compliance can be a concern in pediatric populations, clinical symptoms were clearly documented by both the surgical team and the parents, minimizing the risk of misclassification. Some authors suggest that exploration of the ulnar nerve may be warranted in cases of closed medial pinning if symptoms persist beyond 3 to 6 weeks [18]. However, in our experience, conservative observation is often sufficient for mild neurapraxia without motor deficits or worsening signs. Revision surgery, such as pin removal or repositioning, should be considered only when symptoms do not resolve or if clinical deterioration is observed.

The most notable finding from our study is the potential for a mini-incision over the medial epicondyle to reduce the risk of ulnar nerve injury during cross-pinning. This technique allows for better visualization of anatomical landmarks and should be considered in challenging cases with significant edema. Our findings support those of Umar Hasan et al., who recommended lateral pinning, noting the higher risk of ulnar nerve injury with cross-pinning despite similar functional outcomes [19]. Similarly, a meta-analysis by Xing et al. of 19 randomized controlled trials reported an increased incidence of ulnar nerve injury with cross-pinning [20]. The fact that no ulnar nerve injuries occurred in our lateral pinning group highlights a primary advantage of this technique.

Limitations

Our study has several limitations. First, it is a retrospective study, lacking both randomization and a large sample size. Additionally, the variation in the number of pins used be-

https://doi.org/10.5455/annalsmedres.2025.06.143

tween groups may have influenced mechanical stability and could potentially affect outcomes. Future prospective, randomized studies with larger patient cohorts are needed to confirm our findings.

CONCLUSION

Both lateral and cross-pinning techniques yield similar radiological and functional outcomes. To reduce the risk of ulnar nerve injury during cross-pinning, we recommend using a stab incision over the medial epicondyle.

Ethics Committee Approval: Ethical approval for this study was obtained from the University of Health Sciences Istanbul Training and Research Hospital Clinical Research Ethics Committee (approval number: 91 date: 19.04.2025).

Informed Consent: Written informed consent was obtained from the patient's parents for their anonymized information to be published in this article.

Peer-review: Externally peer-reviewed.

Conflict of Interest: The authors declare no conflicts of interes in this study.

Author Contributions: BA: Conception, Design, Analysis and Interpretation, Writing; SBT: Data collection, Writing, Analysis and interpretation; ASK: Conception, Materials, Data collection; AŞ: Writing- Literature Review, Supervision, Critical Review.

Financial Disclosure: The authors received no financial support for this article.

REFERENCES

1. Vuillermin C, May C, Kasser J. Closed Reduction and Percutaneous Pinning of Pediatric Supracondylar Humeral Fractures. *JBJS Essent Surg Tech.* 2018;8(2):e10. doi: 10.2106/JBJS.ST.16.00011.
2. Maccagnano G, Noia G, Coviello M, Stigliani C, Cassano GD. et al. Surgical strategies in pediatric supracondylar humeral fractures: our experience. *Acta Biomed.* 2023;94(S2):e2023170. doi: 10.23750/abm.v94iS2.13814.
3. Muslu O, Cengiz T, Aydın Şimşek Ş, Yurtbay A, Keskin D. Radiological and Clinical Outcomes of Pediatric Patients With a Supracondylar Humerus Fracture Surgically Treated With Closed Reduction and Percutaneous Pinning. *Cureus.* 2023;15(11):e49358. doi: 10.7759/cureus.49358.
4. Mahan ST, Miller PE, Park J, Sullivan N, Vuillermin C. Fully displaced pediatric supracondylar humerus fractures: Which ones need to go at night? *J Child Orthop.* 2022;16(5):355-365. doi: 10.1177/18632521221119540.
5. Graff C, Dounas GD, Sung J, Kumawat M, Huang Y, Todd M. Management of iatrogenic ulnar nerve palsies after cross pinning of pediatric supracondylar humerus fractures: A systematic review. *J Child Orthop.* 2022;16(5):366-373. doi: 10.1177/18632521221124632.
6. Vescio A, Carlisi G, Macrì VR, Sanzo F, Gigliotti G. et al. The Effect of Fracture Patterns, Pinning Configuration, Surgeon Experience and Subspecialty on Short-Term Radiological Outcomes of Pediatric Supracondylar Humeral Fractures Treated in the Prone Position: A Case-Series. *Healthcare (Basel).* 2023;11(19):2648. doi: 10.3390/healthcare11192648.
7. Kumar V, Singh A. Fracture Supracondylar Humerus: A Review. *J Clin Diagn Res.* 2016;10(12):RE01-RE06. doi: 10.7860/JCDR/2016/21647.8942.
8. Transtrum MB, Sanchez D, Griffith S, Godinez B, Singh V. et al. Predictors Associated with the Need for Open Reduction of Pediatric Supracondylar Humerus Fractures: A Meta-analysis of the Recent Literature. *JB JS Open Access.* 2024;9(3):e24.00011. doi: 10.2106/JBJS.OA.24.00011.
9. Bašković M, Pešorda D, Zaninović L, Hasandić D, Lohman Vuga K, Pogorelić Z. Management of Pediatric Elbow Fractures and Dislocations. *Children (Basel).* 2024;11(8):906. doi: 10.3390/children11080906.
10. Naik LG, Sharma GM, Badgire KS, Qureshi F, Waghchoure C, Jain V. Cross Pinning Versus Lateral Pinning in the Management of Type III Supracondylar Humerus Fractures in Children. *J Clin Diagn Res.* 2017;11(8):RC01-RC03. doi: 10.7860/JCDR/2017/28481.10351.
11. Radaideh AM, Rusan M, Obeidat O, Al-Nusair J, Albustami IS, Mohaidat ZM, Sunallah AW. Functional and radiological outcomes of different pin configuration for displaced pediatric supracondylar humeral fracture: A retrospective cohort study. *World J Orthop.* 2022;13(3):250-258. doi: 10.5312/wjo.v13.i3.250.
12. Zionts LE, McKellop HA, Hathaway R. Torsional strength of pin configurations used to fix supracondylar fractures of the humerus in children. *J Bone Joint Surg Am.* 1994;76(2):253-6. doi: 10.2106/00004623-199402000-00013.
13. Lee SS, Mahar AT, Miesen D, Newton PO. Displaced pediatric supracondylar humerus fractures: biomechanical analysis of percutaneous pinning techniques. *J Pediatr Orthop.* 2002;22(4):440-3. PMID: 12131437.
14. Zhao H, Xu S, Liu G, Zhao J, Wu S, Peng L. Comparison of lateral entry and crossed entry pinning for pediatric supracondylar humeral fractures: a meta-analysis of randomized controlled trials. *J Orthop Surg Res.* 2021;16(1):366. doi: 10.1186/s13018-021-02505-3.
15. Yawar B, Khan MN, Asim A, Qureshi A, Yawar A. et al. Comparison of Lateral and Crossed K-wires for Paediatric Supracondylar Fractures: A Retrospective Cohort Study. *Cureus.* 2022;14(7):e27267. doi: 10.7759/cureus.27267.
16. Na Y, Bai R, Zhao Z, Han C, Kong L. et al. Comparison of lateral entry with crossed entry pinning for pediatric supracondylar humeral fractures: a meta-analysis. *J Orthop Surg Res.* 2018;13(1):68. doi: 10.1186/s13018-018-0768-3.
17. Combs K, Frick S, Kiebzak G. Multicenter Study of Pin Site Infections and Skin Complications Following Pinning of Pediatric Supracondylar Humerus Fractures. *Cureus.* 2016;8(12):e911. doi: 10.7759/cureus.911.
18. Brauer CA, Lee BM, Bae DS, Waters PM, Kocher MS. A systematic review of medial and lateral entry pinning versus lateral entry pinning for supracondylar fractures of the humerus. *J Pediatr Orthop.* 2007(2):181-6. doi: 10.1097/bpo.0b013e3180316cf1.
19. Hasan SU, Pervez A, Usmani SUR, Tahseen MU, Asghar S. et al. Comparative analysis of pinning techniques for supracondylar humerus fractures in paediatrics: A systematic review and meta-analysis of randomized controlled trials. *J Orthop*. 2023;44:5-11. doi: 10.1016/j.jor.2023.08.005.
20. Xing B, Dong B, Che X. Medial-lateral versus lateral-only pinning fixation in children with displaced supracondylar humeral fractures: a meta-analysis of randomized controlled trials. *J Orthop Surg Res.* 2023;18(1):43. doi: 10.1186/s13018-023-03528-8.

https://doi.org/10.5455/annalsmedres.2025.06.143

Ann Med Res

Current issue list available at Ann Med Res

Annals of Medical Research

journal page: annalsmedres.org

Rim enhancement, drainage, and inflammatory response in patients with anterior versus posterior lingual abscesses

Kadir Sinasi Bulut [a,*], Fatih Gul [b], Ali Ozturk [a], Tuba Saadet Deveci Bulut [c], Burak Celik [a], Serkan Serifler [a], Mehmet Ali Babademez [a]

[a] Ankara Yıldırım Beyazıt University, Faculty of Medicine, Department of Otolaryngology, Head and Neck Surgery, Ankara, Türkiye
[b] Lokman Hekim University, Faculty of Medicine, Department of Otolaryngology, Head and Neck Surgery, Ankara, Türkiye
[c] Ankara City Hospital, Department of Biochemistry, Ankara, Türkiye
*Corresponding author: kadirsinasibulut@gmail.com (Kadir Sinasi Bulut)

MAIN POINTS

- Posterior lingual abscesses exhibited larger diameters (27.43±11.64 mm) and significantly longer hospital stays (9.29±1.89 days) than anterior abscesses.
- Surgical drainage markedly reduced WBC count by day 5 (9.31±2.59 vs 13.27±4.48, p=0.039) and shortened hospitalization (7.08±1.49 vs 10.00±1.82 days, p=0.005).
- Rim enhancement on contrast-enhanced computed tomography did not correlate with abscess size, inflammatory markers, or length of stay (p>0.05).
- S. agalactiae and other viridans streptococci predominated among cultured pathogens.
- Early, localization-specific, multidisciplinary management optimizes outcomes in lingual abscess patients.

Cite this article as: Bulut KS, Ozturk A, Deveci Bulut TS, Celik B, Serifler S, Babademez MA, Gul F. Rim enhancement, drainage, and inflammatory response in patients with anterior versus posterior lingual abscesses. *Ann Med Res*. 2025;32(11):486–492. doi: 10.5455/annalsmedres.2025.05.133.

ABSTRACT

Aim: Lingual abscesses are rare but potentially serious infections of the tongue, with limited data available in the literature. This study aimed to compare the clinical, radiological, and laboratory features of anterior and posterior lingual abscesses and evaluate the impact of drainage on patient outcomes.

Materials and Methods: This retrospective case series included 17 patients diagnosed with lingual abscess between February 2019 and March 2025. Patients were categorized based on anatomical localization (anterior vs. posterior). Demographic data, symptoms, laboratory values (WBC, CRP, etc), computed tomography findings, treatment modalities, and outcomes were analyzed. Subgroup comparisons were performed based on abscess location, drainage status, and rim enhancement.

Results: Of the 17 patients, 10 had anterior and 7 had posterior abscesses. Posterior abscesses were larger and associated with significantly longer hospital stays (p = 0.004). Drainage was associated with significantly shorter hospitalization (p = 0.005) and greater reduction in white blood cell counts by day 5 (p = 0.046). Rim enhancement on computed tomography was not significantly associated with clinical or laboratory outcomes. Streptococcus species were the most commonly isolated pathogens. No major complications or airway interventions were required.

Conclusion: Posterior lingual abscesses demonstrate a more severe clinical course than anterior abscesses. Surgical drainage is associated with improved inflammatory markers and faster clinical recovery. Rim enhancement alone may not reliably reflect disease severity. These findings support the importance of early diagnosis and individualized management based on anatomical location and clinical progression.

Keywords: Tongue disease, Abscess, Drainage, Mediators of inflammation

Received: May 26, 2025 **Accepted:** Aug 08, 2025 **Available Online:** Nov 25, 2025

INTRODUCTION

Lingual abscesses are infrequent but significant pathological conditions that primarily affect the parenchyma of the tongue and are typically of an infectious origin [1,2]. Research on lingual abscesses in the literature is exceedingly limited, predominantly comprising sporadically published case reports [2,3], with approximately 50 reports over the past three decades. This paucity of data has resulted in a significant gap in knowledge, leading to variability in diagnostic practices and lingual abscess treatment strategies. Although early diagnosis and appropriate treatment can reduce morbidity and mortality rates, the absence of comprehensive data on this condition complicates its clinical management [1].

Lingual abscesses are typically categorized into two primary types based on their anatomical location: anterior and posterior [1]. These distinct localizations contribute to consider-

able differences in clinical presentations, diagnostic methodologies, and therapeutic strategies [1,2]. In particular, the diagnosis of posterior lingual abscesses poses greater diagnostic challenges and is associated with a heightened risk of airway obstruction, often necessitating prompt medical intervention [4,5]. Anterior lingual abscesses are usually associated with trauma (e.g., biting or foreign bodies), whereas posterior abscesses more often result from underlying conditions, such as infected thyroglossal cysts or lingual tonsillitis. Poor oral hygiene, dental infections, immunosuppression, and chronic tobacco use are additional risk factors [1,2,6–8].

Accurate diagnosis requires detailed history, examination, and often contrast-enhanced CT, especially for posterior abscesses and deep neck involvement [5,8,9]. The management of lingual abscesses mainly focuses on securing the airway, performing abscess drainage, and administering appropriate antibiotic therapy [1,2,6]. Airway management is of paramount importance, especially in cases of posterior abscesses or in patients exhibiting respiratory distress [1,6]. Abscess drainage may be accomplished through surgical incision and drainage or needle aspiration, with broad-spectrum antibiotics being essential for effective treatment [1,5,6,10].

This study was designed to offer comprehensive data on the differentiation, prognosis, and management of lingual abscesses, addressing the limited information currently available in the literature. By filling existing gaps in the literature, the findings will contribute to the enhancement of management strategies for patients with lingual abscesses.

MATERIALS AND METHODS

Study population

The Institutional Scientific and Ethical Review Board approved this retrospective case series under approval number (TABED 2-25-1131). This single-center, observational study reviewed data from patients diagnosed with a lingual abscess between February 2019 and March 2025 at the ENT Department of a tertiary referral center.

Although the literature on lingual abscess is limited, the minimum required sample size for this study was determined based on previously published case series and systematic reviews. A large effect size (Cohen's d = 1.2) was assumed for comparisons between anterior and posterior groups. The sample size was calculated using a significance level (alpha) of 0.05 and a power (1-β) of 0.80. According to the power analysis conducted with G*Power software (version 3.1.9.6), at least 7 cases per group (a total of 14 cases) would be sufficient to detect a statistically significant difference between groups. The final study population included 17 patients, categorized into two groups based on anatomical localization: anterior lingual abscess (n = 10) and posterior lingual abscess (n = 7), thus meeting the required sample size. Written informed consent was obtained from all participants prior to their participation in the study.

Data collection and variables

Patient data, including demographic characteristics (age, gender, smoking history, and comorbidities), clinical presentation, radiological findings, laboratory results, microbiological culture data, treatment modalities, and clinical outcomes, were retrospectively retrieved from electronic medical records. Each case was categorized by abscess localization as either anterior or posterior lingual abscess. Anatomical distinction between anterior and posterior lingual abscesses was determined using the sulcus terminalis as the dividing line, with the foramen cecum at its apex serving as a reference point. Abscesses located anterior to the terminal sulcus were classified as anterior lingual abscesses, whereas those posterior to this anatomical landmark were classified as posterior lingual abscesses.

The assessed clinical variables included symptoms at presentation (e.g., sore throat, dysphagia, trismus, and dyspnea), hospitalization duration, and drainage status (performed vs not performed). Radiological parameters included the maximum abscess diameter and the presence or absence of rim enhancement on contrast-enhanced computed tomography.

Laboratory parameters, including white blood cell count (WBC), neutrophil count, lymphocyte count, large unstained cells (LUC), and C-reactive protein (CRP) levels, were evaluated on admission (day 0) and day 5 of hospitalization. All laboratory data were obtained using validated automated analyzers. Additionally, microbiological culture results from drained abscess material were recorded where available.

To identify differences in clinical course, laboratory trends, and outcomes, comparative analyses were performed between anterior and posterior lingual abscess groups, patients who underwent drainage and those who did not, and patients with and without rim enhancement on CT imaging.

Laboratory analysis

C-reactive protein (CRP) levels were measured using the Atellica CH C-reactive protein_2 (CRP_2) method on Siemens Atellica CI AutoAnalyzer systems via turbidimetric analysis. CBC results were obtained using the Siemens ADVIA 2120i hematology AutoAnalyzer systems.

Statistical analysis

Statistical analysis of the data obtained in the study was performed using IBM SPSS Statistics for Windows, Version 29.0 (IBM Corp., Armonk, NY, USA). Continuous variables were expressed as mean ± standard deviation (SD), whereas categorical variables were expressed as frequencies and percentages (%). The Shapiro-Wilk test was used to assess the normality of the distribution of continuous variables. For normally distributed data, the homogeneity of variances between groups was evaluated using Levene's test for equality of variances. If the variances were equal, the independent samples t-test was applied; otherwise, the results from the adjusted t-test were reported. Fisher's exact test was used to compare categorical

https://doi.org/10.5455/annalsmedres.2025.05.133

Table 1. Comparison of Demographic, Clinical, Radiological, and Treatment Characteristics Between Anterior and Posterior Lingual Abscess Groups.

		Anterior lingual abscess group (n=10)	Posterior lingual abscess group (n=7)	p value
Age, y (mean ± SD)		50.90 ± 7.85	54.71± 14.18	0.486
Sex, n (%)	Female	3 (30)	2 (28.5)	*ns*
	Male	7 (70)	5 (71.5)	
Smoking status, n (%)	Yes	9 (90)	4 (57.1)	0.250
	No	1 (10)	3 (42.9)	
Clinical presentation, n (%)	Neck pain	-	1 (14.2)	-
	Sore throat	8 (80)	6 (85.7)	-
	Odinophagia	6 (60)	5 (71.5)	-
	Dysphagia	9 (90)	7 (100)	-
	Fewer	1 (10)	1 (14.2)	-
	Dyspnea	1 (10)	1 (14.2)	-
	Trismus	-	2 (28.5)	-
	Neck swelling	-	1 (14.2)	-
	Restricted cervical mobility	-	1 (14.2)	-
Maximum diameter of abscess, mm (mean ± SD)		18.70 ± 8.82	27.43 ± 11.64	0.098
Length of stay, day (mean ± SD)		6.7 ± 1.25	9.29 ± 1.89	**0.004**
Result of drainage attempt, n (%)	Successful	8 (80)	5 (71.4)	*ns*
	Unsuccessful	2 (20)	2 (28.6)	
Amount of drainage, mL (mean ± SD)		2.50 ± 1.69	3.60± 2.88	0.399
Etiology, n (%)	Idiopathic	7 (70)	4 (57.1)	-
	Odontogenic	1 (10)	1 (14.2)	-
	Surgery/trauma	2 (20)	-	-
	Acute tonsillitis	-	1 (14.2)	-
	Epiglottitis	-	1 (14.2)	-

Ns: Non-Significant.

Table 2. Comparison of Radiological and Clinical Characteristics Between Drained and Non-Drained Lingual Abscess Groups.

	Non-drained lingual abscess group (n=4)	Drained lingual abscess group (n=13)	p value
Rim enhancement on CT, n (%)			
Presence	1(25)	9(69.2)	0.250
Absence	3(75)	4(30.8)	
Length of Stay, day (mean ± SD)	10.00 ± 1.82	7.08 ± 1.49	**0.005**
Maximum diameter of abscess, mm (mean ± SD)	14.75 ± 2.63	24.62 ± 11.21	**0.011**

variables. A p-value of <0.05 was considered statistically significant.

RESULTS

Demographic findings

A total of 17 patients were included in this study. Of these, 10 (58.8%) and 7 (41.2%) patients were categorized in the anterior and posterior lingual abscess groups, respectively. There was no statistically significant difference in the mean age between the anterior and posterior groups (50.90 ± 7.85 years vs. 54.71 ± 14.18 years, respectively, p=0.486). Gender distribution was similar between the groups, with 30% females and 70% males in the anterior group and 28.5% females and 71.5% males in the posterior group (p=1.000). Although smoking was more prevalent in the anterior group (90% vs. 57.1%), the difference was not statistically significant (p = 0.25) (Table 1).

Clinical findings

The most common presenting symptoms in both groups were sore throat (80% in the anterior group and 85.7% in the posterior group) and dysphagia (90% and 100%, respectively). Additional clinical features such as trismus (28.5%), neck swelling (14.2%), and limited cervical motion (14.2%) were more frequently observed in the posterior group than in the anterior group (Table 1).

Radiological findings

The posterior group had a larger average abscess diameter (27.43 ± 11.64 mm) than the anterior group (18.70 ± 8.82 mm), although this difference was not statistically significant (p=0.098). On contrast-enhanced computed tomography, rim enhancement was more frequently observed in the drained abscess group (69.2%) than in the non-drained abscess group (25%), but this difference was not statistically sig-

https://doi.org/10.5455/annalsmedres.2025.05.133

Table 3. Admission (d0) and Day 5 (d5) Laboratory Results of Lingual Abscesses by Anterior and Posterior Locations, Rim Enhancement Presence, and Drainage Status.

	Anterior lingual abscess group (n=10) mean ± SD	Posterior lingual abscess group (n=7) mean ± SD	p value
WBC $_{(d0)}$	12.60 ± 2.01	15.42 ± 4.16	0.136
WBC $_{(d5)}$	8.88 ± 3.16	12.20 ± 2.97	**0.046**
Neutrophile $_{(d0)}$	9.57 ± 2.41	12.20 ± 4.89	0.226
Neutrophile $_{(d5)}$	5.17 ± 3.07	8.53 ± 3.40	0,051
Lymphocyte $_{(d0)}$	2.12 ± 0.85	2.08 ± 0.83	0.93
Lymphocyte $_{(d5)}$	2.71 ± 0.95	2.82 ± 1.48	0.855
LUC $_{(d0)}$	0.13 ± 0.054	0.17 ± 0.081	0.242
LUC $_{(d5)}$	0.16 ± 0.03	0.16 ± 0.05	0.976
CRP $_{(d0)}$	39.89 ± 21.52	74.93 ± 47.89	0.105
CRP $_{(d5)}$	13.25 ± 8.65	25.58 ± 21.13	0.115
	Rim enhancement presence on CT (n=11) mean ± SD	Rim enhancement absence on CT (n=6) mean ± SD	p value
WBC $_{(d0)}$	13.37 ± 3.21	14.47 ± 3.62	0.528
WBC $_{(d5)}$	9.78 ± 3.19	11.10 ± 3.98	0.465
Neutrophile $_{(d0)}$	10.23 ± 3.50	11.44 ± 4.39	0.542
Neutrophile $_{(d5)}$	5.85 ± 2.97	7.84 ± 4.40	0.283
Lymphocyte $_{(d0)}$	2.09 ± 0.83	2.11 ± 0.87	0.962
Lymphocyte $_{(d5)}$	2.92 ± 1.35	2.46± 0.68	0.362
LUC $_{(d0)}$	0.14 ± 0.063	0.15 ± 0.079	0.755
LUC $_{(d5)}$	0.17 ± 0.047	0.13 ± 0.029	**0.046**
CRP $_{(d0)}$	63.24 ± 42.05	37.95 ± 12.42	0.176
CRP $_{(d5)}$	18.18 ± 18.16	18.60 ± 11.64	0.960
	Non-drained lingual abscess group (n=4) mean ± SD	Drained lingual abscess group (n=13) mean ± SD	p value
WBC $_{(d0)}$	14.63 ± 3.14	12.65 ± 4.29	0.411
WBC $_{(d5)}$	13.27 ± 4.48	9.31 ± 2.59	**0.039**
Neutrophile $_{(d0)}$	11.90 ± 3.49	9.43 ± 4.54	0.337
Neutrophile $_{(d5)}$	10.19 ± 4.81	5.43 ± 2.27	0.141
Lymphocyte $_{(d0)}$	1.72 ± 0.77	2.22 ± 0.82	0.308
Lymphocyte $_{(d5)}$	1.93 ± 0.54	3.01 ± 1.18	0.103
LUC $_{(d0)}$	0.13 ± 0.054	0.17 ± 0.081	0.921
LUC $_{(d5)}$	0.16 ± 0.06	0.16 ± 0.04	0.894
CRP $_{(d0)}$	44.57 ± 45.36	49.62 ± 40.89	0.835
CRP $_{(d5)}$	19.12 ± 30.64	13.47 ± 10.77	0.564

Abbreviations: WBC, White Blood Cell; LUC, Large Unstained Cells; CRP, C-reactive protein;CT Computer Tomography. The units of the WBC, Neutrophil, Lymphocyte, and LUC parameters are $x10^9$/L, and the unit of CRP is mg/L.

Table 4. Difference in Laboratory Results of Lingual Abscesses by Anterior and Posterior Locations, Rim Enhancement Presence, and Drainage Status Between Admission (d0) and Day 5 (d5).

	Difference WBC $_{(d0\text{-}d5)}$ mean ± SD	p value	Difference Neutrophile $_{(d0\text{-}d5)}$ mean ± SD	p value	Difference CRP $_{(d0\text{-}d5)}$ mean ± SD	p value
Anterior lingual abcess group (n=10) Posterior lingual abcess group (n=7)	3.72 ± 2.13 3.22 ± 3.96	0.369	3.45 ± 2.39 3.39 ± 5.29	0.489	22.6 ± 16.5 39.4 ± 49.9	0.211
Non-drained lingual abscess group (n=4) Drained lingual abscess group (n=13)	1.36 ± 1.48 4.18 ± 2.96	**0.046**	2.34 ± 3.36 3.76 ± 3.87	0.259	15.4 ± 19.10 33.84 ± 39.97	0.18
Rim enhancement presence on CT (n=11) Rim enhancement absence on CT (n=6)	3.59 ± 2.92 3.37 ± 3.17	0.886	3.01 ± 3.19 4.18 ± 4.72	0.550	38.66 ± 37.42 12.75 ± 19.60	0.138

Abbreviations: WBC, White Blood Cell; CRP, C-reactive protein; CT Computer Tomography. The units of the WBC, Neutrophil, Lymphocyte, and LUC parameters are $x10^9$/L, and the unit of CRP is mg/L.

nificant (p=0.25). When rim enhancement was evaluated in relation to clinical parameters, the mean length of hospital stay was 7.36 ± 1.80 days in rim enhancement-positive patients and 8.50 ± 2.25 days in rim enhancement-negative patients, without a statistically significant difference (p=0.273). Similarly, the maximum abscess diameter was comparable between rim enhancement-positive and -negative patients (22.18 ± 10.36 mm vs. 22.50 ± 12.27 mm, p=0.576) (Table 2) (Figure 1). In one patient, both pre- and posttreatment contrast-enhanced CT images were available, demon-

https://doi.org/10.5455/annalsmedres.2025.05.133

Table 5. Microbial culture results in lingual abscess cases.

Pathogens observed in cases of lingual abscesses	n (%)
No proliferation	4 (23.5)
No culture	4 (23.5)
S. Agalactia	2 (11.7)
S. Anginosus	1 (5.8)
S. Constellatus	1 (5.8)
S. Hominis	1 (5.8)
S. Mitis-S. Oralis	1 (5.8)
S. Salivarius	1 (5.8)
S. Pneumoniae	1 (5.8)
S. Intermedius	1 (5.8)

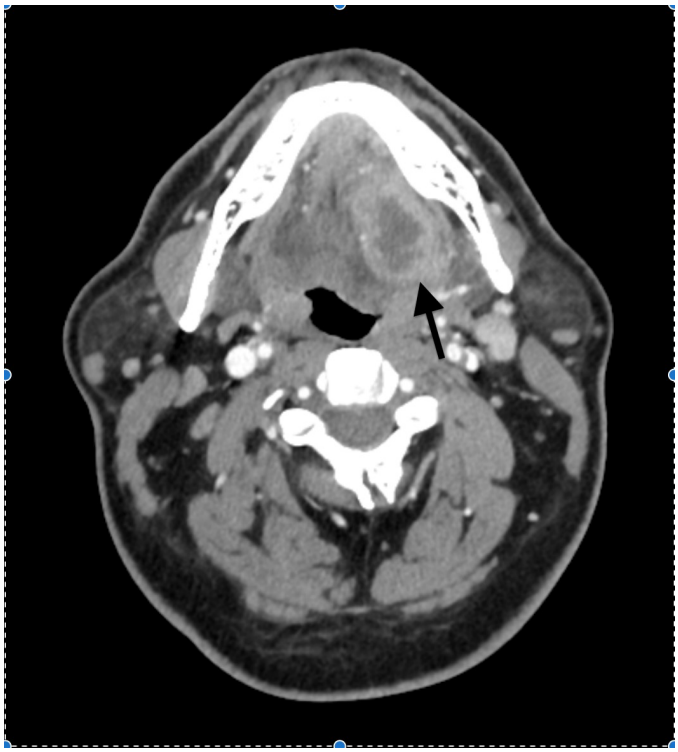

Figure 1. A contrast-enhanced axial computed tomography image showing a tongue abscess (arrow) characterized by a hypodense lesion with peripheral rim enhancement on the tongue.

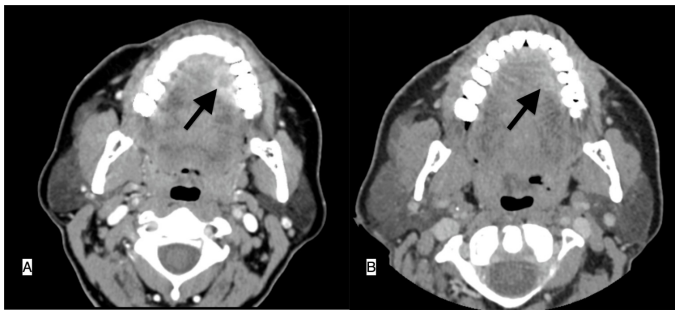

Figure 2. (A) Contrast-enhanced axial computed tomography image obtained before treatment shows a hypodense abscess with enhancement of the peripheral rim of the tongue (arrow). (B) Axial CT demonstrates near-complete resolution of the abscess on the ninth day after drainage (arrow).

strating marked abscess resolution following surgical drainage (Figure 2).

Clinical course and treatment

Patients with posterior lingual abscess had a significantly longer hospital stay (9.29 ± 1.89 days vs. 6.7 ± 1.25 days, p=0.004). Drainage was attempted with similar success rates in both groups (anterior group, 80%; posterior group, 71.4%; p = 1.000). Patients who underwent drainage had significantly larger mean abscess diameters than those who did not (24.62 ± 11.21 mm vs. 14.75 ± 2.63 mm, p=0.011). Additionally, the length of hospital stay was significantly shorter in patients who underwent drainage than in those who did not (7.08 ± 1.49 days vs. 10.00 ± 1.82 days, p = 0.005). Although the mean volume of drained abscess material was higher in the posterior group (3.60 ± 2.88 mL vs. 2.50 ± 1.69 mL), the difference was not statistically significant (p =0.399) (Table 1).

Etiological findings

The most common etiology of the abscess was idiopathic in both groups (70% in the anterior group, 57.1% in the posterior group). While infectious causes, such as acute tonsillitis and epiglottitis, were more common in the posterior group, trauma and odontogenic infections were more frequently identified in the anterior group (Table 1).

Laboratory findings

Comparison between anterior and posterior lingual abscess groups

White blood cell (WBC) and neutrophil counts at admission (day 0) were higher in the posterior group than in the anterior group (WBC: 15.42 ± 4.16 vs. 12.60 ± 2.01, p=0.136; neutrophils: 12.20 ± 4.89 vs. 9.57 ± 2.41, p=0.226), but these differences were not statistically significant. On day 5, however, the posterior group had significantly higher WBC counts (12.20 ± 2.97 vs. 8.88 ± 3.16, p=0.046). Although the neutrophil counts also showed an increasing trend in the posterior group, the statistical significance was marginal (p=0.051). Lymphocyte and large unstained cell (LUC) counts were similar between the groups (p>0.05). CRP levels were higher in the posterior group on days 0 and 5 (CRP day 0: 74.93 ± 47.89 vs. 39.89 ± 21.52, p=0.105), but these differences were not statistically significant (Table 3).

Comparison between patients with and without rim enhancement

When patients with rim enhancement on CT were compared with those without, no statistically significant differences in WBC, neutrophil, or CRP levels were observed on either day 0 or day 5 (p>0.05). However, day 5 LUC values were significantly lower in patients without rim enhancement (rim enhancement present: 0.17 ± 0.047, absent: 0.13 ± 0.029, p=0.046) (Table 3).

Comparison between patients with and without drainage

On day 5, WBC counts were significantly lower in patients who underwent drainage (9.31 ± 2.59 vs. 13.27 ± 4.48,

https://doi.org/10.5455/annalsmedres.2025.05.133

p=0.039). There were no statistically significant differences in other laboratory parameters (neutrophils, lymphocytes, LUC, CRP) between patients who did and did not undergo drainage (p>0.05) (Table 3).

Changes in laboratory parameters (Comparison between days 0 and 5)

When comparing changes in WBC, neutrophil, and CRP levels between the anterior and posterior groups from day 0 to day 5, no statistically significant differences were observed (p>0.05). However, a significant difference was observed in the change in WBC levels between patients who underwent drainage and those who did not. The reduction in WBC count was more pronounced in patients who underwent drainage (4.18 ± 2.96 vs. 1.36 ± 1.48, p=0.046). No significant differences in neutrophil or CRP changes were observed between the groups.

No significant differences were observed in laboratory parameter changes based on the presence of rim enhancement (Table 4).

Microbiological culture results

According to the microbiological culture results from the abscess material, 23.5% of the samples showed no growth, and cultures were not obtained in another 23.5% of cases.

Among the positive cultures, S. agalactiae was the most frequently isolated pathogen (11.7%). Other Streptococcus species, including Streptococcus anginosus, Streptococcus constellatus, Streptococcus hominis, Streptococcus mitis/oralis, Streptococcus salivarius, Streptococcus pneumoniae, and Streptococcus intermedius, were isolated in 5.8% of samples (Table 5).

DISCUSSION

This study comprehensively evaluated the clinical, radiological, and laboratory characteristics of lingual abscesses according to their anterior and posterior localizations, the impact of drainage procedures on clinical outcomes, and the distribution of microbiological pathogens. Our findings demonstrated that lingual abscesses exhibit different clinical courses based on their anatomical localization, directly influencing clinical decision-making and management strategies.

Posterior lingual abscesses had larger dimensions and significantly longer hospital stays than anterior abscesses. The anatomical proximity to the base of the tongue renders posterior abscesses particularly hazardous regarding potential airway obstruction, thus necessitating prioritized clinical intervention. This observation aligns with reports in the literature from various case studies and small patient series [6]. Buendia et al reported that patients with posterior lingual abscesses frequently required emergent intubation and experienced delays in diagnosis. Our study objectively addresses these clinical risks, demonstrating significantly larger abscess diameters and extended hospital stays in the posterior group than in the anterior group.

The significant decrease in WBC levels observed in patients undergoing drainage suggests rapid suppression of the systemic inflammatory response following the removal of infected material. Additionally, the notably shorter hospital stay in patients who underwent drainage indicates that drainage positively impacts not only laboratory parameters but also clinical recovery. This finding closely corresponds with Brook's (2004) concept of "early recovery through source control" [11,12]. Numerous studies have highlighted the critical role of early drainage in the successful management of head and neck infections [13,14].

Our study revealed that the presence of rim enhancement on contrast-enhanced CT scans, although commonly used to support abscess diagnosis, did not show a significant correlation with clinical severity or improvement in inflammatory laboratory markers. This suggests that rim enhancement may reflect the abscess' morphological features without necessarily indicating its clinical behavior or prognosis. In contrast, Liu et al. demonstrated that rim enhancement was significantly associated with positive surgical drainage in pediatric retropharygeal abscess, emphasizing its potential role as a radiologic predictor of purulence rather than systemic severity. These differing findings may reflect anatomical and pathological distinctions between lingual and retropharyngeal abscesses and underscore the need for disease-specific imaging criteria in abscess evaluation [11].

The microbiological culture results revealed no microbial growth in 23.5% of the samples, whereas cultures were not obtained in another 23.5%. Among the positive cultures, Streptococcus agalactiae and other viridans group streptococci (e.g., S. mitis, S. oralis, and S. salivarius) were the most frequently isolated pathogens. This distribution suggests that lingual abscesses are predominantly derived from the oral flora. Brook (2002) highlighted streptococci and anaerobic bacteria as common causative agents in lingual and adjacent tissue abscesses, recommending beta-lactam/lactamase inhibitor combinations and agents such as clindamycin for empirical therapy [12]. Our inability to employ anaerobic culture techniques represents a limitation; however, even the aerobic flora data provide valuable guidance for treatment planning.

The multidisciplinary approach is especially crucial in cases of posterior lingual abscess, which may present with nonspecific symptoms and are often difficult to detect on physical examination alone. Early collaboration between otolaryngologists, anesthesiologists, and radiologists facilitates timely diagnosis and safe management of patients with cancer. Advanced imaging and endoscopic assessment are essential in guiding drainage procedures in the clinical setting, minimizing complications, and optimizing patient outcomes.

https://doi.org/10.5455/annalsmedres.2025.05.133

Limitations

This study is presented as a retrospective case series due to the rare nature of lingual abscesses and the small sample size. The statistical power for subgroup analyses is limited, and the clinical significance of subgroup comparisons should be interpreted with caution. The retrospective and single-center design further restricts the generalizability of our results. Although our findings provide valuable insights into the clinical course and management of lingual abscesses, larger prospective multicenter studies are needed to confirm these observations and better define the clinical relevance of subgroup differences.

CONCLUSION

In conclusion, a multidisciplinary approach is essential for the diagnosis and management of lingual abscess. In cases with posterior localization, airway monitoring must be prioritized, and urgent drainage and imaging support should be provided when necessary. Drainage procedures significantly reduce the inflammatory response and shorten hospital stays. Although radiological findings, such as rim enhancement, can support diagnosis, clinical and laboratory data should primarily guide treatment decisions. Detailed microbiological analysis is crucial for targeted antibiotic therapy. Considering the limited data available in the literature, advanced prospective and multicenter studies on lingual abscess are warranted.

Ethics Committee Approval: This retrospective cohort study was approved by the Ankara Bilkent City Hospital No. 2 Medical Research Scientific and Ethical Evaluation Board under approval number (TABED 2-25-1131).

Informed Consent: Informed consent was obtained from all participants.

Peer-review: Externally peer-reviewed.

Conflict of Interest: The authors declare no conflict of interest.

Author Contributions: Conception: KSB, AO; Design: KSB, AO, FG; Supervision: TSDB, MAB; Materials: TSDB, BC; Data Collection and/or Processing: SS, FG, BC, AO; Analysis and/or Interpretation: KSB, FG; Literature Review: KSB, MAB, BC; Writing: KSB, TSDB, SS; Critical Review: SS, MAB.

Financial Disclosure: This study was not funded by any specific grants from public, commercial, or non-profit funding agencies.

REFERENCES

1. Srivanitchapoom C, Yata K. Lingual Abscess: Predisposing Factors, Pathophysiology, Clinical Manifestations, Diagnosis, and Management. *Int J Otolaryngol.* 2018;2018:4504270. doi: 10.1155/2018/4504270.
2. Safia A, Shehadeh R, Merchavy S. Anterolateral Lingual Abscess in a Young Adult: A Comprehensive Case Study. *Ear Nose Throat J.* 2024:1455613241233922. doi: 10.1177/01455613241233922.
3. Pallagatti S, Sheikh S, Kaur A, Puri N, Singh R, Arya S. Tongue abscess: a rare clinical entity. *J Investig Clin Dent*. 2012;3(3):240-3. doi: 10.1111/j.2041-1626.2011.00101.x.
4. Antoniades K, Hadjipetrou L, Antoniades V. Acute tongue abscess. Report of three cases. *Oral Surg.* 2004;97(5):570-573. doi: 10.1016/j.tripleo.2003.11.011.
5. Vellin JF, Crestani S, Saroul N, Bivahagumye L, Gabrillargues J, Gilain L. Acute abscess of the base of the tongue: a rare but important emergency. *J Emerg Med.* 2011;41(5):e107-10. doi: 10.1016/j.jemermed.2008.04.047.
6. Saro-Buendía M, Urquiza PS, González JA, Navarro MJL, Mazón M, Carceller MA. Posterior Lingual Abscess: A Case Report. *Arch Acad Emerg Med.* 2023;11(1):e18. doi: 10.22037/aaem.v11i1.1860.
7. Sands M, Pepe J, Brown RB. Tongue Abscess: Case Report and Review. *Clin Infect Dis.* 1993;16(1):133-5. doi: 10.1093/clinids/16.1.133.
8. Bekele K, Markos D. Lingual abscess: A case report. *Int Med Case Rep J.* 2017;10:285-287. doi: 10.2147/IMCRJ.S140255.
9. Sánchez Barrueco Á, Melchor Díaz MA, Huerta IJ, Juncos JMM, Álvarez CA. Recurrent lingual abscess. *Acta Otorrinolaringol Esp.* 2012;63(4):318-320. doi: 10.1016/j.otoeng.2011.01.007.
10. Balatsouras DG, Eilopoulos PN, Kaberos AC. Lingual abscess: diagnosis and treatment. *Head Neck.* 2004;26(6):550-4. doi: 10.1002/hed.20018.
11. Liu Y, Nicotera DJ, Islam AA, Dunsky K, Lieu JEC. Prognostic Factors for Retropharyngeal Abscess in Children undergoing Surgery or Antibiotic Therapy. *Laryngoscope.* 2024;134(4):1955-1960. doi: 10.1002/lary.31064.
12. Brook I. Microbiology and management of peritonsillar, retropharyngeal, and parapharyngeal abscesses. *J Oral Maxillofac Surg.* 2004;62(12):1545-50. doi: 10.1016/j.joms.2003.12.043.
13. Wang LF, Kuo WR, Tsai SM, Huang KJ. Characterization of life-threatening deep cervical space infections: A review of one hundred ninety-six cases. *Am J Otolaryngol.* 2003;24(2):111-7. doi: 10.1053/ajot.2003.31.
14. Huang TT, Liu TC, Chen PR, Tseng FY, et al. Deep neck infection: Analysis of 185 patients. *Head Neck.* 2004;26(10):854-60. doi: 10.1002/hed.20014.

Ann Med Res

Current issue list available at Ann Med Res

Annals of Medical Research

journal page: annalsmedres.org

Diagnostic and prognostic utility of systemic inflammation indices in cervical dysplasia

Yagmur Soykan [a,b,*], Ahmet Elturk [c], Cennet Meltem Alaybeyoglu [c]

[a] Yuksek Ihtisas Hospital, Department of Obstetrics and Gynecology, Division of Gynecologic Oncology, Kırıkkale, Türkiye
[b] Gazi University, Faculty of Medicine, Department of Medical Biology and Genetics, Ankara, Türkiye
[c] Cengiz Gokcek Women's and Children's Hospital, Department of Obstetrics and Gynecology, Gaziantep, Türkiye
*Corresponding author: dryagmursoykan@gmail.com (Yagmur Soykan)

MAIN POINTS

- In a cohort with chronic cervicitis, LSIL, and HSIL, CBC-derived indices (SII, NLR, PLR) showed no significant differences across grades, limiting their diagnostic/grading utility.
- Multivariable logistic regression indicated modest inverse associations: each unit increase in lymphocyte count and PLR reduced HSIL odds by 0.2% and 2.5%, respectively.
- High-risk HPV genotypes (16/18) were significantly more frequent in HSIL than in LSIL/chronic cervicitis.
- These findings suggest that systemic inflammation indices alone have limited prognostic value, whereas HPV genotyping remains more clinically informative.

Cite this article as: Soykan Y, Elturk A, Alaybeyoglu CM. Diagnostic and prognostic utility of systemic inflammation indices in cervical dysplasia. *Ann Med Res*. 2025;32(11):493--498. doi: 10.5455/annalsmedres.2025.05.117.

ABSTRACT

Aim: This study investigated the diagnostic and prognostic potential of the Systemic Immune-Inflammation Index (SII), Neutrophil-Lymphocyte Ratio (NLR), and Platelet-Lymphocyte Ratio (PLR) in cervical dysplasia, evaluating their correlation with disease presence and severity for potential clinical applications in risk assessment and patient management.

Materials and Methods: In this retrospective study, the SII, NLR, and PLR values were analyzed using parameters obtained from the routine complete blood count of 215 patients whose cervical dysplasia grades were evaluated through colposcopic biopsy.

Results: HPV DNA types 16 and 18 were detected in 114 (53.0%) of 215 patients, while 101 (47.0%) tested positive for non-16/18 hr-HPV DNA types. No statistically significant differences were observed in WBC, neutrophil, platelet, lymphocyte, SII, NLR, and PLR values across the chronic cervicitis, LSIL (low-grade squamous intraepithelial lesion), and HSIL (high-grade squamous intraepithelial lesion) groups ($p < 0.05$). However, logistic regression analysis for HSIL risk identified lymphocyte count (OR = 0.998) and PLR (OR = 0.975) as significant predictors, where a one-unit increase in each was associated with a 0.2% and 2.5% decrease in the odds of HSIL, respectively.

Conclusion: SII, NLR, and PLR values in diagnosing or grading the presence or severity of cervical dysplasia, indicating that these systemic inflammatory markers alone may have limited value as diagnostic or prognostic tools. Further validation through larger prospective studies is warranted to more comprehensively elucidate the role of these markers.

Keywords: Systemic immune-inflammation index (SII), Platelet-lymphocyte ratio, Neutrophil-lymphocyte ratio, Complete blood count, Cervical intraepithelial neoplasia

Received: May 20, 2025 **Accepted:** Aug 18, 2025 **Available Online:** Nov 25, 2025

INTRODUCTION

Cervical cancer is the fourth most common cancer among women worldwide [1]. Globally, it remains a significant cause of mortality, accounting for over 300,000 female deaths annually [2]. Infection with Human Papilloma Virus (HPV) is implicated in approximately 99% of cervical cancer cases [3]. The development of most of these cancers is attributed to persistent infection with high-risk HPV genotypes, including HPV 16, 18, 31, 33, 35, 39, 45, 51, 52, 56, 58, 59, and 66 [4]. HPV types 16 and 18 are responsible for over 70% of cervical cancer diagnoses [4]. While the majority (approximately 90%) of HPV infections undergo spontaneous regression within 1-3 years [3], persistent infection, facilitated by viral integration into the host cell genome and mechanisms that evade immune surveillance, can lead to the progression of cervical lesions from preneoplastic conditions (CIN2-3) to invasive cervical carcinoma. Approximately 10% of women with HPV infection exhibit signs of oncogenic transformation of the cervix [5].

The crucial role of the local immune response to HPV infection in the pathogenesis of cervical intraepithelial neoplasia

(CIN) lesions has long been recognized [6]. The binding of the major L1 capsid protein to heparan sulfate proteoglycans on the keratinocyte surface initiates HPV entry into host cells [7]. The early viral genes, particularly E6 and E7, are expressed following cellular entry. These oncoproteins target and inactivate the tumor suppressor proteins p53 and pRb [8], leading to cell cycle dysregulation. In hr-HPV infections, viral DNA often integrates into the host genome, disrupting the E2 gene and overexpressing E6 and E7 oncoproteins [9]. This genomic instability contributes to the accumulation of cellular abnormalities that progress through stages of precancerous lesions: CIN1 (mild dysplasia), CIN2 (moderate dysplasia), and CIN3 (severe dysplasia/carcinoma in situ). According to the Lower Anogenital Squamous Terminology (LAST) classification, CIN1 is categorized as a low-grade squamous intraepithelial lesion (LSIL), whereas CIN2 and CIN3 are classified as high-grade squamous intraepithelial lesions (HSIL) [10,11]. Despite extensive research into the dynamics of CIN regression, persistence, and progression, morphologic assessment alone cannot reliably predict the clinical outcome of these lesions.

Emerging evidence strongly suggests that systemic inflammation may also play a significant role in CIN pathogenesis and progression [12]. Systemic inflammation is increasingly recognized as a key factor in various chronic diseases, including the development of precancerous lesions and their progression to cancer. The potential of chronic inflammation to drive carcinogenesis is a widely accepted concept; however, sustained inflammatory processes may be critical in malignant transformation and tumor development [13].

The number of inflammatory cells and platelets in the systemic circulation and indices derived from their ratios are considered important indicators of the systemic immune response to cancer [14]. Studies have indicated that the Systemic Immune-Inflammation Index (SII), Neutrophil-to-Lymphocyte Ratio (NLR), and Platelet-to-Lymphocyte Ratio (PLR) are associated with poor prognosis in various solid tumors and correlate with tumor size, stage, and lymph node metastasis [15].

However, the current data regarding the association between systemic inflammation and CIN lesions are inconsistent, necessitating further investigation. This study was based on the hypothesis that changes in systemic inflammatory markers—specifically the SII, NLR, and PLR—reflect the progression of CIN; therefore, these indices could serve as accessible and cost-effective tools for distinguishing between grades of cervical dysplasia.

MATERIALS AND METHODS

This retrospective, observational, cross-sectional study enrolled 215 patients who underwent colposcopic biopsy at Cengiz Gokçek Obstetrics and Gynecology Hospital and Kırıkkale Yuksek Ihtisas Hospital between February 2022 and October 2024. The study protocol received ethical approval from the Ethics Committee of Kırıkkale University (decision date: 2025.03.12, decision number: 2025.03.07). This study was conducted and reported in accordance with the STROBE guidelines for cross-sectional studies.

The study included women aged 30–65 years who had an indication for colposcopic examination based on abnormal PAP smear (Thin-prep) screening results or positive high-risk HPV DNA (HC2; Qiagen, Hilden, Germany) test results. Colposcopy-guided biopsies were classified as either HSIL or LSIL according to the LAST criteria [10]. The study groups were established based on the pathological findings: patients with chronic cervicitis (n = 98), patients with CIN 1 biopsy results (LSIL, n = 63), and patients with CIN 2 and 3 biopsy results (HSIL, n = 54). Routine blood samples were collected on the biopsy day. Participants were managed according to the American Society for Colposcopy and Cervical Pathology guidelines [16], with follow-up or surgical intervention determined by the colposcopic biopsy results. All accessible and eligible patient records within the study period were analyzed.

Exclusion criteria encompassed patients with acute and chronic inflammatory diseases, hematologic disorders, a history of cancer, prior radiotherapy or chemotherapy, the use of anti-inflammatory, immunosuppressive, or anticoagulant agents, and other sexually transmitted infections .

Hematological indices were calculated from complete blood count data. The NLR was calculated by dividing the absolute neutrophil count by the absolute lymphocyte count. The PLR was calculated by dividing the absolute platelet count by the absolute lymphocyte count. The SII was calculated using the following formula: (platelet count × neutrophil count) / lymphocyte count.

Statistical analysis

Statistical analyses were performed using the IBM SPSS Statistics, Version 27.0 (IBM Corp., Armonk, NY, USA) package program. Descriptive statistics were presented as mean ± standard deviation (SD) or median with interquartile range (IQR), depending on data distribution. The normality of distribution was assessed using visual inspection and the Shapiro–Wilk test.

For normally distributed continuous variables with homogeneity of variance (tested by Levene's test), one-way analysis of variance (ANOVA) was applied to compare the differences among the three groups. For nonnormally distributed variables or in case of unequal variances, the Kruskal–Wallis H test was used. The categorical variables were compared using Pearson's chi-square test. To evaluate the relationship between hematological parameters and the risk of HSIL and LSIL, we performed binary logistic regression analysis (Backward LR method). Assumptions for logistic regression, including log-odds linearity and multicollinearity, were tested and met.

https://doi.org/10.5455/annalsmedres.2025.05.117

Table 1. Association between HPV genotypes and the severity of cervical dysplasia.

Variables	LSIL (n=63)		HSIL (n=54)		Chronic cervicitis (n = 98)		Statistical analysis*
	n	%	n	%	n	%	
HPV types							
HPV 16-18	31	49.2	39	72.2	44	44.9	x^2=10.957
Types other than HPV16-18	32	50.8	15	27.8	54	55.1	**p=0.004**

*Pearson-x^2 crosstabs.

Table 2. Comparative analysis of quantitative findings across study groups.

Parameters	LSIL (n=63) X±S.S	HSIL (n=54) X±S.S	Chronic cervicitis (n = 98) X±S.S	Statistical analysis*
Age (years)	45.59±10.17	43.89±8.78	44.94±9.98	x^2=0.668 p=0.716
Hemoglobin(g/dL)	12.76±1.47	12.76±1.62	13.07±1.36	x^2=2.231 p=0.328
WBC(mcL)	7410.48±2016.32	7589.44±2026.98	7545.71±1811.63	F=0.145 p=0.865
Neutrophil(mcL)	4519.68±1476.55	4714.07±1740.86	4554.08±1341.01	x^2=0.187 p=0.911
Platelet (103/μL)	284904.76±71273.38	284925.93±82030.79	295948.98±56656.38	F=0.700 p=0.498
Lymphocyte(mcL)	2171.75±722.12	2170.56±565.95	2317.45±691.34	F=1.264 p=0.285
NLR	2.28±0.98	2.26±0.96	2.13±0.93	x^2=1.846 p=0.397
PLR	141.90±48.21	137.75±47.36	140.85±53.94	x^2=0.286 p=0.867
SII	644273.69±319708.65	640145.43±322440.51	632410.59±306284.63	x^2=0.010 p=0.995

WBC: White blood cell, NLR: Neutrophil-Lymphocyte Ratio, PLR: Platelet-Lymphocyte Ratio, SII: Systemic Immune-Inflammation Index. *For data exhibiting a normal distribution, the statistics of the "ANOVA" test (F-statistic) was employed for the comparison of measurement values across three or more independent groups. For data not conforming to a normal distribution, the statistics of the "Kruskal-Wallis H" test (x^2-statistic) were used for the comparison of measurement values among three or more independent groups.

Table 3. Analysis of factors influencing the LSIL probability using binary logistic regression.

Parameters	B	S.H.	Wald	s	p	OR	95 percent confidence interval (OR) Lower	Upper
Age (years)	0.013	0.016	0.691	1	0.406	1.013	0.982	1.046
Hemoglobin(g/dL)	-0.094	0.108	0.756	1	0.384	0.911	0.738	1.124
WBC(mcL)	0.001	0.000	0.762	1	0.383	1.000	1.000	1.001
Neutrophil(mcL)	-0.001	0.000	2.457	1	0.117	0.999	0.998	1.000
Platelet(10^3/μL)	0.000	0.000	0.214	1	0.644	1.001	1.000	1.000
Lymphocyte(mcL)	0.000	0.001	0.239	1	0.625	1.001	0.998	1.001
NLR	0.759	0.807	0.884	1	0.347	2.135	0.439	10.381
PLR	-0.014	0.013	1.230	1	0.267	0.986	0.962	1.011
SII	0.001	0.001	0.071	1	0.790	1.001	1.000	1.000
Constant	0.871	2.815	0.096	1	0.757	2.389		

CCR: 70.7% [Hosmer-Lemeshow Test x^2=3.771; p=0.877]. WBC: White blood cell, NLR: Neutrophil-Lymphocyte Ratio, PLR: Platelet-Lymphocyte Ratio, SII: Systemic Immune-Inflammation Index.

Table 4. Analysis of factors influencing the HSIL probability using binary logistic regression.

Parameters	B	S.H.	Wald	s	p	OR	95 percent confidence interval (OR) Lower	Upper
Lymphocyte(mcL)	-0.002	0.001	5.441	1	**0.020**	0.998	0.997	0.999
PLR	-0.026	0.012	4.892	1	**0.027**	0.975	0.953	0.997
Constant	3.440	1.872	3.377	1	**0.046**	31.196		

CCR: 74.9% [Hosmer-Lemeshow Test x^2=97.90; p=0.280]. PLR: platelet-to-lymphocyte ratio.

https://doi.org/10.5455/annalsmedres.2025.05.117

RESULTS

Analysis of the age distribution across the study groups revealed mean ages of 44.94±9.98 years in the chronic cervicitis group, 45.59±10.17 years in the LSIL group, and 43.89±8.78 years in the HSIL group. No significant difference in age was observed between the groups (p = 0.716). Regarding HPV DNA typing, 114 cases tested positive for HPV types 16 and 18, whereas 101 cases tested positive for high-risk HPV types other than 16/18. Specifically, 32 (50.9%) patients with LSIL and 54 (55.1%) patients with chronic cervicitis tested positive for high-risk HPV types other than 16/18, whereas 39 (72.2%) patients with HSIL tested positive for HPV 16-18. A statistically significant association was found between the study groups and HPV types (p < 0.05) (Table 1).

Comparison of the chronic cervicitis, LSIL, and HSIL groups revealed no statistically significant differences in age, hemoglobin, white blood cell count (WBC), neutrophil count, platelet count, lymphocyte count, NLR, PLR, and SII values (p > 0.05) (Table 2).

Logistic regression analysis to assess the risk of LSIL indicated that none of the included parameters had a significant effect on LSIL status (p > 0.05) (Table 3). In contrast, logistic regression analysis for HSIL risk identified lymphocyte count and PLR as significant parameters (p < 0.05). A one-unit increase in lymphocyte count was associated with a 0.2% decrease in the odds of HSIL (OR = 0.998). Similarly, a one-unit increase in PLR was associated with a 2.5% decrease in the odds of HSIL (OR = 0.975) (Table 4).

DISCUSSION

Given the growing interest in inflammation-related biomarkers for cervical disease assessment, this study examined the utility of systemic immune-inflammation indices—namely SII, NLR, and PLR—in differentiating histopathological grades of cervical dysplasia in HPV-positive patients. Despite analyzing a well-defined cohort using colposcopic biopsy data, we observed no significant differences in routine inflammatory parameters across chronic cervicitis, LSIL, and HSIL groups. However, logistic regression analysis revealed that higher lymphocyte count and PLR were inversely associated with HSIL risk, suggesting a possible protective role or immune response modulation.

The increasingly acknowledged role of chronic inflammation in cervical carcinogenesis warrants attention [12]. Immune inflammation indices offer potential clinical utility as readily accessible parameters that reflect the systemic inflammatory milieu. A body of evidence suggests a possible correlation between these indices and the severity and prognosis of cervical lesions [17,18].

The significant role of inflammatory indices in the pathogenesis and clinical trajectory of cervical cancer and advanced-stage dysplasia has been substantiated in the existing literature. Afsar et al. reported significantly elevated inflammatory indices in individuals diagnosed with cervical cancer, proposing their potential as diagnostic adjuncts for distinguishing malignant status [19]. Similarly, Lima et al. demonstrated an association between elevated NLR levels and diminished overall and disease-free survival in invasive cervical neoplasia, concluding that NLR could serve as an independent adverse prognosticator [20]. Moreover, studies [21-23] have identified NLR and WBC count as potential prognostic markers for predicting recurrence risk following excisional procedures in patients with CIN, highlighting the central role of systemic inflammation in CIN recurrence post-LEEP and the utility of preoperative NLR levels as a robust independent prognostic factor for recurrence after surgical excision of CIN. These cumulative findings underscore the importance of the inflammatory response in the clinical management of cervical cancer and its precursor lesions, and highlight the potential clinical applications of inflammatory indices. No significant association in low-grade dysplasia (LSIL) within our cohort supports the hypothesis that inflammatory markers may play a more prominent role in disease progression or in more advanced stages.

Mantoani et al. evaluated data from 51 patients with low- and high-grade squamous intraepithelial lesions, employing colposcopic image analysis to quantify lesion areas and examine corresponding laboratory parameters. Their analysis revealed an inverse correlation between lesion area and NLR (r = -0.446, P = 0.001), PLR (r = -0.438, P = 0.001), and absolute leukocyte count (r = -0.351, P = 0.011) across the entire CIN patient cohort. Furthermore, they established an optimal lesion area cutoff of 21.019 pixels squared (58.87 mm squared) for predicting the absence of residual lesions in patients with CIN 2/3 undergoing excisional surgery [24]. Although our study did not identify significant intergroup differences in inflammatory indices, the findings of Mantoani et al. lend credence to the notion that CIN represents a systemic perturbation potentially manifesting as alterations in NLR, PLR, and leukocyte counts. Conversely, Tas et al. suggested that while NLR and PLR may aid in differentiating precancerous cervical pathologies from overt cervical cancer, their utility in predicting LSIL and HSIL appears limited [25]. Consistent with this, Küçükyurt and Çetin reported no significant variations in inflammatory indices such as NLR and PLR among the CIN I, CIN II, and CIN III groups [26]. The lack of significant differences in SII, NLR, and PLR values across the groups in our study suggests that when considered in isolation, these markers may not possess sufficient discriminatory power for the diagnosis of cervical dysplasia.

The results of our logistic regression analysis regarding HSIL risk indicated a significant influence of both lymphocyte count and PLR (p < 0.05). Specifically, a 0.2% reduction in the odds of HSIL was associated with each unit increment in lymphocyte count (OR = 0.998). Similarly, each unit increase in PLR value correlated with a 2.5% reduction in HSIL odds (OR = 0.975). These observations imply that the systemic inflammatory response plays a complex role in the develop-

https://doi.org/10.5455/annalsmedres.2025.05.117

ment of advanced cervical intraepithelial neoplasia. A study assessing the prognostic value of preoperative PLR levels and HR-HPV infection in predicting HSIL recurrence following LEEP at 3- and 5-year intervals demonstrated that elevated PLR levels and HR-HPV infection were associated with an increased risk of HSIL recurrence/residual disease, suggesting their potential as markers for clinical management [27]. Conventionally, a low lymphocyte count and elevated PLR are associated with an unfavorable prognosis in certain malignancies [28,29]. However, the inverse relationship observed in our study warrants further investigation to elucidate the underlying mechanisms contributing to these unexpected findings. This counterintuitive association may be attributed to a complex immune response, where a higher lymphocyte count could reflect an effective antiviral or antitumoral activity. Similarly, an elevated PLR within a certain physiological range might signal a reactive thrombopoietic state rather than a protumorigenic process. These hypotheses warrant further experimental validation.

The significant association between HPV type and lesion grade in our study reinforces the well-established understanding that more severe lesions are associated with high-risk HPV types, particularly HPV 16/18. The interplay between HPV infection and inflammation is multifaceted. Bilir et al demonstrated significantly higher hematological inflammatory markers, such as SIRI and NLR, in women with persistent HPV infection, suggesting their potential utility in predicting persistent HPV infection [30]. Hammes et al. showed a positive correlation between macrophage infiltration in the cervical epithelium and the progression and transformation of CIN lesions to cancer, with inflammation intensity correlated with lesion grade [31]. Kemp et al. reported elevated systemic pro-inflammatory cytokine levels in women with persistent HPV infection [32]. Trinchieri posits that HPV infection may initiate inflammatory pathways in later stages, thereby facilitating tumor progression [33]. This observation provides a readily available parameter for enhanced surveillance of patients with persistent HPV infection for cervical cancer prevention. No significant association was found between SII, NLR, PLR, and varying CIN grades in our study, suggesting that these markers may not be sufficiently reliable as standalone diagnostic tools for low-grade cervical dysplasia. This implies a potential limitation in the utility of these indices for routine screening or primary diagnostic purposes in clinical practice. However, the observed inverse relationship between lymphocyte count and PLR with HSIL risk in logistic regression warrants continued scrutiny. The significant association between HPV type and lesion grade, coupled with the higher prevalence of HPV 16/18 positivity in the HSIL group, aligns with existing literatüre. Typing in risk stratification emphasizes the necessity of implementing HPV type-specific follow-up and management algorithms in clinical practice [34]. This study has certain limitations, including its retrospective design, which may impact the generalizability of the findings. Additionally, the sample size for some subgroup analyses may be limited. Future studies should adopt prospective, longitudinal designs, include larger and more diverse populations, and consider incorporating molecular or immunological biomarkers alongside hematological indices to enhance diagnostic precision.

CONCLUSION

Future studies should adopt a prospective and multidimensional design to better elucidate the clinical utility of hematological inflammatory markers in cervical dysplasia. Therefore, multimodal approaches, integrating inflammatory indices with other clinical and pathological factors, may provide a more holistic perspective in the management of cervical dysplasia.

Ethics Committee Approval: The study protocol received ethical approval from the Ethics Committee of Kırıkkale University (decision date: 2025.03.12, decision number: 2025.03.07).

Availability of data and materials: The datasets used and analyzed during the current study are available from the corresponding author on reasonable request.

Informed Consent: As the study was conducted retrospectively, informed consent from the patients was not required.

Peer-review: Externally peer-reviewed.

Conflict of Interest: The authors have no potential conflicts of interest to declare.

Author Contributions: YS: Conceptualization, Design, Data curation, Formal analysis, Methodology, Project administration, Writing-original draft, Writing-review and editing, Investigation, Software, Supervision; AE: Data curation, Validation, Visualization, Writing-original draft, Writing-review and editing; CMA: Data curation, Validation, Visualization, Writing-original draft, Writing-review and editing.

Financial Disclosure: None.

REFERENCES

1. Sung H, Ferlay J, Siegel RL, et al. Global Cancer Statistics 2020: GLOBOCAN Estimates of Incidence and Mortality Worldwide for 36 Cancers in 185 Countries. *CA Cancer J Clin.* 2021;71(3):209-249. doi: 10.3322/caac.21660.
2. Singh D, Vignat J, Lorenzoni V et al. Global estimates of incidence and mortality of cervical cancer in 2020: a baseline analysis of the WHO Global Cervical Cancer Elimination Initiative. *Lancet Glob Health.* 2023;11(2):e197-e206. doi: 10.1016/S2214-109X(22)00501-0.
3. Okunade KS. Human papillomavirus and cervical cancer. *J Obstet Gynaecol.* 2020;40(5):602-608. doi: 10.1080/01443615.2019.1634030. Erratum in: *J Obstet Gynaecol.* 2020;40(4):590. doi: 10.1080/01443615.2020.1713592.
4. Ahmed HG, Bensumaidea SH, Alshammari FD, et al. Prevalence of human papillomavirus subtypes 16 and 18 among Yemeni patients with cervical cancer. *Asian Pac J Cancer Prev.* 2017;18(6):1543-1548. doi: 10.22034/APJCP.2017.18.6.1543.

https://doi.org/10.5455/annalsmedres.2025.05.117

5. Molina MA, Steenbergen RDM, Pumpe A, Kenyon AN, Melchers WJG. HPV integration and cervical cancer: a failed evolutionary viral trait. *Trends Mol Med.* 2024;30(9):890-902. doi: 10.1016/j.molmed.2024.05.009.
6. Zhu R, Wang W, Yang A et al. Interactions between vaginal local cytokine IL-2 and high-risk human papillomavirus infection with cervical intraepithelial neoplasia in a Chinese population-based study. *Front Cell Infect Microbiol.* 2023;13:1109741. doi: 10.3389/fcimb.2023.1109741.
7. Schiller JT, Day PM, Kines RC. Current understanding of the mechanism of HPV infection. *Gynecol Oncol.* 2010;118(1 Suppl):S12-S17. doi: 10.1016/j.ygyno.2010.04.004.
8. Yeo-Teh NSL, Ito Y, Jha S. High-risk human papillomaviral oncogenes E6 and E7 target key cellular pathways to achieve oncogenesis. *Int J Mol Sci.* 2018;19(6):1706. doi: 10.3390/ijms19061706.
9. Porter VL, Marra MA. The drivers, mechanisms, and consequences of genome instability in HPV-driven cancers. *Cancers (Basel).* 2022;14(19):4623. doi: 10.3390/cancers14194623.
10. Darragh TM, Colgan TJ, Cox JT, et al. The Lower Anogenital Squamous Terminology Standardization Project for HPV-Associated Lesions: background and consensus recommendations from the College of American Pathologists and the American Society for Colposcopy and Cervical Pathology. *J Low Genit Tract Dis.* 2012;16(3):205-42. doi: 10.1097/LGT.0b013e31825c31dd. Erratum in: *J Low Genit Tract Dis.* 2013;17(3):368.
11. World Health Organization Classification of Tumors of Female Reproductive Organs Fourth Edition. *WHO OMS.* Available from: https://apps.who.int/bookorders/anglais/detart1.jsp?codlan=1&codcol=70&codcch=4006. Accessed January 10, 2020.
12. Fernandes JV, Medeiros DE, Fernandes TA, Azevedo DE, et al. Link between chronic inflammation and human papillomavirus-induced carcinogenesis (Review). *Oncol Lett.* 2015;9(3):1015-1026. doi: 10.3892/ol.2015.2884.
13. Grivennikov SI, Greten FR, Karin M. Immunity, inflammation, and cancer. *Cell.* 2010;140(6):883-899. doi: 10.1016/j.cell.2010.01.025.
14. Wu S, Liu Z, Li X, Gao S, Xia P. Association between systemic immune-inflammation index and the risk of all-cause, cancer and non-cancer mortality in the general population: results from national health and nutrition examination survey 2005-2018. *BMC Public Health.* 2025;25(1):227. doi: 10.1186/s12889-025-21423-1.
15. Liu F, Yin P, Jiao B, Shi Z, Qiao F, Xu J. Detecting the preoperative peripheral blood systemic immune-inflammation index (SII) as a tool for early diagnosis and prognosis of gallbladder cancer. *BMC Immunol.* 2025;26(1):7. doi: 10.1186/s12865-025-00683-x.
16. Perkins RB, Guido RL, et al. Response to Letter to the Editor Regarding: 2019 ASCCP Risk-Based Management Consensus Guidelines for Abnormal Cervical Cancer Screening Tests and Cancer Precursors. *J Low Genit Tract Dis.* 2020;24(4):426. doi: 10.1097/LGT.0000000000000562.
17. Xu L, Song J. Elevated neutrophil-lymphocyte ratio can be a biomarker for predicting the development of cervical intraepithelial neoplasia. *Medicine (Baltimore).* 2021;100(28):e26335. doi: 10.1097/MD.0000000000026335.
18. Chun S, Shin K, Kim KH, et al. The neutrophil-lymphocyte ratio predicts recurrence of cervical intraepithelial neoplasia. *J Cancer.* 2017;8(12):2205-2211. doi: 10.7150/jca.19173.
19. Afsar S, Turan G, Guney G, Sahin G, Talmac MA, Afsar CU. The Relationship between Furin and Chronic Inflammation in the Progression of Cervical Intraepithelial Neoplasia to Cancer: A Cross-Sectional Study. *Cancers (Basel).* 2023;15(19):4878. doi: 10.3390/cancers15194878.
20. Lima PSV, Mantoani PTS, Murta EFC, Nomelini RS. Laboratory parameters as predictors of prognosis in uterine cervical neoplasia. *Eur J Obstet Gynecol Reprod Biol.* 2021;256:391-396. doi: 10.1016/j.ejogrb.2020.11.044.
21. Farzaneh F, Faghih N, Hosseini MS, Arab M, Ashrafganjoei T, Bahman A. Evaluation of Neutrophil-Lymphocyte Ratio as a Prognostic Factor in Cervical Intraepithelial Neoplasia Recurrence. *Asian Pac J Cancer Prev.* 2019;20(8):2365-2372. doi: 10.31557/APJCP.2019.20.8.2365.
22. Zhai F, Mu S, Song Y, Zhang M, Zhang C, Lv Z. Associations Between Preoperative Inflammatory Indices and Residual or Recurrent Cervical Intraepithelial Neoplasia Post Loop Electrosurgical Excision Procedure. *J Inflamm Res.* 2024;17:8741-8751. doi: 10.2147/JIR.S485698.
23. Origoni M, Cantatore F, Candotti G, Candiani M. Prognostic Significance of Neutrophil/Lymphocytes Ratio (NLR) in Predicting Recurrence of Cervical Dysplasia. *Biomed Res Int.* 2022;2022:1149789. doi: 10.1155/2022/1149789.
24. Mantoani PTS, Vieira JF, Menchete TT, et al. CIN extension at colposcopy: relationship to treatment and blood parameters. *J Obstet Gynaecol Can.* 2022;44(3):255-260. doi: 10.1016/j.jogc.2021.10.008.
25. Tas M, Yavuz A, Ak M, Ozcelik B. Neutrophil-to-Lymphocyte Ratio and Platelet-to-Lymphocyte Ratio in Discriminating Precancerous Pathologies from Cervical Cancer. *J Oncol.* 2019;2019:2476082. doi: 10.1155/2019/2476082.
26. Küçükyurt A, Çetin A. Cervical intraepithelial neoplasia (cin) and the importance of leukocytes, platelets, mean platelet volume, platelet distribution width, red cell distribution width, plateletcrit, neutrophil/lymphocyte, platelet/lymphocyte, lymphocyte/monocyte ratios in diagnosis. *TRSGO Dergisi.* 2024;24(2):74-83.
27. Huang G, Gao H, Chen Y, et al. PPlatelet-to-Lymphocyte Ratio (PLR) as the Prognostic Factor for Recurrence/Residual Disease in HSIL Patients After LEEP. *J Inflamm Res.* 2023;16:1923-1936. doi: 10.2147/JIR.S406082.
28. Zhao J, Huang W, Wu Y et al. Prognostic role of pretreatment blood lymphocyte count in patients with solid tumors: a systematic review and meta-analysis. *Cancer Cell Int.* 2020;20:15. doi: 10.1186/s12935-020-1094-5.
29. Templeton AJ, Ace O, McNamara MG, et al. Prognostic role of platelet to lymphocyte ratio in solid tumors: a systematic review and meta-analysis. *Cancer Epidemiol Biomarkers Prev.* 2014;23(7):1204-1212. doi: 10.1158/1055-9965.EPI-14-0146.
30. Bilir F, Chkhikvadze M, Yilmaz AY, Kose O, Arıöz DT. Prognostic value of systemic inflammation response index in patients with persistent human papilloma virus infection. *Ginekol Pol.* 2022;93(9):705-709. doi: 10.5603/GP.a2021.0200.
31. Hammes LS, Tekmal RR, Naud P, et al. Macrophages, inflammation and risk of cervical intraepithelial neoplasia (CIN) progression–clinicopathological correlation. *Gynecol Oncol.* 2007;105(1):157-165. doi: 10.1016/j.ygyno.2006.11.023.
32. Kemp TJ, Hildesheim A, García-Piñeres A et al. Elevated systemic levels of inflammatory cytokines in older women with persistent cervical human papillomavirus infection. *Cancer Epidemiol Biomarkers Prev.* 2010;19(8):1954-1959. doi: 10.1158/1055-9965.EPI-10-0184.
33. Trinchieri G. Innate inflammation and cancer: Is it time for cancer prevention? *F1000 Med Rep.* 2011;3:11. doi: 10.3410/M3-11.
34. Eroglu S, Asgin N. Frequency and genotype distribution of high-risk human papillomavirus types in Karabuk province, Turkey: A hospital-based cross-sectional study. *Ann Med Res.* 2020;27(3):765–769. doi: 10.5455/annalsmedres.2019.12.787.

Ann Med Res

Current issue list available at Ann Med Res

Annals of Medical Research

journal page: annalsmedres.org

A comparative study of nerve-sparing techniques in open radical prostatectomy: Antegrade versus retrograde

Serkan Ozcan [a,*], Hakan Tekinaslan [b], Osman Kose [a], Enis Mert Yorulmaz [a], Sacit Nuri Gorgel [a], Yigit Akin [a]

[a] *İzmir Katip Çelebi University, Faculty of Medicine, Department of Urology, İzmir, Türkiye*
[b] *Menderes State Hospital, Clinic of Urology, İzmir, Türkiye*
**Corresponding author: drserkanozcan@hotmail.com (Serkan Ozcan)*

MAIN POINTS

- This study provides a direct comparison between antegrade and retrograde nerve-sparing techniques in open radical prostatectomy.
- The retrograde approach was associated with reduced operative time and shorter hospitalization.
- The antegrade approach resulted in lower intraoperative blood loss, indicating superior hemostatic control.
- Despite similar surgical margin rates, biochemical recurrence was more frequent in the antegrade group, likely due to a higher prevalence of high-grade tumors. Postoperative continence, erectile function, and anastomotic stricture rates were comparable between groups.
- Both techniques are safe and effective; surgical approach should be selected based on tumor characteristics and surgeon expertise.

Cite this article as: Ozcan S, Tekinaslan H, Kose O, Yorulmaz EM, Gorgel SN, Akin Y. A comparative study of nerve-sparing techniques in open radical prostatectomy: Antegrade versus retrograde. *Ann Med Res*. 2025;32(11):499--505. doi: 10.5455/annalsmedres.2025.05.119.

ABSTRACT

Aim: To compare perioperative, oncological, and functional outcomes between antegrade and retrograde nerve-sparing techniques in open radical prostatectomy (ORP).

Materials and Methods: This retrospective study included 278 patients who underwent open radical prostatectomy (ORP) performed by a single surgeon between 2016 and 2025. Patients were divided based on the nerve-sparing approach: antegrade (n=90) or retrograde (n=188). Demographic characteristics, perioperative variables, pathological outcomes, biochemical recurrence (BCR), urinary continence, and erectile function were evaluated. Multivariable logistic regression analysis was used to determine independent predictors of BCR.

Results: Retrograde ORP demonstrated a shorter operative time compared with the antegrade technique (151.1 vs. 166.5 minutes, p<0.001), whereas the antegrade group was associated with lower intraoperative blood loss (437 vs. 517 mL, p=0.047). Biochemical recurrence was significantly higher in the antegrade group (33.3% vs. 18.8%, p=0.008). Postoperative functional outcomes, including urinary continence (p=0.524) and erectile function (p=0.230), were comparable between the groups. In multivariable logistic regression, the retrograde approach independently reduced the risk of biochemical recurrence (OR 0.38; 95% CI: 0.19--0.76; p=0.0058).

Conclusion: It is evident that both techniques are safe and effective in ORP. The retrograde approach was associated with more favourable oncological outcomes, whereas the antegrade technique provided better intraoperative hemostasis. The choice of surgical approach should be individualized based on tumor characteristics and surgeon expertise.

Keywords: Prostatectomy, Nerve-sparing, Prostate cancer, Open surgery, Biochemical recurrence

Received: May 16, 2025 **Accepted:** Sep 05, 2025 **Available Online:** Nov 25, 2025

INTRODUCTION

Radical prostatectomy (RP) remains a standard curative treatment for clinically localized prostate cancer, offering durable oncological control and long-term survival benefits [1]. Currently, RP can be performed through three main surgical modalities: open radical prostatectomy (ORP), laparoscopic radical prostatectomy (LRP), and robot-assisted laparoscopic prostatectomy (RALP). Minimally invasive approaches, particularly RALP, have gained popularity due to shorter recovery, lower blood loss, and improved cosmesis. However, their adoption is limited by high costs, steep learning curves, and a lack of availability in low-resource settings [2,3]. Therefore, ORP remains a relevant and accessible surgical option, particularly in healthcare systems with limited access to advanced Technologies [4].

In this context, ORP continues to be a viable and widely performed surgical option. Despite technological advances, functional complications such as erectile dysfunction (ED)

and urinary incontinence remain major concerns following RP. Preservation of the neurovascular bundles (NVBs) is critical for maintaining postoperative continence and sexual function. Several factors influence functional outcomes, including nerve-sparing technique, surgeon experience, and patient-specific anatomy [5]. Two principal NVB preservation techniques have been described in ORP: the antegrade approach, which dissects from base to apex, and the retrograde approach, which proceeds in the opposite direction [6,7]. Both aim to minimize NVB trauma, but data comparing their relative efficacy is limited and inconclusive, particularly in open surgery.

Additionally, advances in surgical energy devices such as the Harmonic scalpel have improved hemostasis and reduced collateral tissue injury, potentially enhancing outcomes in nerve-sparing procedures [8]. Nonetheless, few studies have directly compared antegrade and retrograde nerve-sparing techniques using standardized surgical methods and instrumentation.

This study aims to compare the perioperative, oncological, and functional outcomes of antegrade versus retrograde nerve-sparing techniques in ORP. All procedures were performed with a consistent technique and energy device, minimizing confounding factors and enhancing the reliability of comparisons.

MATERIALS AND METHODS

Study design and surgical technique

This retrospective study analyzed a cohort of 278 patients who underwent open radical prostatectomy (ORP) at Atatürk Training and Research Hospital between 2016 and 2025. Patients were stratified into two groups based on the nerve-sparing technique employed: antegrade (n=90) or retrograde (n=188). To ensure procedural consistency, all operations were performed by a single urologist using a standardized surgical method and the Harmonic scalpel for hemostasis. During the study period, neither laparoscopic nor robotic-assisted radical prostatectomy was available, making ORP the exclusive surgical approach for all patients. The study protocol was approved by the Non-Interventional Clinical Research Ethics Committee of İzmir Kâtip Çelebi University Faculty of Medicine (Approval No: 2025/0172; Date: March 2025).

The nerve-sparing approach was chosen intraoperatively by the surgeon, based on anatomical factors such as prostate size, apical configuration, and vascular pattern. Therefore, the study was not randomized. Tumor grade and stage were not used to determine the surgical approach. This may introduce selection bias, but the use of a single surgeon, uniform technique, and consistent instrumentation minimizes variability and enhances comparability. This is discussed in the discussion section.

Patient selection and data collection

The inclusion criteria were as follows: prostate adenocarcinoma, radical prostatectomy performed at our institution, complete clinical and follow-up data, and a preoperative IIEF-5 score of at least 21. Exclusion criteria were prior pelvic surgery, metastatic disease, neoadjuvant therapy, or missing data.

Demographic and clinical variables recorded included age, body mass index (BMI), preoperative PSA, and presence of diabetes. Operative data included surgical technique, operative time, estimated blood loss, transfusion requirement, and length of hospital stay. Oncological parameters included biopsy and postoperative ISUP grade, Gleason score, surgical margin status, biochemical recurrence, duration of follow-up, and overall survival.

Since the present study compared the outcomes of two nerve-sparing techniques in patients who underwent nerve-sparing radical prostatectomy; the patients who received non-nerve-sparing surgery were excluded to ensure comparable results in terms of complications such as postoperative erectile function and incontinence.

Definitions and outcome measures

Urinary continence was defined as needing one protective pad per day. Erectile function was evaluated using the IIEF-5 questionnaire, with scores $\leq$12 indicating significant dysfunction. Biochemical recurrence (BCR) was defined as a PSA level $\geq$0.2 ng/mL confirmed by two consecutive measurements. Disease-free survival was defined as the interval from surgery to either BCR or the latest follow-up.

Statistical analysis

All statistical procedures were conducted using the IBM SPSS Statistics for Windows, Version 25.0 (Armonk, NY: IBM Corp.). The distribution of continuous variables was tested using the Kolmogorov–Smirnov test. Comparisons were made using the Mann–Whitney U test or independent samples t-test. Categorical variables were analyzed using Pearson's chi-square test. A p-value less than or equal to 0.05 was considered statistically significant.

Independent predictors of biochemical recurrence were identified using a multivariable logistic regression model. This included surgical approach (retrograde vs. antegrade), preoperative PSA, pathological ISUP grade, age, diabetes mellitus, and BMI. The model provided odds ratios (ORs) and 95% confidence intervals. All independent variables were entered simultaneously into the multivariable logistic regression model (enter method).

A post-hoc power analysis was conducted to confirm sufficient statistical power. This analysis used G*Power version 3.1, applying the Demidenko method for logistic regression. It found an observed OR of 0.38 for surgical approach, an event rate of 33%, and a total sample size of 278. The power was calculated as 0.86 (α = 0.05).

https://doi.org/10.5455/annalsmedres.2025.05.119

Table 1. Demographic, operative, oncological, and functional outcomes in the nerve-sparing radical prostatectomy groups. Continuous variables are expressed as median (interquartile range) for non-normally distributed data or mean ± SD for normally distributed data. Categorical variables are presented as number of patients (percentage within group).

Parameter	Antegrade group (n = 90)	Retrograde group (n = 188)	p value
Demographic Data			
Age (years)	65.89 ± 5.70	65.79 ± 6.23	0.880
Body Mass Index (kg/m²)	26.31 ± 2.89	25.74 ± 3.75	0.035
Preoperative PSA (ng/mL)	11.04 ± 9.54	12.13 ± 14.76	0.783
Diabetes Mellitus *	20 (22.20%)	24 (12.70%)	0.214
Operative Findings			
Operation Time (minutes)	160 (145-180)	148 (130-175)	<0.001
Intraoperative Blood Loss (mL)	430 (360-510)	510 (420-620)	0.047
Blood Transfusion required *	10 (11.10%)	30 (16.00%)	0.090
Hospital Stay (days)	7 (5-10)	6 (4-8)	0.042
Oncological Outcomes			
Positive Surgical Margin *	35 (38.90%)	63 (33.70%)	0.397
Biochemical Recurrence *	30 (33.30%)	35 (18.80%)	0.008
Overall Survival (alive) *	84 (93.30%)	176 (94.10%)	0.799
Functional Outcomes			
Urinary Incontinence *	35 (38.60%)	65 (34.50%)	0.524
Erectile Dysfunction *	87 (96.70%)	175 (93.10%)	0.230
Anastomotic Stricture *	20 (22.20%)	33 (17.60%)	0.354

* Variables analyzed by Chi-square test are indicated with an asterisk. Non-normally distributed continuous variables were compared using the Mann–Whitney U test. A p <0.05 was considered statistically significant.

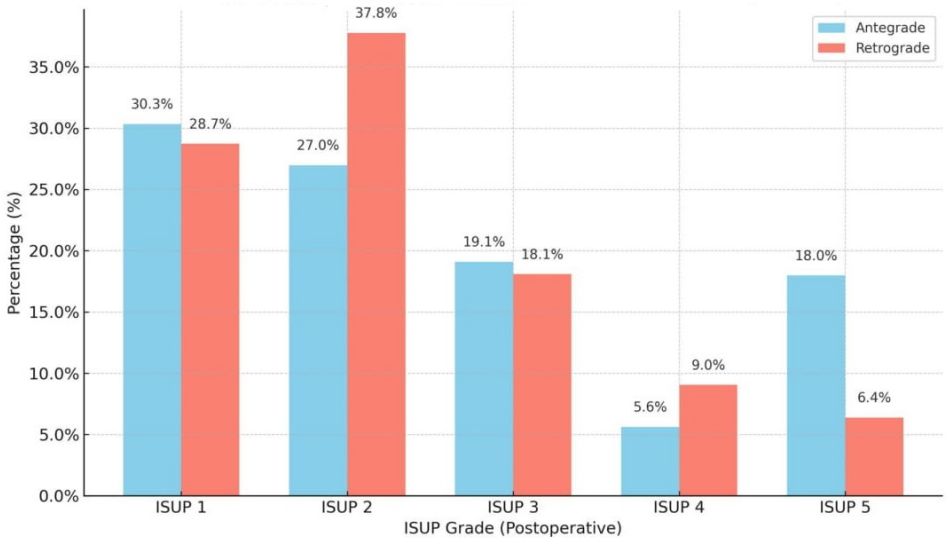

Figure 1. Postoperative pathological ISUP grade distribution in the antegrade (blue) andretrograde (red) groups. The chart depicts the percentage of patients in each group who hadfinal pathology ISUP grades 1 through 5. A significantly higher fraction of tumors were ISUPgrade 5 in the antegrade group, whereas the retrograde group had more grade 2 tumors (Chi-square p = 0.026). Data are expressed as percentages.

Prior to the multivariable logistic regression, multicollinearity among the independent variables was assessed. No significant collinearity was detected, and all variance inflation factor (VIF) values were below 2.5.

RESULTS

A total of 278 patients were included in the study, with 90 undergoing antegrade prostatectomy versus 188 undergoing retrograde open radical prostatectomy. Demographic and baseline clinical characteristics were comparable between the two groups. The mean age was approximately 66 years, and preoperative PSA levels did not differ significantly. The retrograde group had a slightly lower BMI (25.74 vs. 26.31 kg/m², p = 0.035). The prevalence of diabetes mellitus was similar (22.2% vs. 12.7%, p = 0.214).

From a surgical perspective, the retrograde approach demon-

https://doi.org/10.5455/annalsmedres.2025.05.119

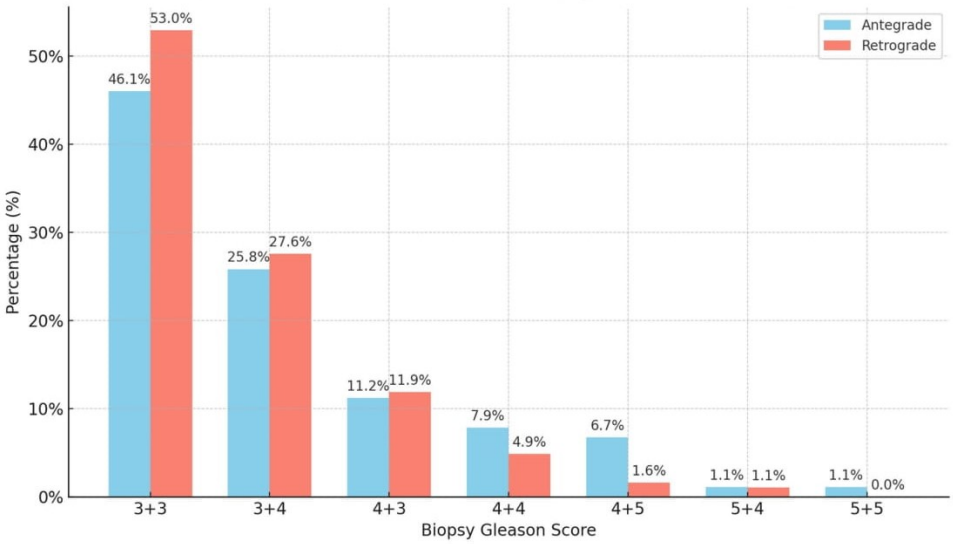

Figure 2. Distribution of biopsy Gleason scores in the antegrade (blue) and retrograde (red) groups. The percentage of patients with Gleason score 6, 7, 8, 9, or 10 on biopsy is shown foreach surgical group. Both the antegrade and retrograde approaches yielded similar Gleasonscore distributions at diagnosis (p>0.20), with over half of patients in each group having Gleason 6 disease on initial biopsy.

strated some advantages. It was associated with a shorter operative time (151.1 vs. 166.5 minutes, $p < 0.001$), although the antegrade approach resulted in lower intraoperative blood loss (437 vs. 517 mL, $p = 0.047$). There were more blood transfusions in the retrograde group (16.0% vs. 11.1%), but this was not significant ($p = 0.090$). The length of hospital stay was longer in the antegrade group (7.4 vs. 6.5 days, $p = 0.042$).

The median follow-up period was 62 months (range: 12–109) in the antegrade group and 59 months (range: 13–108) in the retrograde group. Oncological outcomes are summarised in Table 1. The rate of positive surgical margins was similar (38.9% vs. 33.7%, $p = 0.397$). However, more cases of biochemical recurrence occurred in the antegrade group (33.3% vs. 18.8%, $p = 0.008$). Overall survival was excellent and comparable (93.3% vs. 94.1%, $p = 0.799$).

Postoperative functional outcomes were similar (Table 1). The prevalence of urinary incontinence (≥2 pads/day) was 38.6% in the antegrade group and 34.5% in the retrograde group ($p = 0.524$). Erectile dysfunction rates were high in both groups (96.7% vs. 93.1%, $p = 0.230$). Anastomotic stricture occurred in 22.2% of the antegrade group and 17.6% of the retrograde group ($p = 0.354$).

Table 2 presents the distribution of biopsy and pathological Gleason and ISUP grades. Biopsy Gleason and ISUP grades did not differ significantly between groups ($p = 0.207$ and $p = 0.169$, respectively). In contrast, postoperative pathological ISUP scores demonstrated a significant difference ($p = 0.026$). The retrograde group had a higher proportion of intermediate-grade disease (notably ISUP 2), while the antegrade group exhibited a greater prevalence of high-grade tumors (notably ISUP 5) (Table 2 and Figure 1).

Similarly, the postoperative Gleason score distribution showed a non-significant trend toward higher grade tumors (scores 9–10) in the antegrade group ($p = 0.086$). These findings suggest that the retrograde technique may be associated with a more favorable pathological grade distribution despite comparable biopsy findings (Figure 2).

A multivariable logistic regression analysis was conducted to determine independent predictors of biochemical recurrence (Table 3). Pathological ISUP grade (OR = 2.01; 95% CI: 1.57–2.61; $p < 0.001$), preoperative PSA level (OR = 1.06; 95% CI: 1.03–1.09; $p = 0.0003$), and surgical approach (OR = 0.38; 95% CI: 0.19–0.76; $p = 0.0058$) were identified as significant predictors of recurrence. Age showed a borderline association (OR = 1.06; 95% CI: 0.99–1.11; $p = 0.052$), while diabetes mellitus and BMI were not associated with recurrence ($p = 0.45$ and $p = 0.57$, respectively). Notably, the surgical approach was coded as 0 = antegrade (reference) and 1 = retrograde; thus, the retrograde technique was associated with a 62% reduction in the odds of biochemical recurrence.

A post-hoc power analysis using G*Power version 3.1 (Demidenko method for logistic regression) demonstrated an achieved power of 0.86 ($\alpha = 0.05$), based on an observed odds ratio of 0.38, an event rate of 33%, and a total sample size of 278, indicating sufficient statistical power for the observed effect.

DISCUSSION

This study offers a direct comparison between the antegrade and retrograde nerve-sparing techniques in open radical prostatectomy, an area with limited comparative data in the existing literature. Our results highlight that each technique

https://doi.org/10.5455/annalsmedres.2025.05.119

Table 2. Distribution of biopsy and postoperative Gleason scores and ISUP grades in antegrade and retrograde groups.

Score category	Antegrade group	Retrograde group
Biopsy Gleason Score		
Gleason 6 (3+3)	41 (46.10%)	98 (53.00%)
Gleason 7 (3+4)	23 (25.80%)	51 (27.60%)
Gleason 7 (4+3)	10 (11.20%)	22 (11.90%)
Gleason 8 (4+4)	7 (7.90%)	9 (4.90%)
Gleason 9 (4+5)	6 (6.70%)	3 (1.60%)
Gleason 9 (5+4)	1 (1.10%)	2 (1.10%)
Gleason 10 (5+5)	1 (1.10%)	0 (0.00%)
Biopsy ISUP Grade		
ISUP 1	40 (45.50%)	98 (52.40%)
ISUP 2	27 (30.70%)	53 (28.30%)
ISUP 3	9 (10.20%)	24 (12.80%)
ISUP 4	6 (6.80%)	9 (4.80%)
ISUP 5	6 (6.80%)	3 (1.60%)
Postoperative Gleason		
Gleason 6 (3+3)	27 (30.30%)	53 (28.60%)
Gleason 7 (3+4)	24 (27.00%)	71 (38.40%)
Gleason 7 (4+3)	17 (19.10%)	32 (17.30%)
Gleason 8 (3+5)	1 (1.10%)	0 (0.00%)
Gleason 8 (4+4)	2 (2.20%)	10 (5.40%)
Gleason 9 (4+5)	3 (3.40%)	7 (3.80%)
Gleason 9 (5+4)	11 (12.40%)	9 (4.90%)
Gleason 10 (5+5)	4 (4.50%)	3 (1.60%)
Postoperative ISUP		
ISUP 1	27 (30.30%)	54 (28.70%)
ISUP 2	24 (27.00%)	71 (37.80%)
ISUP 3	17 (19.10%)	34 (18.10%)
ISUP 4	5 (5.60%)	17 (9.00%)
ISUP 5	16 (18.00%)	12 (6.40%)

*ISUP: International Society of Urological Pathology. Percentages are calculated out of the number of patients with available data in each group. Denominators vary slightly across categories due to missing data. There were no significant between-group differences in biopsy Gleason or biopsy ISUP distributions (p>0.05); the postoperative ISUP distribution differed significantly between groups (p = 0.026).

Table 3. Multivariate logistic regression model predicting biochemical recurrence.

Variable	Odds Ratio (OR)	95% Confidence Interval	p-value
Pathological ISUP	2.01	(1.57 – 2.61)	<0.001
Preoperative PSA	1.06	(1.03 – 1.09)	0.0003
Surgical Approach[1]	0.38	(0.19 – 0.76)	0.0058
Age	1.06	(0.89 – 1.00)	0.052
Diabetes Mellitus	0.73	(0.31 – 1.66)	0.45
BMI	0.97	(0.88 – 1.07)	0.57

presents distinct advantages and limitations across perioperative, oncologic, and functional outcomes.

The antegrade approach was associated with a significantly longer mean operative time (166.5 ± 32.2 vs. 151.1 ± 49.8 minutes, p <0.001), potentially reflecting the careful dissection along anatomical planes and the stepwise vascular control that defines this technique, including early ligation of the prostatic pedicles and delayed division of the dorsal venous complex (DVC) [9–11]. Notably, the antegrade group exhibited significantly less intraoperative bleeding compared to the retrograde group (437 ± 142 mL vs. 517 ± 188 mL, p = 0.047). While transfusion requirements did not reach statistical significance, they were numerically lower in the antegrade group (11.1% vs. 16.0%, p = 0.090). This may be attributed to earlier exposure and control of venous structures during antegrade dissection, facilitating more effective hemostasis in line with previous reports [12,13]. Despite improved bleeding control, patients in the antegrade group experienced a slightly longer hospital stay (7.4 ± 3.95 vs. 6.5 ± 2.75 days, p = 0.042). Although this difference is statistically significant, its clinical relevance may be minimal, possibly reflecting a marginally slower immediate recovery. Importantly, aside from a lower body mass index in the retrograde group (25.74 ± 3.75 vs. 26.31 ± 2.89, p = 0.035), both groups were demographically similar, suggesting that perioperative differences likely stem from surgical technique rather than patient-related factors.

Oncologic efficacy appeared largely comparable between the two techniques. Positive surgical margin rates were similar (38.9% antegrade vs. 33.7% retrograde, p = 0.397), consistent with prior studies suggesting that nerve-sparing technique whether antegrade or retrograde does not compromise margin status or oncologic control [14,15]. However, the antegrade group showed a significantly higher rate of biochemical recurrence (33.3% vs. 18.8%, p = 0.008), despite similar margin positivity. This discrepancy may be explained by differences in tumor characteristics; the antegrade cohort had a higher proportion of high-grade tumors on final pathology, with ISUP grade 5 observed more frequently (18.0% vs. 6.4%, p = 0.026). Thus, the increased biochemical recurrence in the antegrade group may reflect a greater tumor burden rather than inadequate surgical clearance. Furthermore, the retrograde technique may allow for finer dissection near the prostatic apex and neurovascular bundles, enabling more complete excision of malignant tissue in anatomically challenging areas [14].

These findings indicate that both techniques remain viable options in the surgical management of localized prostate cancer, each with specific advantages: the antegrade technique offers better hemostasis, while the retrograde technique is associated with lower biochemical recurrence potentially due to enhanced apex dissection or a lower incidence of high-grade disease.

Rates of anastomotic stricture were comparable between groups, suggesting similar long-term safety. The equivalent stricture rates and survival outcomes support the notion that both nerve-sparing approaches are safe and oncologically sound when performed by experienced surgeons [16–18].

Postoperative functional outcomes were also similar between techniques, with no statistically significant differences in continence or erectile function. Urinary incontinence (defined as ≥2 pads/day) affected 38.6% of patients in the antegrade group and 34.5% in the retrograde group (p = 0.524), which

https://doi.org/10.5455/annalsmedres.2025.05.119

aligns with the wide variation in continence rates reported in the literature (ranging from 30–69%) (5). Erectile dysfunction was prevalent in both groups, as expected in this patient population. Clinically significant erectile dysfunction (IIEF-5 $\leq$12) was observed in 96.7% of antegrade and 93.1% of retrograde patients (p = 0.230), reflecting the inherent challenge of nerve preservation in open surgery and the strict definition employed. Nonetheless, a slight clinical trend favoring the retrograde group was observed in both continence and potency rates. This may be due to more delicate nerve-sparing at the apex with the retrograde technique, possibly facilitating better preservation of the neurovascular bundles and improved functional recovery.

Supporting this notion, Ko et al. found that a retrograde nerve-sparing technique in robotic prostatectomy yielded significantly better early potency recovery without affecting continence [15]. Likewise, de Carvalho et al. reported improved functional outcomes with a modified retrograde approach that preserved the dorsal vein complex during robotic prostatectomy[14]. Our findings are in line with these observations: although not statistically significant in our cohort, the retrograde technique appears at least equivalent and potentially advantageous when functional outcomes are a clinical priority.

Our multivariable analysis highlighted that both pathological ISUP grade and preoperative PSA level were significant predictors of biochemical recurrence. Notably, even after adjusting for these variables, the retrograde surgical approach remained independently protective, reducing the risk of recurrence by 62%, and thereby suggesting a potentially favorable oncologic impact. Although age demonstrated borderline significance, neither diabetes mellitus nor BMI were predictive. Furthermore, the robustness of these findings was supported by a post-hoc power analysis (power = 0.86, α = 0.05), confirming the adequacy of the sample size for the observed effect.

All procedures were performed by an experienced surgeon using standardized techniques and consistent instrumentation, minimizing variability. Open surgery was chosen over laparoscopic or robotic approaches due to the surgeon's expertise and procedural consistency; robotic surgery was not available during the study period. The inclusion of a large number of cases from a high-volume center enhanced the study's ability to detect clinically meaningful differences between the techniques.

However, the retrospective design introduces potential bias, particularly due to the absence of randomization and potential differences in tumor characteristics. Intraoperative decisions may have been influenced by unmeasured confounders. The surgeon's experience likely improved over the nine-year period, and learning curve effects were not analyzed separately.

Functional outcomes were based on patient-reported measures (pad count, IIEF-5) without objective clinical validation. Although patients with IIEF-5 scores below 21 were excluded, documentation of preoperative erectile function was limited. Interpretation of postoperative functional outcomes particularly in older patients should therefore be made with caution.

Interaction effects between covariates (e.g., surgical technique and pathological grade) were not evaluated, which may limit interpretation of combined influences on recurrence risk.

Finally, the findings may not be generalizable, as all surgeries were performed by a single surgeon at a single center. While follow-up was adequate for assessing biochemical recurrence, longer-term data are needed to draw definitive conclusions regarding oncologic durability and late functional outcomes.

Conclusion

Both antegrade and retrograde nerve-sparing techniques in open radical prostatectomy represent safe and effective options for the treatment of organ-confined prostate cancer. The retrograde approach was associated with shorter operative time, lower rates of biochemical recurrence, and a trend toward improved functional outcomes, whereas the antegrade technique offered superior intraoperative hemostasis. The choice of surgical technique should be individualized based on patient and tumor characteristics, as well as surgeon expertise. These findings warrant further validation in prospective, multicenter trials.

A preliminary version of this study was delivered as an oral presentation at the Turkish Association of Urology Scientific Meeting, held at İzmir Kâtip Çelebi University Faculty of Medicine in March 2025.

Ethics Committee Approval: Ethical clearance for this research (approval code: 2025/0172) was obtained from the Non-Interventional Clinical Research Ethics Board of İzmir Kâtip Çelebi University, Faculty of Medicine.

Informed Consent: Not applicable, as the study was conducted retrospectively using anonymized patient data.

Peer-review: Externally peer-reviewed.

Conflict of Interest: The authors declare that they have no competing interests that could have influenced the outcomes of this study.

Author Contributions: Concept: H.T.; Design: H.T., E.M.Y.; Supervision: S.N.G.; Materials: H.T., S.Ö., O.K.; Data Collection and Processing: H.T., E.M.Y., S.Ö.; Analysis and Interpretation: H.T.; Literature Search: H.T., O.K.; Writing Manuscript: S.Ö.; Critical Review: S.N.G., Y.A.

Financial Disclosure: This study received no funding or financial assistance during its conception, authorship, or publication process.

https://doi.org/10.5455/annalsmedres.2025.05.119

REFERENCES

1. Goolam AS, la Rosa AHD, Manoharan M. Surgical Management of Organ-Confined Prostate Cancer with Review of Literature and Evolving Evidence. *Indian J Surg Oncol.* 2018;9(2):225-231. doi: 10.1007/s13193-016-0594-1.
2. Nelson JB. Debate: Open radical prostatectomy vs. laparoscopic vs. robotic. *Urol Oncol.* 2007;25(6):490-493. doi: 10.1016/j.urolonc.2007.05.018.
3. Carbonara U, Srinath M, Crocerossa F, et al. Robot-assisted radical prostatectomy versus standard laparoscopic radical prostatectomy: an evidence-based analysis of comparative outcomes. *World J Urol.* 2021;39(10):3721-3732. doi: 10.1007/s00345-021-03687-5.
4. Pereira R, Joshi A, Roberts M, Yaxley J, Vela I. Open retropubic radical prostatectomy. *Transl Androl Urol.* 2021;9(6):3025-3035. doi: 10.21037/tau.2019.09.15.
5. Alivizatos G, Skolarikos A. Incontinence and erectile dysfunction following radical prostatectomy: a review. *ScientificWorldJournal.* 2005;5:747-758. doi: 10.1100/tsw.2005.94.
6. Kyriazis I, Spinos T, Tsaturyan A, Kallidonis P, Stolzenburg JU, Liatsikos E. Different Nerve-Sparing Techniques during Radical Prostatectomy and Their Impact on Functional Outcomes. *Cancers (Basel).* 2022;14(7):1601. doi: 10.3390/cancers14071601.
7. Cathelineau X, Sanchez-Salas R, Barret E, et al. Radical prostatectomy: evolution of surgical technique from the laparoscopic point of view. *Int Braz J Urol.* 2010;36(2):129-139. doi: 10.1590/S1677-55382010000200002.
8. Delto JC, Wayne G, Yanes R, Nieder AM, Bhandari A. Reducing robotic prostatectomy costs by minimizing instrumentation. *J Endourol.* 2015;29(5):556-560. doi: 10.1089/end.2014.0533.
9. Yilmaz Y, Kose O, Can E, et al. Comparative outcomes of antegrade open radical prostatectomy with electrosurgical devices versus retrograde technique without devices. *Ann Med Res.* 2020;27(2):442-7. doi: 10.5455/annalsmedres.2019.10.635.
10. Gomella LG, Kundavaram C. Radical Retropubic Prostatectomy. *Prostate Cancer: Science and Clinical Practice.* 2016:265-273. doi: 10.1016/B978-0-12-800077-9.00030-X.
11. Chopra S, Srivastava A, Tewari A. Robotic radical prostatectomy: The new gold standard. *Arab J Urol.* 2012;10(1):23-31. doi: 10.1016/j.aju.2011.12.005.
12. Wang Y, Cheng X, Xiong Q, Cheng S. The progress of dorsal vascular complex control strategy in radical prostatectomy. *J Int Med Res.* 2023;51(2):3000605231152091. doi: 10.1177/03000605231152091.
13. Carini M, Masieri L, Minervini A, Lapini A, Serni S. Oncological and Functional Results of Antegrade Radical Retropubic Prostatectomy for the Treatment of Clinically Localised Prostate Cancer. *Eur Urol.* 2008;53(3):554-61. doi: 10.1016/j.eururo.2007.07.004.
14. de Carvalho PA, Barbosa JABA, Guglielmetti GB, et al. Retrograde Release of the Neurovascular Bundle with Preservation of Dorsal Venous Complex During Robot-assisted Radical Prostatectomy: Optimizing Functional Outcomes. *Eur Urol.* 2020;77(5):628-635. doi: 10.1016/j.eururo.2018.07.003.
15. Ko YH, Coelho RF, Sivaraman A, et al. Retrograde versus antegrade nerve sparing during robot-assisted radical prostatectomy: Which is better for achieving early functional recovery? *Eur Urol.* 2013;63(1):169-177. doi: 10.1016/j.eururo.2012.09.051.
16. Kao TC, Cruess DF, Garner D, et al. Multicenter patient self-reporting questionnaire on impotence, incontinence and stricture after radical prostatectomy. *J Urol.* 2000;163(3):858-864. doi: 10.1016/S0022-5347(05)67819-6.
17. Carlsson S, Nilsson AE, Schumacher MC, et al. Surgery-related Complications in 1253 Robot-assisted and 485 Open Retropubic Radical Prostatectomies at the Karolinska University Hospital, Sweden. *Urology.* 2010;75(5):1092-1097. doi: 10.1016/j.urology.2009.09.075.
18. Kundu SD, Roehl KA, Eggener SE, Antenor JA V., Han M, Catalona WJ. Potency, continence and complications in 3,477 consecutive radical retropubic prostatectomies. *J Urol.* 2004;172(6 Pt 1):2227-2231. doi: 10.1097/01.ju.0000145222.94455.73.

https://doi.org/10.5455/annalsmedres.2025.05.119

Ann Med Res

Current issue list available at Ann Med Res

Annals of Medical Research

journal page: annalsmedres.org

Evaluation of clinical, radiological characteristics, and treatment outcomes of pediatric pseudotumor cerebri syndrome cases

Arzu Eroglu [a,*], Demet Aydogdu [b], Ahmet Guven [c], Huseyin Caksen [c]

[a]Balıkesir Atatürk City Hospital, Clinic of Pediatrics, Division of Pediatric Neurology, Balıkesir, Türkiye
[b]Necmettin Erbakan University, Meram Faculty of Medicine, Department of Radiology, Konya, Türkiye
[c]Necmettin Erbakan University, Meram Faculty of Medicine, Department of Pediatrics, Division of Pediatric Neurology, Konya, Türkiye
*Corresponding author: mdarzueroglu@hotmail.com (Arzu Eroglu)

MAIN POINTS

- Headache, vomiting, and visual disturbances are the most common symptoms of pediatric PTCS.
- High-dose acetazolamide, initiated early, can prevent long-term visual complications.
- MRI findings such as empty sella and optic nerve sheath distension support diagnosis in the absence of papilledema.
- Secondary PTCS is often associated with medications (e.g., cyclosporine) and vitamin imbalances.
- OCT and visual field testing are critical for monitoring treatment response.

Cite this article as: Eroglu A, Aydogdu D, Guven A, Caksen H. Evaluation of clinical, radiological characteristics, and treatment outcomes of pediatric pseudotumor cerebri syndrome cases. *Ann Med Res*. 2025;32(11):506–511. doi: 10.5455/annalsmedres.2025.05.129.

ABSTRACT

Aim: This study aims to evaluate the clinical, radiological, and treatment outcomes of pediatric patients diagnosed with Pseudotumor Cerebri Syndrome.

Materials and Methods: This retrospective study included 21 children diagnosed with definite or possible Pseudotumor Cerebri Syndrome according to the revised Friedman diagnostic criteria, out of 115 patients evaluated between 2017 and 2019 at a pediatric neurology clinic. Clinical findings, radiological features, treatment responses, and prognosis were analyzed.

Results: The study cohort was predominantly female (85.7%), with a mean age of 12.8 years. The most common presenting symptoms were headache, visual disturbances, and vomiting. A key diagnostic finding was elevated cerebrospinal fluid (CSF) opening pressure (>280 mmH_2O), observed in 67% of patients. Two-thirds of the cases (66.6%) were classified as Primary Pseudotumor Cerebri Syndrome, while the remaining third (33.4%) were secondary, most frequently attributed to drug exposure or vitamin imbalances. The majority of patients showed significant clinical improvement following medical treatment with high-dose acetazolamide. Only a few required adjunctive therapies such as topiramate or corticosteroids, and recurrence was documented in only a single case. Additionally, MRI findings supportive of the diagnosis were present in a subset of patients.

Conclusion: Early diagnosis and treatment of Pseudotumor Cerebri Syndrome in children can prevent permanent visual complications. A multidisciplinary approach, including ophthalmology and pediatric neurology, is essential for accurate diagnosis, effective treatment, and favorable outcomes.

Keywords: Pseudotumor cerebri syndrome, Pediatric neurology, Increased intracranial pressure, Acetazolamide treatment, Papilledema

Received: May 21, 2025 **Accepted:** Sep 17, 2025 **Available Online:** Nov 25, 2025

INTRODUCTION

Pseudotumor cerebri syndrome (PTCS), also known as idiopathic intracranial hypertension, is a rare but significant condition in children, with an incidence of approximately 0.6–0.71 per 100,000 [1,2]. It is characterized by increased intracranial pressure (ICP) in the absence of structural brain lesions, hydrocephalus, or central nervous system infection, and typically presents with headache, nausea, vomiting, and visual disturbances [3].

The etiology is multifactorial; obesity, rapid weight gain, certain medications (e.g., tetracyclines, corticosteroids, vitamin A derivatives), and systemic diseases are among the risk factors [4–6]. One proposed mechanism is the impaired absorption of cerebrospinal fluid (CSF) at the level of the arachnoid villi [7-9].

In 2013, Friedman et al. [2] proposed revised diagnostic criteria incorporating clinical, radiological, and CSF pressure measurements, which are now widely used in pediatric practice. Early diagnosis is of critical importance, as delayed treatment may lead to irreversible vision loss [10,11].

This study aims to describe the demographic, clinical, radiological, and treatment characteristics of pediatric PTCS pa-

tients followed in a tertiary care center in Turkey and to compare the findings with established diagnostic frameworks, including the revised Friedman criteria.

MATERIALS AND METHODS

This retrospective study was conducted at the Pediatric Neurology Department of Necmettin Erbakan University Meram Medical Faculty between January 2017 and January 2019. Patient records were reviewed based on International Classification of Diseases (ICD) codes H53, H54.0, H47.1, R51, and G93.2 to identify cases potentially related to increased intracranial pressure.

A total of 115 pediatric patients were initially identified. Of these, 21 met the revised Friedman criteria for definite or possible PTCS. Data collected included age, gender, presenting symptoms, imaging findings, etiology, treatment modalities, and clinical outcomes.

The required minimum sample size was calculated using G*Power 3.1 software for a two-tailed Mann–Whitney U test, with an alpha error of 0.05, a desired power of 0.80, and a large effect size (Cohen's d = 0.8) based on previous pediatric PTCS studies. This calculation yielded a minimum sample size requirement of 42 participants (21 per group). In our study, 21 children met the diagnostic criteria for PTCS. Post-hoc power analysis for the comparison of CSF opening pressure between definitive and possible PTCS cases demonstrated a very large effect size (Cohen's d = 2.58) and a power of 0.998, indicating that our sample size was sufficient to detect clinically significant differences in this primary outcome despite the rarity of the condition.

Lumbar punctures (LP) were performed in the lateral decubitus position under sedation by the same pediatric neurologist, and cerebrospinal fluid (CSF) opening pressures were recorded. A CSF opening pressure $\geq$280 mmH_2O was considered elevated [1,12].

Vitamin D deficiency was defined as <20 ng/mL, and insufficiency as 20–30 ng/mL. Normal vitamin A levels were considered 26–49 μg/dL. Papilledema severity was graded as mild (grades 1–2) or severe (grades 3–4).

Neuroimaging findings were evaluated based on six criteria from Friedman's diagnostic framework: empty sella, optic nerve tortuosity and perineural fluid distension, optic disc flattening or bulging, Meckel's cave and cavernous sinus enlargement, transverse sinus stenosis, and enlarged arachnoid villi. All imaging studies were reviewed and interpreted by a single pediatric radiologist.

Treatment responses were assessed through clinical examination, optical coherence tomography (OCT), and visual field testing. Patients were followed at 1, 3, 6, and 12 months after treatment initiation. Recurrence within the first-year post-treatment was also evaluated.

Ethical approval was obtained from the Non-Pharmaceutical and Non-Medical Device Research Ethics Committee of Necmettin Erbakan University Meram Medical Faculty (Approval No: 2019/1657).

Statistical analysis

Statistical analyses were performed using IBM SPSS Statistics for Windows, Version 21 (Armonk, NY: IBM Corp.). Descriptive data are presented as frequencies and percentages. Continuous variables were expressed as median (minimum–maximum) in line with data distribution, and compared between primary and secondary PTCS groups using the Mann–Whitney U test for nonparametric data and the chi-square test (exact method) for categorical variables. A p-value <0.05 was considered statistically significant.

RESULTS

A total of 115 pediatric patients were screened, and 21 were diagnosed with definite or possible Pseudotumor Cerebri Syndrome (PTCS) according to the revised diagnostic criteria by Friedman et al. [2]. Of these, 18 (85.7%) were female and 3 (14.3%) were male, with a mean age of 12.8 years (range: 3–17 years). The most common presenting symptoms were headache, vomiting, and blurred vision. Elevated cerebrospinal fluid (CSF) opening pressure (>280 mmH_2O) was observed in 67% (14/21) of patients.

Fourteen patients (66.7%) were classified as primary PTCS, and seven (33.3%) as secondary PTCS. In the secondary group, drug exposure—particularly cyclosporine and growth hormone therapy—was the leading etiology (43%) [13]. Due to incomplete medical records, obesity status could not be assessed for patients in the primary PTCS group.

Seven patients (33.3%) were categorized as "possible PTCS." The demographic characteristics, clinical findings, and diagnostic classification details are presented in Table 1. In patients without papilledema or with normal CSF pressure, brain MRI findings were evaluated separately. Severe papilledema (grades 3–4) was present in 8 patients (38.1%) Table 2. Radiological findings among "possible PTCS" patients included optic disc flattening/bulging in 5 patients (71%), empty sella in 4 patients (57%), optic nerve tortuosity with perineural fluid accumulation in 2 patients (29%), Meckel's cave and cavernous sinus enlargement in 1 patient (14%), and enlarged arachnoid villi in 1 patient (14%) [14,15]. Transverse sinus stenosis was not observed in any patient, likely due to incomplete MR venography studies. Representative MRI findings of PTCS patients are shown in Figure 1.

Initial treatment consisted of high-dose acetazolamide (30 mg/kg/day in three divided doses). Topiramate was used in patients with acetazolamide intolerance or insufficient response. Of the 12 patients initially treated with acetazolamide, 2 required switching to topiramate due to metabolic acidosis. In 3 patients with elevated CSF pressure and severe papilledema (grades 3–4), corticosteroids were added to acetazolamide. In 4 patients, treatment was limited to removal of

https://doi.org/10.5455/annalsmedres.2025.05.129

Table 1. Demographic, etiological, and clinical characteristics of the patients.

Patient	Sex	Age (years)	Complaint	NE	ES	MRI Findings	BOSp (cmH_2O)	Etiology	Additional Findings	Friedman Diagnosis
1	F	9	Headache + Diplopia	N	+	None	35	Primary	-	Definitive
2	F	15	Headache, N/V, VLS	N	+	3*	35	Secondary	Cyclosporine	Definitive
3	F	10	Headache, N/V, VLS	N	+	2,3*	12	Primary	-	Possible
4	F	9	Headache, N/V, VLS	N	+	1*	25	Primary	-	Possible
5	F	11	Headache, N/V, VLS	N	+	None	22	Primary	-	Possible
6	M	8	Headache, N/V, VLS	N	+	1,2*	29	Secondary	Vitamin A deficiency	Definitive
7	F	13	Headache, N/V, VLS	N	+	1,2*	28	Primary	-	Definitive
8	F	14	Headache, N/V, VLS	N	+	1,2*	32	Secondary	Hyperthyroidism	Definitive
9	F	17	Headache, N/V, VLS	N	+	None	35	Secondary	Vitamin B12 deficiency	Definitive
10	F	15	Headache, N/V, VLS	N	+	None	40	Primary	-	Definitive
11	M	16	Headache, N/V, VLS	N	+	1,2*	28	Primary	-	Definitive
12	F	17	Headache, N/V, VLS	N	+	2*	31	Primary	-	Definitive
13	F	17	Headache, N/V, VLS	N	+	1,3*	15	Primary	-	Possible
14	F	16	Headache, N/V, VLS	N	+	None	38	Primary	-	Definitive
15	F	11	Headache, N/V, VLS	N	+	6*	24	Secondary	Growth hormone	Possible
16	F	17	Headache, N/V, VLS	N	+	3,4*	26	Primary	-	Possible
17	M	3	Headache, N/V, VLS	N	+	1-4*	28	Secondary	Growth hormone	Definitive
18	F	15	Headache, N/V, VLS	N	+	4*	31	Secondary	DiGeorge Syndrome	Definitive
19	F	11	Headache, N/V, VLS	N	+	1,2,3*	-	Primary	-	Possible
20	F	17	Headache, N/V, VLS	N	+	None	32	Primary	-	Definitive
21	F	9	Headache, N/V, VLS	N	+	None	29	Primary	-	Definitive

*NE: Neurological Examination; ES: Eye Signs (Papilledema); MRI: Magnetic Resonance Imaging findings; BOSp: Cerebrospinal Fluid Opening Pressure; AF: Additional Findings; N/V: Nausea/Vomiting; VLS: Visual Loss Symptoms.

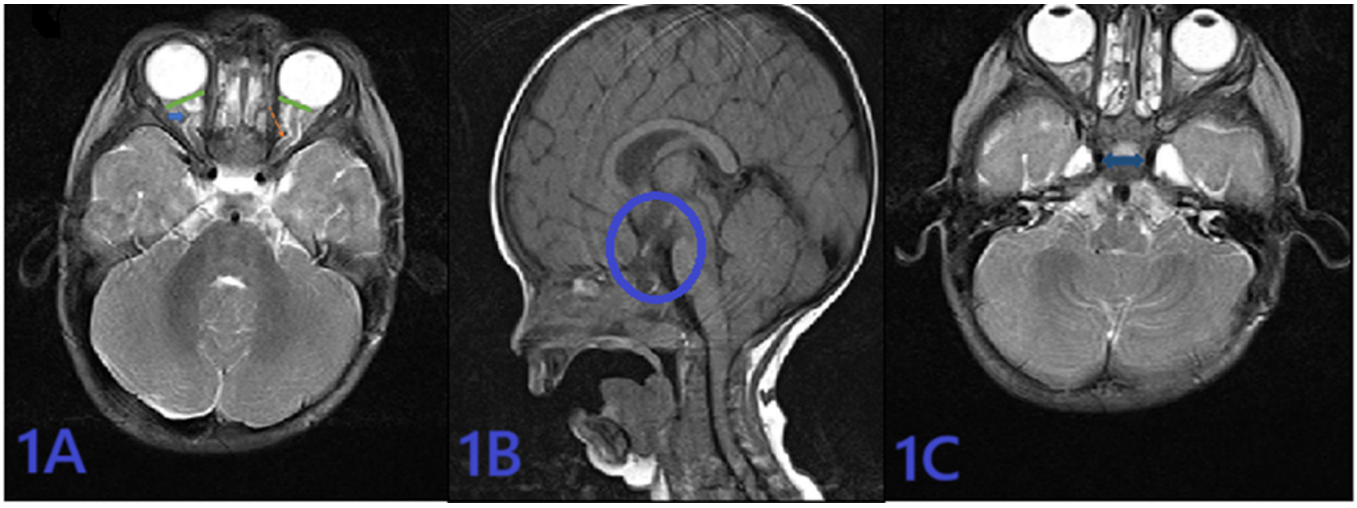

Figure 1. Brain MRI Findings in Patients with PTCS; 1A: Axial T2-weighted images showing bilateral optic nerve tortuosity, increased perineural fluid, and flattening/bulging of the optic disc. 1B: Sagittal T1-weighted images showing an empty sella appearance with the suprasellar cistern extending toward the pituitary. 1C: Axial T2-weighted images demonstrating bilateral enlargement of Meckel's cave spaces.

the underlying etiology (e.g., discontinuation of growth hormone therapy, correction of vitamin deficiencies) [16,17].

Treatment monitoring included clinical evaluation, optical coherence tomography (OCT), and visual field testing. Follow-up visits were scheduled at week 2, and at 1, 3, and 6 months, with a final evaluation at 1 year. Treatment adjustments were made based on clinical status at week 2 and visual field results at month 1. Most patients demonstrated marked improvement within 3 months. Patients with mild papilledema (grades 1–2) had no visual field loss and recovered by month 1, while those with severe papilledema (grades 3–4) improved by month 3.

Only one patient, with secondary PTCS due to cyclosporine toxicity, experienced recurrence within the one-year follow-up period [13]. Patients with mild papilledema and no significant MRI findings responded well to medical treatment alone. Conversely, patients with severe papilledema or notable MRI findings required lumbar puncture and closer follow-up.

No statistically significant differences were found between primary and secondary PTCS groups regarding CSF opening pressure (p=0.80), sex (p=0.18), or age (p=0.30) Table 3. A graphical summary of patient selection, classification, clinical and radiological findings, and treatment outcomes is provided

https://doi.org/10.5455/annalsmedres.2025.05.129

Table 2. Characteristics of patients defined according to possible PTCS criteria.

Etiology	Papilledema Grade	CSF Pressure (cmH_2O)	Brain MRI Findings*
Primary PTCS	Grade 3	12	2,3
Primary PTCS	Grade 2	25	1
Primary PTCS	Grade 2	22	-
Primary PTCS	Grade 2	15	1,3
Primary PTCS	-	26	3,4
Primary PTCS	Grade 2	-	1,2,3
Secondary PTCS†	Grade 2	24	6

*MRI findings based on PTCS-specific criteria: (1) Empty sella, (2) Optic nerve tortuosity with increased perineural fluid, (3) Optic disc flattening and bulging, (4) Meckel's cave and cavernous sinus enlargement, (5) Transverse sinus stenosis, (6) Enlarged arachnoid villi. † Secondary PTCS due to growth hormone use.

Table 3. Demographic and Cerebrospinal Fluid (CSF) pressure characteristics of primary and secondary PTCS patients.

Characteristics	Primary PTCS (n=14)	Secondary PTCS (n=7)	p-value
Gender (F/M)	13 / 1	5 / 2	0.18
Age (years)	13(9-17)	15(3-17)	0.30
CSF Pressure (cmH_2O)	26(12-40)	28.5 (15-38)	0.80

in Figure 2.

DISCUSSION

This study provides a comprehensive overview of pediatric Pseudotumor Cerebri Syndrome (PTCS), reaffirming key clinical, radiological, and therapeutic characteristics in agreement with previously published literature. Similar to earlier reports, our data show a predominant female representation (85.7%) and a mean age of 12.8 years, highlighting the susceptibility of adolescent girls to PTCS [1,3,4,17]. Headache, vomiting, and visual disturbances were the most frequent presenting symptoms, consistent with hallmark features of increased intracranial pressure (ICP) described in prior studies [3,9,18].

Two-thirds of our cohort were diagnosed with primary PTCS, and one-third with secondary PTCS, a distribution comparable to earlier epidemiological findings [6,15,19]. Secondary cases were most often associated with cyclosporine use, growth hormone therapy, and vitamin imbalances (particularly excess vitamin A and vitamin D deficiency) [16,13,20]. The only recurrence during follow-up occurred in a patient with cyclosporine-induced PTCS, underlining the necessity of identifying and eliminating underlying etiologies [13].

Papilledema grade emerged as an important prognostic indicator. Severe papilledema (grades 3–4) was linked to more pronounced symptoms, higher rates of visual field defects, and increased need for combination therapy—findings consistent with Tovia et al. and other literature that emphasize the correlation between papilledema severity and treatment intensity [10,21].

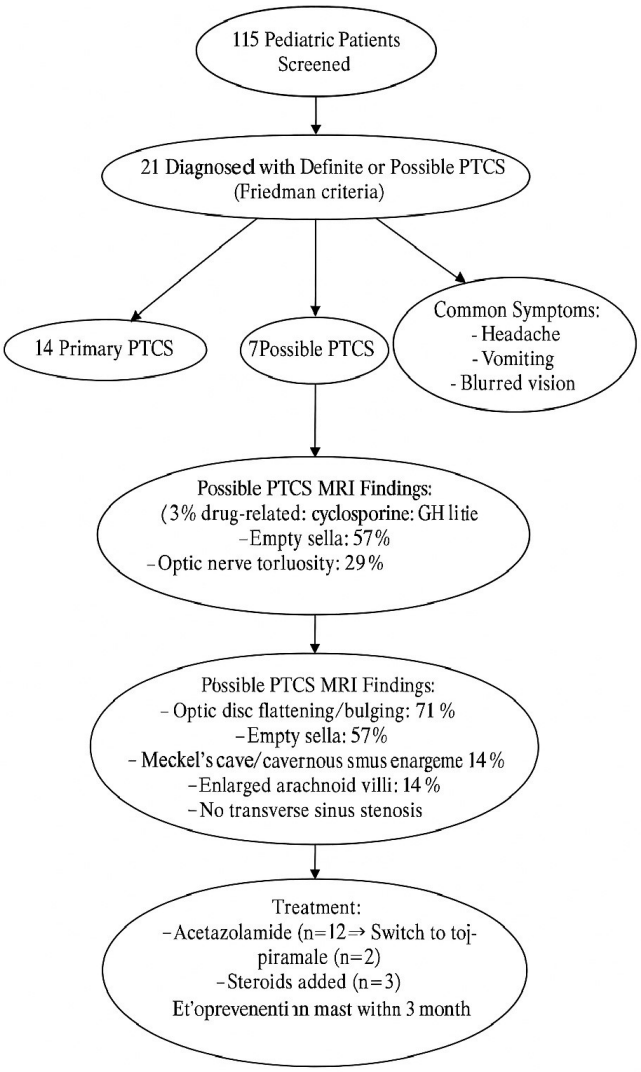

Figure 2. Study Flow Diagram; Flowchart illustrating the study process, from initial screening of 115 pediatric patients to final classification into definite or possible PTCS according to the revised Friedman criteria. The figure summarizes demographic distribution, key presenting symptoms, cerebrospinal fluid (CSF) pressure findings, major radiological signs, and the division into primary and secondary PTCS groups. Treatment modalities (acetazolamide, topiramate, corticosteroids, and etiology-specific interventions) and follow-up outcomes, including recurrence, are also depicted.

Neuroimaging played a pivotal role, especially in "possible PTCS" cases without papilledema. The most common findings—optic disc flattening, empty sella, and optic nerve sheath distension—align with the revised Friedman criteria [2] and were similarly highlighted by Görkem et al. and Maralani et al. [14,15]. Transverse sinus stenosis was absent, likely due to incomplete MR venography, as noted in other cohorts [15,20].

Pharmacological management yielded favorable outcomes. High-dose acetazolamide remained the primary therapy and was effective in most cases, confirming results from Celebisoy et al. [11]. Topiramate and corticosteroids were effective alternatives when acetazolamide was ineffective or poorly tolerated [12]. Only one patient required surgical intervention,

https://doi.org/10.5455/annalsmedres.2025.05.129

supporting prior observations that medical therapy is generally sufficient in pediatric PTCS [10].

Continuous ophthalmologic monitoring using optical coherence tomography (OCT) and visual field testing allowed for objective assessment of treatment efficacy and early detection of complications, as emphasized in pediatric PTCS management guidelines [17,21].

Our results align with international findings but also provide region-specific data from a Turkish tertiary center. Comparable demographic and clinical patterns reported by Değerliyurt et al. and Sager et al. support the applicability of the Friedman criteria in diverse populations [20,21].

Strengths of this study include standardized diagnostic protocols, consistent follow-up, and a uniform treatment approach. Limitations involve the retrospective design, single-center scope, relatively small sample size, and incomplete data on obesity and MR venography, which may have restricted further subgroup analysis.

Despite these limitations, our findings contribute to the understanding of pediatric PTCS, underscore the value of Friedman's diagnostic framework, and emphasize the importance of multidisciplinary management involving pediatric neurology, ophthalmology, and radiology to optimize outcomes.

CONCLUSION

This study highlights the clinical and radiological spectrum of pediatric PTCS and supports the diagnostic utility of the revised Friedman criteria. High-dose acetazolamide is confirmed as an effective first-line therapy, with OCT and visual field monitoring essential for preventing long-term visual impairment. Radiological features particularly optic disc bulging and empty sella are useful in diagnosing cases without papilledema. Radiological examples (Figure 1) illustrate the role of MRI in confirming diagnosis. A multidisciplinary approach ensures timely intervention and improved prognosis. Further multicenter, prospective studies are warranted to validate and expand these findings.

Ethics Committee Approval: This study was approved by the Ethics Committee of Necmettin Erbakan University Meram Faculty of Medicine (Approval No: 2019/1657).

Informed Consent: Since the study is a retrospective study, informed consent is not required.

Peer-review: Externally peer-reviewed.

Conflict of Interest: The authors declare that they have no conflict of interest.

Author Contributions: AE: Conseption, Design, Materials, Analysis and Interpretation, Data Collection and Precessing, Literature Review, Writing; DA: Supervision, Analysis and Interpretation, Literature Review, Critical Review; ASG: Supervision, Critical Review; HC: Supervision, Critical Review.

Financial Disclosure: No financial support was received for this study.

REFERENCES

1. Per H, Canpolat M, Gümüş H, et al. Clinical spectrum of the pseudotumor cerebri in children: etiological, clinical features, treatment and prognosis. *Brain Dev.* 2013;35(6):561–8. doi: 10.1016/j. braindev.2012.08.008.
2. Friedman DI, Liu GT, Digre KB. Revised diagnostic criteria for the pseudotumor cerebri syndrome in adults and children. *Neurology.* 2013;81(13):1159–65. doi: 10.1212/WNL.0b013e3182a55f17.
3. Standridge SM. Idiopathic intracranial hypertension in children: a review and algorithm. *Pediatr Neurol.* 2010;43(5):377–90. doi: 10.1016/j. pediatrneurol.2010.08.001.
4. Couch R, Camfield PR, Tibbles JA. The changing picture of pseudotumor cerebri in children. *Can J Neurol Sci.* 1985;12(1):48–50. doi: 10.1017/s0317167100046588.
5. Benzimra JD, Simon S, Sinclair AJ, Mollan SP. Sight-threatening pseudotumour cerebri associated with excess vitamin A supplementation. *Pract Neurol.* 2015;15(1):72–3. doi: 10.1136/practneurol-2014-000934.
6. Distelmaier F, Tibussek D, Schneider DT, Mayatepek E. Seasonal variation and atypical presentation of idiopathic intracranial hypertension in prepubertal children. *Cephalalgia.* 2007;27(12):1261–4. doi: 10.1111/j.1468-2982.2007.01442.x.
7. Aylward SC, Way AL. Pediatric intracranial hypertension: a current literature review. *Curr Pain Headache Rep.* 2018;22(2):14. doi: 10.1007/s11916-018-0665-9.
8. Hamedani AG, Witonsky KFR, Cosico M, et al. Headache characteristics in children with pseudotumor cerebri syndrome. *Headache.* 2018;58(9):1339–46. doi: 10.1111/head.13362.
9. Tibussek D, Schneider DT, Vandemeulebroecke N, et al. Clinical spectrum of the pseudotumor cerebri complex in children. *Childs Nerv Syst.* 2010;26(3):313–21. doi: 10.1007/s00381-009-1018-0.
10. Tovia E, Reif S, Oren A, et al. Treatment response in pediatric patients with pseudotumor cerebri syndrome. *J Neuroophthalmol.* 2017;37(4):393–7. doi: 10.1097/WNO.0000000000000512.
11. Celebisoy N, Gökçay F, Sirin H, Akyürekli O. Treatment of idiopathic intracranial hypertension: Topiramate vs acetazolamide, an open-label study. *Acta Neurol Scand.* 2007;116(5):322–7. doi: 10.1111/j.1600-0404.2007.00892.x.
12. Orssaud C, Dureau P, Zerah M, et al. Benign childhood intracranial hypertension. *J Fr Ophtalmol.* 2001;24(1):54–9. PMID: 11240472.
13. Costa KM, Almeida JB, Félix RH, Silva Júnior MF. Pseudotumor cerebri associated with cyclosporin use following renal transplantation. *J Bras Nefrol.* 2010;32(1):136–9. doi: 10.1590/S0101-28002010000100023.
14. Görkem SB, Doğanay S, Canpolat M, et al. MR imaging findings in children with pseudotumor cerebri and comparison with healthy controls. *Childs Nerv Syst.* 2015;31(3):373–80. doi: 10.1007/s00381-014-2579-0.
15. Maralani PJ, Hassanlou M, Torres C, et al. Accuracy of brain imaging in the diagnosis of idiopathic intracranial hypertension. *Clin Radiol.* 2012;67(7):656–63. doi: 10.1016/j. crad.2012.01.020.
16. Morente GB, Sánchez JT, Colmenero CG, García EM, Molina-Carballo A. Pseudotumor cerebri associated with cyclosporine use in severe atopic dermatitis. *Pediatr Dermatol.* 2015;32(2):237–9. doi: 10.1111/pde.12273.
17. Wall M, Kupersmith MJ, Kieburtz KD, et al. The idiopathic intracranial hypertension treatment trial: clinical profile at baseline. *JAMA Neurol.* 2014;71(6):693–701. doi: 10.1001/jamaneurol.2014.133.
18. Barmherzig R, Szperka CL. Pseudotumor cerebri syndrome in children. *Curr Pain Headache Rep*. 2019;23(8):58. doi: 10.1007/s11916-019-0795-8.
19. Masri A, Jaafar A, Noman R, et al. Intracranial hypertension in children: etiologies, clinical features, and outcome. *J Child Neurol.* 2015;30(12):1562–8. doi: 10.1177/0883073815574332.

https://doi.org/10.5455/annalsmedres.2025.05.129

20. Değerliyurt A, Teber S, Karakaya G, et al. Pseudotumor cerebri in children: experience of a tertiary care hospital. *Brain Dev.* 2014;36(8):690–9. doi: 10.1016/j. braindev.2013.09.005.

21. Sager G, Kaplan AT, Yalçin SÖ, et al. Evaluation of the signs and symptoms of pseudotumor cerebri syndrome in pediatric population. *Childs Nerv Syst.* 2021;37(10):3067–72. doi: 10.1007/s00381-021-05230-6.

https://doi.org/10.5455/annalsmedres.2025.05.129

Ann Med Res

Current issue list available at Ann Med Res

Annals of Medical Research

journal page: annalsmedres.org

Risk of hepatitis B reactivation in rheumatic patients receiving tocilizumab treatment

Bayram Kizilkaya [a], Osman Cure [b,*], Serdar Durak [c]

[a] Recep Tayyip Erdoğan University, Training and Research Hospital, Department of Internal Medicine, Rize, Türkiye
[b] Recep Tayyip Erdogan University, Faculty of Medicine, Department of Rheumatology, Rize, Türkiye
[c] Private Levent Hospital, Clinic of Gastroenterology, Istanbul, Türkiye
*Corresponding author: creosman61@gmail.com (Osman Cure)

MAIN POINTS

- No HBV reactivation was observed during tocilizumab therapy, one HBsAg-positive patient achieved HBsAg seroclearance under antiviral treatment.
- In HBsAg-negative/anti-HBc-positive patients, vigilant monitoring without routine antiviral prophylaxis may be sufficient, as no reactivation occurred in this group.
- These findings suggest that tocilizumab may have a low risk of HBV reactivation, though larger prospective studies are needed for confirmation.

Cite this article as: Kizilkaya B, Cure O, Durak S. Risk of hepatitis B reactivation in rheumatic patients receiving tocilizumab treatment. *Ann Med Res*. 2025;32(11):512–517. doi: 10.5455/annalsmedres.2025.05.106.

ABSTRACT

Aim: This study aimed to investigate the relationship between tocilizumab, a biological agent widely used for treating rheumatic diseases, and hepatitis B virus reactivation (HBVr).

Materials and Methods: The electronic records of all patients who received tocilizumab in our rheumatology outpatient clinic between July 2018 and August 2024 were retrospectively reviewed. Demographic data, baseline and followup HBV serological markers, liver biochemistry, and antiviral prophylaxis details were extracted and analyzed.

Results: A total of 54 patients were included (76.2 % female; mean age 57.5 ± 14.3 years). While HBsAg, anti-HBc IgGG and anti-HBs were requested for all patients before treatment, HBsAg was positive in 1 of 54 patients (1.9%) and anti-HBc IgG was positive in 26 (48.1%). While antiviral treatment was initiated in 10 (18.5%) of the patients, 9 were HBsAg negative, 1 was HBsAg positive, and 1 was anti-HBc Ig G positive. No patient experienced HBV reactivation during treatment; however, one HBsAg-positive patient achieved HBsAg seroclearance. The mean follow-up period was 50.5 ± 22.9 months.

Conclusion: No patient experienced HBV reactivation during tocilizumab therapy, and a single HBsAgpositive participant on prophylactic tenofovir achieved HBsAg seroclearance. These realworld data suggest that HBsAgnegative/antiHBcpositive individuals may be managed with vigilant biochemical and serological monitoring rather than routine antiviral prophylaxis during tocilizumab treatment. Nevertheless, the retrospective singlecentre design and modest sample size limit the strength and generalizability of these findings; larger prospective studies are required for definitive guidance.

Keywords: Rheumatological disease, Tocilizumab, Hepatitis B virus reactivation

Received: May 03, 2025 **Accepted:** Sep 26, 2025 **Available Online:** Nov 25, 2025

INTRODUCTION

Interleukin-6 (IL-6) is a crucial factor in the regulation of the immune system and is significantly involved in the development of inflammation, infections, and autoimmune disorders. In addition to its proinflammatory effects, IL-6 supports antiviral immunity by enhancing type I interferon signaling and promoting virus-specific $CD8^+$ T-cell responses. Tocilizumab (TCZ) is a monoclonal antibody designed to block the IL-6 receptor, thereby targeting the effects of IL-6. It is employed in the management of several rheumatic conditions, including rheumatoid arthritis, juvenile idiopathic arthritis, and giant cell arteritis [1,2]. IL-6 signaling modulates HBV replication in a context-dependent manner In vitro, IL6 can suppress the formation of covalently closed circular DNA (cccDNA) and reduce HBV transcripts via signal transducer and activator of transcription 3 (STAT3) activation [3]. Conversely, chronic IL6/STAT3 overactivation has been linked to hepatocarcinogenesis in human hepatitis B virus models [4]. This dual role raises the question of whether pharmacological IL6 blockade with tocilizumab could lift a natural brake on HBV replication and precipitate reactivation.

The suppressive effect of IL-6 on HBV replication suggests that tocilizumab treatment may increase the risk of reactivation, especially in latent HBV carriers [5,6]. Several factors affect the risk of HBV reactivation in patients receiving TCZ

treatment. Among these factors, being an HBV carrier, treatment duration, and immune response play an important role [7]. The long-term use of biological therapies for treating rheumatic diseases is a concern for physicians, especially in terms of the risk of HBV infection reactivation [8]. In addition, careful monitoring and early initiation of antiviral therapy are important to prevent HBV reactivation (HBVr) under tocilizumab therapy.

Although several small series from Asia and Western Europe suggest that the risk of HBV reactivation (HBVr) under tocilizumab therapy is lower than with TNF-α inhibitors, most cohorts include fewer than 30 antiHBcpositive patients and seldom report followup beyond 2 years. Moreover, data from countries with intermediate HBV endemicity, such as Türkiye, are scarce.

Therefore, this singlecentre retrospective study aims to provide longterm, realworld evidence on HBVr in tocilizumab treated rheumatic patients from an intermediate prevalence region, including the clinical course of an HBsAgpositive individual who achieved seroclearance.

MATERIALS AND METHODS

Study design and patient selection

This retrospective, single-center cohort study was conducted in the Rheumatology Outpatient Clinic of Recep Tayyip Erdoğan University Training and Research Hospital. All adults (≥ 18 years) who received at least three consecutive doses of tocilizumab for a rheumatic disease between July 1, 2018, and August 31, 2024 were screened. Tocilizumab was prescribed according to the established American College of Rheumatology/European League Against Rheumatism criteria for rheumatoid arthritis, adult-onset Still's disease, and other inflammatory arthritides.

Inclusion criteria

1. Age ≥ 18 years.
2. Receipt of tocilizumab for ≥ 3 months.
3. Complete baseline HBV serology (HBsAg, antiHBs, and antiHBc) within six months before therapy was available.

The exclusion criteria (Figure 1)

1. Tocilizumab exposure < 3 months.
2. Active malignancy or chemotherapy in the previous 12 months.
3. Positive for HCVRNA.
4. Missing baseline HBV tests or < 6 months of follow-up data.

HBV reactivation within the first two dosing cycles of tocilizumab has rarely been reported. Most published series indicate that events occur after ≥ 12 weeks of continuous exposure when cumulative immunomodulation becomes clinically relevant [9]. Therefore, patients who received < 3 months of TCZ were excluded to ensure a uniform exposure window in which reactivation could plausibly occur and to guarantee at least one scheduled HBVDNA assessment.

Because this was an exploratory real-world analysis, all eligible patients during the study window were included without an a priori sample size calculation.

Antiviral prophylaxis was initiated at the discretion of the treating physician (gastroenterology or infectious diseases specialist). In practice, all HBsAg-positive patients received prophylaxis, whereas HBsAg-negative/anti-HBc-positive patients received either prophylaxis or close monitoring. This approach reflects real-world variability and is broadly consistent with recommendations of international guidelines [8].

Data collection

Demographic variables (age, sex), primary rheumatic diagnosis, comorbidities, prior immunosuppressive therapy, tocilizumab initiation date, and longitudinal laboratory data (HBV serology, HBV DNA, liver enzymes) were retrieved from the hospital's electronic medical record system (Akgun®, version 25.4.) using a standardized casereport form. Two independent investigators crosschecked all entries for accuracy.

Serum HBVDNA was quantified at baseline, at months 3 and 6, and every six months thereafter. An unscheduled test was also performed whenever alanine aminotransferase (ALT) exceeded 2 × the upper limit of normal or when clinical hepatitis was suspected. This schedule followed the national HBV reactivation surveillance guidelines. Figure 1 shows the flow chart of the study participants.

The study protocol was approved by the Recep Tayyip Erdoğan University Ethics Committee (Approval No. 2024/219) and conformed to the principles of the Declaration of Helsinki.

Definitions and explanations

Within six months before initiating tocilizumab therapy, patients underwent HBV screening, including tests for HBsAg and anti-HBc. Individuals with HBsAg positivity for more than six months were classified as having chronic hepatitis B. Those who tested negative for HBsAg but positive for anti-HBc were considered to have a resolved HBV infection [10]. During patient follow-up, HBV reactivation was identified either by the emergence of detectable HBV DNA in those who initially had undetectable levels, indicating a significant rise—typically tenfold—or by a new onset of HBsAg positivity in individuals who were previously negative [9]. Hepatitis is characterized by a rise in serum alanine aminotransferase

https://doi.org/10.5455/annalsmedres.2025.05.106

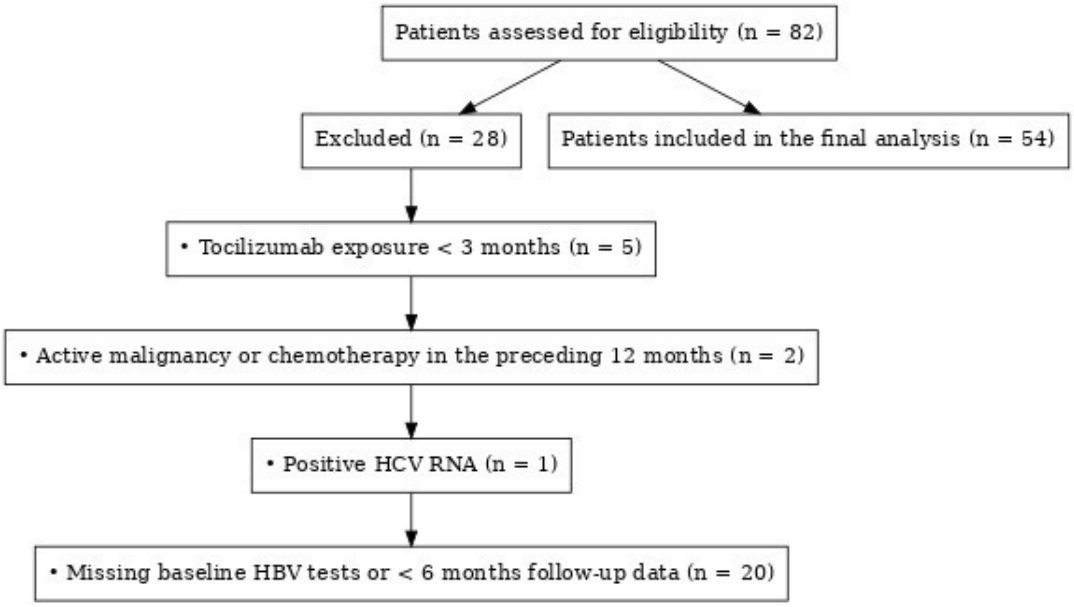

Figure 1. Flow chart of the study participants.

Table 1. Demographic and clinical characteristics of the patients included.

Variables		p
Male / Female, n (%)	12 (22.2) / 42 (77.8)	
Age, mean ± SD	57.52 ± 14.34	0.376
Male	54.25 ± 16.01	
Female	58.45 ± 13.90	
Rheumatological disease, n (%)		
Rheumatoid arthritis	49 (90.7)	
Adult Still's disease	2 (3.7)	
Temporal arteritis	1 (1.9)	
Polyarteritis Nodosa	1 (1.9)	
FMF	1 (1.9)	
Chronic diseases, n (%)		
HT	36 (66.7)	
DM	5 (9.3)	
CKD	2 (3.7)	
COPD	1 (1.9)	

FMF: Familial Mediterranean fever, HT: Hypertension, DM: Diabetes mellitus, CKD: Chronic kidney disease; COPD, chronic obstructive pulmonary disease.

(ALT) levels to three times or more above the normal upper limit, defined as ALT levels of 45 U/L [11]. HBV-related hepatitis was identified by the presence of liver inflammation accompanied by an increase in HBV DNA levels [12].

Blood immune and viral replication markers in hepatitis B

HBV-related markers in the blood, such as HBsAg, anti-HBs, and anti-HBc, were analyzed using the Roche Cobas e6001 system (Roche Diagnostics, Mannheim, Germany) using the electrochemiluminescence immunoassay technique. Serum HBV DNA was quantified through real-time PCR using the Rotor-Gene Q platform (QIAGEN, Hilden, Germany), with a detection threshold of 12 IU/mL. Standard biochemical tests were performed using a Cobas 8000 Modular Analyzer (Roche Diagnostics, Germany).

Statistical analysis

Statistical analysis was performed using the Statistical Package for the Social Sciences version 22 for Windows. The distribution of continuous variables was assessed using histograms, Q-Q plots, and normality tests (Shapiro-Wilk or Kolmogorov-Smirnov), depending on the number of variables. Continuous variables following a normal distribution are presented as mean ± standard deviation. The independent t-test was utilized to compare the two groups.

RESULTS

The study included 54 patients, of whom 76.2% were females, and the mean age was 57.52 ± 14.34 years. No significant difference was found in age between genders (p = 0.376). Patients most commonly received TCZ treatment due to RA (90.7%). The average follow-up duration was 50.5 ± 22.9 months, with high blood pressure (66.7%) and type 2 diabetes (9.3%) being the most prevalent comorbid conditions (Table 1).

Before treatment, HBsAg, anti-HBc IgGG and anti-HBs tests were requested for all patients. HBsAg and anti-HBc IgG were positive in 1 (1.9%) and 26 (48.1%) of 54 patients, respectively. Antiviral treatment was initiated in 10 (18.5%) of the patients, 6 with entecavir, 3 with tenofovir disoproxil, and 1 with tenofovir alafenamide. Of those who received treatment, nine were HBsAg negative and anti-HBc IgG positive, while 1 was HBsAg positive. While HBVr did not occur in any patient during the treatment, HB Ag seroclearance occurred in the HBs Ag-positive patient.

https://doi.org/10.5455/annalsmedres.2025.05.106

Patient with HBsAg seroclearance

A 47-year-old male patient has been followed up since 2007 due to adult Still's disease. The patient, who had no known chronic disease other than adult Still's disease and had previously received corticosteroid and methotrexate treatments, was started on tocilizumab treatment in 2020 and simultaneously on tenofovir alafenamide treatment. Before treatment, the patient was HBsAg positive, anti-HBe positive, and had a HBV DNA level of 1622 IU/ml. In the 43rd month of treatment, the patient was negative for HBsAg and HBV DNA.

DISCUSSION

Hepatitis B infection is an important health problem in society, and the risk of reactivation, especially among hepatitis B virus carriers, poses a significant safety concern. In addition, chronic hepatitis B infection causes serious complications, such as hepatocellular cancer (HCC) and cirrhosis, causing significant morbidity and mortality. HBV reactivation (HBVr) occurs when the immune response to the virus is retriggered. Conditions of immunosuppression, including the use of anti-tumor necrosis factor (TNF)-α inhibitors, tocilizumab (TCZ), corticosteroids, and other immunosuppressive treatments for rheumatological disorders, can lead to viral reactivation due to their detrimental effects on the immune system's ability to control HBV replication [6,7,13].

In the study conducted by Hong X. et al., the risk of HBVr was found to be low in patients with rheumatoid arthritis who were HBsAg negative/HBV core antibody positive and used TCZ, and it was stated that antiviral treatment was a safe option for prophylaxis [14]. In the study conducted by Rodríguez-Tajes S et al., in 44 HBsAg-negative/anti-HBc-positive patients with COVID-19 treated with TCZ, 61% of the patients received prophylactic entecavir, and HBV DNA positivity was detected in only one patient [15]. Another study reported that anti-HBs had a protective effect in patients with rheumatism treated with TCZ [16]. Studies have also emphasized the importance of early antiviral treatment initiation in preventing HBVr under TCZ treatment [17,18]. In our study, HBVr was not observed during tocilizumab treatment, which is similar to the findings in the literature. However, HBV serology performed before treatment and antiviral treatment initiation significantly reduced the risk of reactivation.

A potentially fatal case of HBV exacerbation has been reported in a patient with rheumatoid arthritis who was HBsAg positive following TCZ treatment [19]. HBVr is quite high in HBs-positive patients with TCZ. HBVr begins in the early stages of treatment with TCZ, and reactivation is almost negligible after the initiation of antiviral prophylaxis [20]. In our study, it was observed that hepatitis B could be controlled with antiviral treatment in patients positive for HBsAg. For example, in a 47-year-old adult patient with Adult Still's disease, tenofovir alafenamide treatment, initiated together with tocilizumab treatment, was found to be effective in providing HBV DNA and HBsAg seroclearance.

Numerous cytokines, such as IL-6, play a role in HBV infection progression. Abnormal IL-6 production has been observed in chronic inflammatory conditions such as hepatitis B and rheumatoid arthritis. IL-6 is a key factor in HBV replication and hepatitis B progression. It has been associated with both hepatitis B advancement and HBV entry and replication processes within the host. The risk of HBVr under TCZ treatment has been a controversial issue. While some studies suggest that IL-6 has a suppressive effect on HBV replication, TCZ may eliminate this suppressive effect and cause reactivation [21,22].

While in vitro data suggest that IL-6 may suppress HBV replication [3], leading to concerns that tocilizumab could theoretically unleash viral activity, our real-world findings do not support this in the context of diligent screening and monitoring. This discrepancy highlights the complexity of the role of IL-6 in HBV pathogenesis, which may differ significantly between in vitro models and complex in vivo human systems, especially when rheumatic disease activity and concomitant therapies simultaneously modulate other immune pathways. On the other hand, some studies have emphasized that HBVr can be prevented by initiating antiviral treatment and that such patients should be closely monitored during the treatment process [23,24]. Although HBVr was not observed in all patients in our study, it was concluded that HBV serological tests should be performed before treatment and antiviral treatment should be initiated. This is an important clinical strategy, especially for patients with HBV.

No HBV reactivation was observed in anti-HBc–positive patients receiving tocilizumab following CAR T-cell therapy, provided that regular HBV DNA monitoring was performed [25]. Isolated clinical observations suggest that IL6 receptor blockade may also benefit patients with postacute sequelae of severe acute respiratory syndrome coronavirus 2 (SARSCoV2) infection ("longCOVID"). In a recent case report, a woman with rheumatoid arthritis and persistent SARSCoV2 antigenemia experienced marked symptomatic and virological improvement after a short course of nirmatrelvir–ritonavir followed by tocilizumab therapy, without any evidence of HBV reactivation or hepatic flare [26]. These observations, together with our 50 month rheumatology cohort, indicate that IL-6 antagonism does not inherently trigger HBVr when evidence based screening and surveillance protocols are applied. Importantly, our study extends the mechanistic overview by Kishimoto & Kang (2022) by providing longterm, realworld data from an intermediate endemic region and by reporting—to our knowledge—the first instance of HBsAg seroclearance under combined tenofovir alafenamide and tocilizumab therapy.

The spontaneous loss of HBsAg in immunocompetent adults occurs at an estimated rate of 0.5%–1% per patient-year [27]. Although spontaneous seroclearance rates may

https://doi.org/10.5455/annalsmedres.2025.05.106

be slightly higher in HBeAg-negative individuals than in HBeAg-positive individuals, our patient's baseline HBeAg negativity coupled with an HBV DNA of 1622 IU/ml still indicated active infection requiring intervention. In contrast, long-term nucleos(t)ide analog (NA) therapy, such as tenofovir, accelerates seroclearance, with cumulative rates of 5%–12% after 3–5 years [28]. Our patient, who received tenofovir alafenamide concomitantly with tocilizumab, became negative for HBsAg after 43 months. This timeline is more consistent with NA-induced rather than spontaneous clearance. Therefore, while the case is clinically interesting, its significance should not be overemphasized, and causality cannot be proven from a single observation. Other factors—such as immune reconstitution once rheumatic disease activity was controlled—may also have contributed to this outcome.

From a healtheconomic perspective, modeling studies indicate that routine nucleos(t)ideanalog prophylaxis is costeffective only in HBsAgpositive patients or in antiHBcpositive individuals exposed to highrisk regimens, whereas close biochemical and virological surveillance is more costefficient than indefinite antiviral therapy in lowrisk antiHBcpositive/antiHBspositive patients [29, 30].

Limitations

This retrospective, singlecentre study enrolled a modest cohort (n = 54) without a parallel control group; therefore, the observed absence of reactivation cannot be causally attributed to tocilizumab exposure alone. The sample size limits statistical power, and the singlecentre setting may reduce generalizability. Potential information and referral biases inherent to ERRs also remain. Larger, prospective, multicenter studies with matched controls are needed to confirm these findings.

CONCLUSION

While no patient using tocilizumab developed hepatitis B reactivation, one patient who was positive for HBs Ag and receiving antiviral treatment developed HBs Ag seroclearance. Although these findings predict that patients with hepatitis B who do not receive antiviral treatment can be followed with careful monitoring after tocilizumab treatment, studies with larger samples are needed to reach definitive conclusions.

Ethics Committee Approval: The study was conducted in accordance with the principles of the Declaration of Helsinki and was approved by the Recep Tayyip Erdoğan University Local Ethics Committee (date: 15.08.2024, no: 2024/219).

Informed Consent: Since this was a retrospective study, informed consent was not obtained.

Peer-review: Externally peer-reviewed.

Conflict of Interest: All authors have no competing financial or nonfinancial interests related to this work.

Author Contributions: BK: Investigation, Writing Supervision, and Methodology. OC: Conceptualization and Writing. SD: Formal analysis and project administration.

Financial Disclosure: This research received no external funding, and all authors confirm that they did not receive any financial support from public, commercial, or notforprofit funding agencies.

REFERENCES

1. Kishimoto T, Kang S. IL-6 Revisited: From Rheumatoid Arthritis to CAR T Cell Therapy and COVID-19. *Annual Rev Immunol.* 2022;40:323-348. doi: 10.1146/annurev-immunol-101220-023458.
2. Aliyu M, Zohora FT, Anka AU, et al. Interleukin-6 cytokine: An overview of the immune regulation, immune dysregulation, and therapeutic approach. *Int Immunopharmacol.* 2022;111:109130. doi: 10.1016/j.intimp.2022.109130.
3. Palumbo GA, Scisciani C, Pediconi N, et al. IL-6 inhibits HBV transcription by targeting the epigenetic control of the nuclear cccDNA minichromosome. *PLoS One.* 2015;10(11):e0142599. doi: 10.1371/journal.pone.0142599.
4. Xu J, Lin H, Wu G, Zhu M, Li M. IL-6/STAT3 Is a Promising Therapeutic Target for Hepatocellular Carcinoma. *Front Oncol.* 2021;11:760971. doi: 10.3389/fonc.2021.760971.
5. Lau G, Yu ML, Wong G, et al. APASL clinical practice guideline on hepatitis B reactivation related to the use of immunosuppressive therapy. *Hepatol Int.* 2021;15(5):1031-1048. doi: 10.1007/s12072-022-10301-2.
6. Loomba R, Liang TJ. Hepatitis B Reactivation Associated With Immune Suppressive and Biological Modifier Therapies: Current Concepts, Management Strategies, and Future Directions. *Gastroenterology.* 2017;152(6):1297-1309. doi: 10.1053/j.gastro.2017.02.009.
7. Snast I, Atzmony L, Braun M, Hodak E, Pavlovsky L. Risk for hepatitis B and C virus reactivation in patients with psoriasis on biologic therapies: A retrospective cohort study and systematic review of the literature. *J Am Acad Dermatol.* 2017;77(1):88-97.e5. doi: 10.1016/j.jaad.2017.01.037.
8. European Association for the Study of the Liver. Electronic address: easloffice@easloffice.eu; European Association for the Study of the Liver. EASL 2017 Clinical Practice Guidelines on the management of hepatitis B virus infection. *J Hepatol.* 2017;67(2):370-398. doi: 10.1016/j.jhep.2017.03.021.
9. Mori S, Fujiyama S. Hepatitis B virus reactivation associated with Antirheumatic therapy: risk and prophylaxis recommendations. *World J Gastroenterol.* 2015;21(36):10274-10289. doi: 10.3748/wjg.v21.i36.10274.
10. Myint A, Tong MJ, Beaven SW. Reactivation of hepatitis B virus: a review of clinical guidelines. *Clin Liver Dis (Hoboken).* 2020;15(4):162-167. doi: 10.1002/cld.883.
11. Pauly MP, Tucker LY, Szpakowski JL, et al. Incidence of hepatitis B virus reactivation and hepatotoxicity in patients receiving long-term treatment with tumor necrosis factor antagonists. *Clin Gastroenterol Hepatol.* 2018;16(12):1964-1973. doi: 10.1016/j.cgh.2018.04.033.
12. Huang SC, Yang HC, Kao JH. Hepatitis B reactivation: diagnosis and management. *Expert Rev Gastroenterol Hepatol.* 2020;14(7):565-578. doi: 10.1080/17474124.2020.1774364.
13. Yip T.C., Gill M., Wong G.L., Liu K. Management of hepatitis B virus reactivation due to treatment of COVID-19. *Hepatol. Int.* 2022;16(2):257–268. doi: 10.1007/s12072-022-10306-x.
14. Hong X, Xiao Y, Xu L, Liu L, Mo H, Mo H. Risk of hepatitis B reactivation in HBsAg−/HBcAb+ patients after biologic or JAK inhibitor therapy for rheumatoid arthritis: A meta-analysis. *Immun Inflamm Dis.* 2023;11(2):e780. doi: 10.1002/iid3.780.
15. Rodríguez-Tajes S, Miralpeix A, Costa J, et al. Low risk of hepatitis B reactivation in patients with severe COVID-19 who receive immunosuppressive therapy. *J Viral Hepat.* 2021;28(1):89–94. doi: 10.1111/jvh.13410.

16. Ko PH, Kuo MH, Kao IT, Wu CY, Tseng CW, Shao SC. The Risk of Hepatitis B Virus Reactivation in Rheumatoid Arthritis Patients Receiving Tocilizumab: A Systematic Review and Meta-Analysis. *Viruses.* 2024;16(1):78. doi: 10.3390/v16010078.
17. Watanabe T, Tanaka Y. Reactivation of hepatitis viruses following immunomodulating systemic chemotherapy. *Hepatol Res.* 2013;43(2):113-21. doi: 10.1111/hepr.12014.
18. Bojito-Marrero L, Pyrsopoulos N. Hepatitis B and Hepatitis C Reactivation in the Biologic Era. *J Clin Transl Hepatol.* 2014;2(4):240-6. doi: 10.14218/JCTH.2014.00033.
19. Sonneveld MJ, Murad SD, van der Eijk AA, de Man RA. Fulminant Liver Failure due to Hepatitis B Reactivation during Treatment with Tocilizumab. *ACG Case Rep J.* 2019;6(12):e00243. doi: 10.14309/crj.0000000000000243.
20. Terrault NA, Lok ASF, McMahon BJ, et al. Update on prevention, diagnosis, and treatment of chronic hepatitis B: AASLD 2018 hepatitis B guidance. *Hepatology.* 2018;67(4):1560–1599. doi: 10.1002/hep.29800.
21. Fang YF, Chang SH, Kuo CF, See LC. Safety outcomes of tocilizumab and tofacitinib treatment for rheumatoid arthritis: Target trial emulation. *Int J Rheum Dis.* 2024;27(11):e15406. doi: 10.1111/1756-185X.15406.
22. Xia C, Liu Y, Chen Z, Zheng M. Involvement of Interleukin 6 in Hepatitis B Viral Infection. *Cell Physiol Biochem.* 2015;37(2):677-86. doi: 10.1159/000430386.
23. Smalls DJ, Kiger RE, Norris LB, Bennett CL, Love BL. Hepatitis B Virus Reactivation: Risk Factors and Current Management Strategies. *Pharmacotherapy.* 2019;39(12):1190-1203. doi: 10.1002/phar.2340.
24. Su YC, Lin PC, Yu HC, Wu CC. Antiviral prophylaxis during chemotherapy or immunosuppressive drug therapy to prevent HBV reactivation in patients with resolved HBV infection: a systematic review and meta-analysis. *Eur J Clin Pharmacol.* 2018;74(9):1111-1119. doi: 10.1007/s00228-018-2487-4.
25. Li P, Zhou L, Ye S, et al. Risk of HBV Reactivation in Patients With Resolved HBV Infection Receiving Anti-CD19 Chimeric Antigen Receptor T Cell Therapy Without Antiviral Prophylaxis. *Front Immunol.* 2021;12:638678. doi: 10.3389/fimmu.2021.638678.
26. Visvabharathy L, Orban ZS, Koralnik IJ. Case report: Treatment of long COVID with a SARS-CoV-2 antiviral and IL-6 blockade in a patient with rheumatoid arthritis and SARS-CoV-2 antigen persistence. *Front Med (Lausanne).* 2022;9:1003103. doi: 10.3389/fmed.2022.1003103.
27. Yeo YH, Ho HJ, Yang HI, et al. Factors Associated With Rates of HBsAg Seroclearance in Adults With Chronic HBV Infection: A Systematic Review and Meta-analysis. *Gastroenterology.* 2019;156(3):635-646.e9. doi: 10.1053/j.gastro.2018.10.027.
28. Maung ST, Decharatanachart P, Chaiteerakij R. Hepatitis B Surface Antigen Seroclearance Rate After Stopping Nucleos(t)ide Analogues in Chronic Hepatitis B-A Systematic Review and Meta-Analysis. *J Gastroenterol Hepatol.* 2025;40(5):1079-1104. doi: 10.1111/jgh.16920.
29. Hwang JP, Huang D, Vierling JM, et al. Cost-effectiveness analysis of hepatitis B virus screening and management in patients with hematologic or solid malignancies anticipating immunosuppressive cancer therapy. *JCO Clin Cancer Inform.* 2019;3:1-12. doi: 10.1200/CCI.18.00097.
30. Loomba R, Liang TJ. Hepatitis B reactivation associated with immunosuppressive and biological modifier therapies: management strategies and future directions. *Gastroenterology.* 2017;152(6):1297-1309. doi: 10.1053/j.gastro.2017.02.009.

https://doi.org/10.5455/annalsmedres.2025.05.106

Ann Med Res

Current issue list available at Ann Med Res

Annals of Medical Research

journal page: annalsmedres.org

Intraventricular migration of intraocular silicone oil: A rare case with computed tomography and magnetic resonance imaging findings

Ali Salbas [a],*, Bilgenur Aksoy [a], Mustafa Fazil Gelal [a]

[a]*Izmir Katip Celebi University, Ataturk Training and Research Hospital, Department of Radiology, Izmir, Türkiye*
**Corresponding author: dralisalbas@gmail.com (Ali Salbas)*

Cite this article as: Salbas A, Aksoy B, Gelal MF. Intraventricular migration of intraocular silicone oil: A rare case with computed tomography and magnetic resonance imaging findings. *Ann Med Res*. 2025;32(11):518–520. doi: 10.5455/annalsmedres.2025.08.215.

ABSTRACT

Intraocular silicone oil (SiO) is widely used as a long-term internal tamponade agent in the surgical treatment of various vitreoretinal disorders. A rare but diagnostically critical complication of SiO is its migration into the brain ventricles. Although few such cases have been reported, this condition may mimic serious pathologies, such as intraventricular hemorrhage. In this case report, intraventricular migration of SiO was identified in an 81-year-old woman with a history of vitreoretinal surgery for diabetic retinopathy–related retinal detachment. The patient presented with dizziness, imbalance, and nausea, and neuroimaging revealed hyperdense layering within the bilateral frontal horns on noncontrast brain computed tomography. These findings may mimic acute intraventricular hemorrhage, highlighting the importance of clinical and radiological correlation for accurate differential diagnosis. Additionally, the patient was concurrently diagnosed with a cerebellar infarction. Awareness of this rare complication may help prevent unnecessary interventions and potential treatment errors in patients presenting with stroke-like symptoms.

Keywords: Intraventricular migration, Silicone oil, Retinal surgery, Intraventricular silicone oil, Neuroimaging

Received: Aug 04, 2025 **Accepted:** Oct 27, 2025 **Available Online:** Nov 25, 2025

INTRODUCTION

Intraocular silicone oil (SiO) is a material widely used as a long-term internal tamponade in the surgical treatment of various vitreoretinal diseases, particularly complicated retinal detachments [1,2]. Its primary indications include proliferative vitreoretinopathy, retinal detachments secondary to diabetic retinopathy, and traumatic retinopathies [2]. The viscosity of SiO and the duration it remains in the eye are key factors that directly influence the risk of developing complications [1]. The most frequently reported ocular complications are cataract, glaucoma, keratopathy, and silicone oil emulsification [2]. The migration of SiO into the ventricular system is another rare but diagnostically important complication [3].

Williams et al first reported the migration of SiO into the ventricles in 1999 [4]. A recent review noted that to date, only 32 cases of intraventricular SiO migration have been reported in the literature [5].

SiO intraventricular migration is mostly asymptomatic and is often incidentally detected during brain imaging performed for unrelated reasons [3]. However, on computed tomography (CT), it may appear as hyperdense layering that can mimic intraventricular hemorrhage (IVH), posing a risk for misdiagnosis and potentially unnecessary interventions [6]. Therefore, a history of previous vitreoretinal surgery plays a critical role in accurately interpreting these imaging findings.

In this case report, we present the intraventricular migration of SiO in a patient with a history of vitreoretinal surgery for diabetic retinopathy-related retinal detachment, who was simultaneously diagnosed with cerebellar infarction. The findings were demonstrated using CT and magnetic resonance imaging (MRI). Given the limited number of reported cases in the literature, this rare complication is shared for its potential to contribute to radiologic differential diagnosis and to emphasize its importance in clinical awareness. This case was considered worthy of reporting because it illustrates the concurrent intraventricular migration of silicone oil and cerebellar infarction, an uncommon coexistence that may lead to confusion in the diagnosis in the emergency setting. Furthermore, the case provides comprehensive radiologic correlation with both CT and MRI findings, reinforcing the value of

multimodality imaging in differentiating silicone oil migration from acute hemorrhagic conditions.

CASE REPORT

An 81-year-old woman presented to the emergency department with a 2-day history of nausea, dizziness, and imbalance. Her medical history included bilateral hip prosthesis surgery, hypertension, and type 2 diabetes mellitus. On physical examination, the patient's gait was ataxic toward the right. Laboratory findings were unremarkable. Electrocardiography (ECG) and transthoracic echocardiography revealed no pathological findings suggestive of a cardioembolic ischemic stroke.

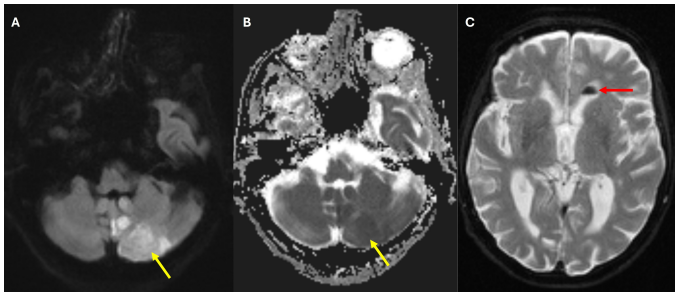

Figure 1. (A) Diffusion-weighted imaging (DWI) and (B) apparent diffusion coefficient (ADC) maps demonstrate diffusion restriction in the left cerebellar hemisphere within the territory of the posterior inferior cerebellar artery (PICA), consistent with early-stage infarction (yellow arrows). (C) Axial DWI (b = 0) sequence reveals a non-dependent, layering hypointense area in the frontal horn of the left lateral ventricle (red arrow), suggestive of migrated intraventricular silicone oil. DWI, diffusion-weighted imaging; ADC, apparent diffusion coefficient.

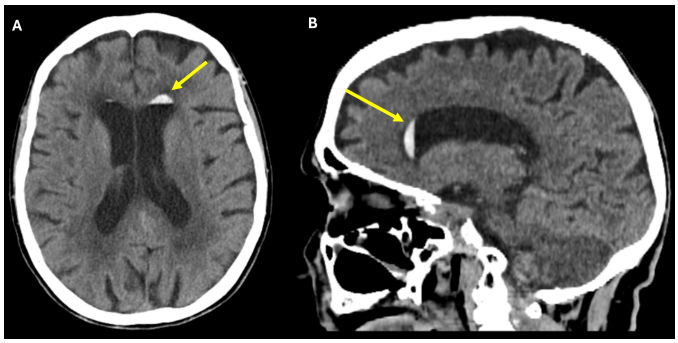

Figure 2. Non-contrast axial (A) and sagittal (B) computed tomography images show a non-dependent, layering hyperdense material in the frontal horn of the left lateral ventricle (yellow arrows). Given that the scan was acquired in the supine position, this appearance is considered atypical for intraventricular hemorrhage.

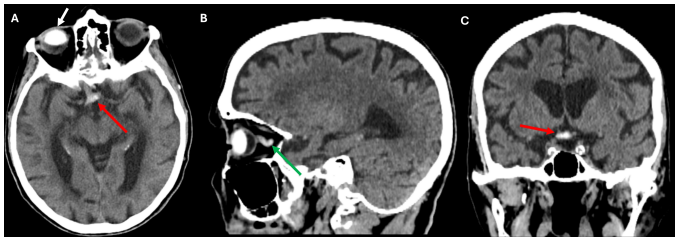

Figure 3. Noncontrast axial (A), sagittal (B), and coronal (C) computed tomography images. Hyperdense intraocular material consistent with silicone oil is observed in the right globe (white arrow, A). Hyperdense foci representing migrated silicone oil are observed at the optic chiasm level (red arrows, A and C). In addition, a hyperdensity consistent with silicone oil is observed along the right optic nerve course (green arrow, B).

Diffusion-weighted imaging (DWI) on MRI revealed diffusion restriction in the left cerebellar hemisphere, consistent with an early-stage infarction in the posterior inferior cerebellar artery (Figure 1). Additionally, a non-dependent, layering hypointense area was observed in the frontal horn of the left lateral ventricle on both apparent diffusion coefficient (ADC) and DWI (b = 0) sequences. Non-contrast brain CT revealed hyperdense layering within the frontal horns of the bilateral lateral ventricles (Figure 2). In the supine-positioned scans, the localization of the layering in the frontal horns was considered atypical for IVH. This hyperdensity was observed to extend along the optic chiasm and the right optic nerve (Figure 3). The presence of hyperdense surgical material within the right bulbus oculi prompted a more detailed investigation of the patient's ophthalmological history. According to the information obtained, approximately 7 years prior, the patient had undergone vitreoretinal surgery at another institution due to tractional retinal detachment secondary to diabetic retinopathy, during which intraocular SiO was injected as a tamponade agent.

On the basis of these findings, it was concluded that SiO within the bulbus oculi had migrated along the optic nerve sheath into the subarachnoid space and subsequently into the intraventricular system. Because the patient presented beyond the accepted time window for intravenous tissue plasminogen activator (tPA) administration, no thrombolytic therapy was initiated. Instead, treatment was continued with 100 mg/day acetylsalicylic acid.

No stroke-related complications developed during six-day hospitalization. The patient was discharged with appropriate recommendations with stable neurological and general condition. A signed informed consent form was obtained from the patient on May 15, 2025. This case report was prepared following the CARE (CAse REport) Guidelines [7,8].

DISCUSSION

Although the intraventricular migration of intraocular SiO is a rare complication, it holds critical diagnostic significance. To date, this condition has been reported in the literature in a few cases [5]. Although the lateral ventricles are the most commonly involved sites, cases with involvement of the third and fourth ventricles have also been described [3].

According to the literature, intraocular SiO migration following ocular injection typically occurs over a period ranging from several months to years (6–120 months). It is usually incidental and asymptomatic [3]. However, on radiological imaging, it may appear as hyperdense layering that can mimic intraventricular hemorrhage, posing a significant diagnostic

https://doi.org/10.5455/annalsmedres.2025.08.215

pitfall—particularly for radiologists, neurosurgeons, and neurologists. In our case, intraventricular migration of silicone oil following vitreoretinal surgery for diabetic retinopathy-related retinal detachment was identified through both CT and MRI. On CT scans, the hyperdense materials observed within the ventricles exhibited characteristic features such as nondependent positioning, providing important clues for differential diagnosis.

These findings can mimic acute hemorrhage due to their similar density, as overlapping Hounsfield Unit (HU) values may complicate the diagnostic process. However, radiological features, such as a globular shape, mobility, and nondependent positioning within the ventricle, are valuable clues for differential diagnosis [3,5]. In addition, the presence of a chemical shift artifact on MRI is considered a significant indicator of intraventricular SiO [9]. Therefore, in patients with a history of vitreoretinal surgery and intraocular SiO injection, the combined assessment of CT and MRI findings is crucial when hyperdense intraventricular lesions are observed, as it significantly impacts clinical management.

A detailed medical history regarding prior vitreoretinal surgery is of critical importance for diagnostic accuracy in elderly patients presenting to the emergency department with stroke-like symptoms. This is because intraventricular SiO can be misinterpreted as intraventricular hemorrhage , potentially leading to the contraindication of thrombolytic therapies such as intravenous tPA. Such a misdiagnosis may result in a fundamental error that significantly alters the patient's treatment course. Although tPA was not indicated in the presented case, overlooking this differential diagnosis in similar clinical scenarios may lead to inappropriate treatment planning. Written informed consent for publication of this case report and accompanying images was obtained from the patient.

CONCLUSION

In conclusion, although the intraventricular migration of SiO is extremely rare, it presents with characteristic and distinguishable radiological features when recognized. Careful correlation of clinical history with imaging findings is essential to avoid misdiagnosis with serious conditions, such as intraventricular hemorrhage, thereby reducing unnecessary interventions and treatment-related errors.

Informed Consent: Written informed consent for publication and accompanying images was obtained from the patient.

Peer-review: Externally peer-reviewed.

Author Contributions: Concept/Design: A.S and B.A.; Data Collection/Processing: A.S., M.F.G and B.A.; Analysis/Interpretation: A.S.; Literature Review: A.S and B.A.; Writing: A.S.; Critical Review: A.S. and M.F.G

Conflict of Interest: None declared by the authors.

Financial Disclosure: The authors declare that none.

REFERENCES

1. Nagpal M, Videkar R. Silicone oil removal. *Expert Rev Ophthalmol.* 2012;7(1):87–96. doi: 10.1586/eop.11.79.
2. Issa R, Xia T, Zarbin MA, et al. Silicone oil removal: post-operative complications. *Eye (Lond).* 2020;34(3):537–43. doi: 10.1038/s41433-019-0551-7.
3. Mathis S, Boissonnot M, Tasu J-P, et al. Intraventricular Silicone Oil. *Medicine (Baltimore).* 2016;95(1):e2359. doi: 10.1097/MD.0000000000002359.
4. Williams RL, Beatty RL, Kanal E, et al. MR Imaging of Intraventricular Silicone: Case Report. *Radiology.* 1999;212(1):151–4. doi: 10.1148/radiology.212.1.r99jl27151.
5. Li W, Wu C, Xue W, et al. Intraventricular silicone oil migration post-retinal detachment surgery: diagnostic features and classification – a case study with literature review. *BMC Ophthalmol.* 2025;25(1):109. doi: 10.1186/s12886-025-03924-0.
6. Filippidis AS, Conroy TJ, Maragkos GA, et al. Intraocular Silicone Oil Migration into the Ventricles Resembling Intraventricular Hemorrhage: Case Report and Review of the Literature. *World Neurosurg.* 2017;102:695.e7-695.e10. doi: 10.1016/j.wneu.2017.03.131.
7. Gagnier JJ, Kienle G, Altman DG, et al. The CARE guidelines: consensus-based clinical case report guideline development. *J Clin Epidemiol.* 2014;67(1):46–51. doi: 10.1016/j.jclinepi.2013.08.003.
8. Riley DS, Barber MS, Kienle GS, et al. CARE guidelines for case reports: explanation and elaboration document. *J Clin Epidemiol.* 2017;89:218–35. doi: 10.1016/j.jclinepi.2017.04.026.
9. Chen JX, Nidecker AE, Aygun N, et al. Intravitreal silicone oil migration into the subarachnoid space and ventricles: A case report and review of literature. *Eur J Radiol Extra.* 2011;78(2):e81–3. doi: 10.1016/j.ejrex.2011.02.004.

https://doi.org/10.5455/annalsmedres.2025.08.215